

Aus dem Institut für Experimentelle und klinische Pharmakologie und Toxikologie
des Universitätsklinikums Hamburg-Eppendorf

Direktor: Prof. Dr. med. T. Eschenhagen

**The role of protein phosphatase inhibitor 1 in the initial phase
after transverse aortic constriction in a murine model**

Dissertation

zur Erlangung des Grades eines Doktors der Medizin
der Medizinischen Fakultät der Universität Hamburg

vorgelegt von

Micha Peeck

aus Geesthacht

Hamburg (2011)

Angenommen von der Medizinischen Fakultät

der Universität Hamburg am: 28.10.2011

Veröffentlicht mit Genehmigung der Medizinischen

Fakultät der Universität Hamburg

Prüfungsausschuss, der Vorsitzende: Prof. Dr. T. Eschenhagen

Prüfungsausschuss: 2. Gutachter: Prof. Dr. A. El-Armouche

Prüfungsausschuss: 3. Gutachter: Prof. Dr. H. Ehmke

Content

1	Introduction	6
1.1	Epidemiology of heart failure	6
1.2	Etiology, pathogenesis and pathophysiology of heart failure	6
1.3	Clinical features and therapy of heart failure.....	8
1.4	The physiologic role of the β -adrenergic signaling cascade.....	8
1.5	Regulation of cardiac protein phosphatase activity	10
1.6	Regulation of I-1.....	11
1.7	The role of the β -adrenergic signaling cascade in heart failure.....	12
1.8	The particular role of PP1 and I-1 in HF.....	15
1.9	Goals and composition of this study	16
2	Material and Methods.....	17
2.1	Origin and handling of mice	17
2.2	Echocardiographic assessment of cardiac parameters.....	19
2.3	Transverse aortic constriction	22
2.4	Animal sacrifice.....	23
2.5	Quantification of mRNA levels	24
2.5.1	Preparation of cDNA.....	24
2.5.2	Principle and design of qPCR	25
2.5.3	qPCR procedure	27
2.6	Proteinbiochemistry	29
2.6.1	Protein extraction.....	29
2.6.2	Quantification of protein using Bradford's method (Bradford. 1976)	29
2.6.3	SDS polyacrylamide gel electrophoresis	30
2.6.4	Transfer of proteins.....	32
2.6.5	Further handling of the membrane.....	33
2.7	Histological Analysis	35
2.8	Statistic analysis	38
3	Results.....	39
3.1	Baseline cardiac function and morphology assessed by echocardiography ..	39
3.2	Baseline cardiac function assessed by left heart catheter	42

3.3	Transverse aortic constriction using a 25G needle	43
3.3.1	Survival.....	43
3.3.2	Comparable development of a minor cardiac hypertrophy	43
3.3.3	I-1 KO mice exhibited worse recovery of cardiac function	45
3.3.4	Induction of hypertrophy was confirmed on a molecular level.....	46
3.3.5	mRNA assessment of I-1 revealed higher levels of I-1 mRNA.....	47
3.3.6	Transverse aortic constriction using a 27G needle	48
3.3.7	Higher mortality rate in I-1 KO ^{TAC} mice	48
3.3.8	All mice exhibited a massive heart failure on day 8 after intervention.....	50
3.3.9	Hypertrophy was attenuated in male KO ^{TAC} mice	51
3.3.10	Contractility was equally diminished in WT ^{TAC} and KO ^{TAC} , while dobutamine response seemed to be slightly attenuated in KO ^{TAC}	53
3.3.11	I-1 mRNA levels were clearly downregulated after TAC.....	57
3.3.12	Pathological hypertrophy markers were massively elevated after TAC.....	58
3.3.13	Immunoblotting showed an increase of PP1 levels after TAC	59
3.3.14	PKA substrates differed in phosphorylation, but results were inconclusive	60
3.3.15	Serca2 levels exhibited a significant decrease in WT ^{TAC} only	63
3.3.16	GSK-3β protein levels conformably increase after TAC	64
3.3.17	Slightly larger cell area in WT ^{TAC} mice	65
4	Discussion.....	67
4.1	Absence of functional differences at baseline is contradictory to earlier reports 67	
4.2	Assessment of the 25G-TAC-Series	68
4.3	Increased mortality in KO ^{TAC} mice unexpected	68
4.4	Stronger impairment of cardiac function in KO ^{TAC} mice resembles survival data 69	
4.4.1	Diminished phosphorylation of cardiac troponin I and C protein might play a pivotal role.....	69
4.5	Comparable hypertrophy response in KO ^{TAC} and WT ^{TAC}	70
4.5.1	Stronger induction of fetal gene program in KO ^{TAC}	70
4.6	Gender specific analysis reveals significant differences	71
4.7	Does failure to adapt cause worse outcome in KO ^{TAC} group?	72

4.8	Conclusion and outlook.....	73
5	Abstract.....	76
6	Abbreviations	77
7	Literature.....	79
8	Acknowledgements	90
9	Curriculum vitae	91
10	Eidesstattliche Versicherung:	92
11	Addendum: Data from the 27G TAC series	93

1 Introduction

1.1 Epidemiology of heart failure

Diseases of the heart and vasculature are the most common cause of death in all industrialized countries. In the United States 80.7 million people, which is 37.1% of the population, had a cardiovascular disease (CVD) of any kind in 2005, and in 2004 diseases of the heart caused 652,486 deaths, which therefore constituted 27.2% of all deaths. The estimated prevalence of heart failure (HF) was 5.3 million in 2005. HF was listed as the underlying cause of death in 57,120 cases, this accounting for 2.4% of all deaths (Miniño et al. 2007; AHA 2007).

HF is the leading cause of hospitalization for people over 65 years of age and has increased as a cause for hospital discharges from 400,000 in 1979 to 1,084,000 in 2005, which resembles a plus of 171%. The direct and indirect costs of HF in 2008 were estimated to be \$34.8 billion (AHA 2007).

The lifetime risk for acquiring HF is 1 in 5 for both men and women (Lloyd-Jones et al. 2002). Since congestive HF is already the leading cause of hospitalization in the elderly and its prevalence will increase due to the growing life expectancy, it is crucial to develop new treatment options as well as to improve primary prevention (Stewart et al. 2003).

1.2 Etiology, pathogenesis and pathophysiology of heart failure

HF, which is defined as a clinical syndrome resulting from the heart's inability to meet the body's circulatory demands, is the final endpoint of many different diseases including coronary heart disease (CHD), pulmonary and arterial hypertension (HTN), valvular heart disease and different forms of cardiomyopathy. HTN has been recognized to be a very common cause for acquiring HF (Levy et al. 1996), even more important in women than in men, in whom myocardial infarction was identified to be an important risk factor (Lloyd-Jones et al. 2002).

Most of these stimuli mentioned above primarily lead to a phase of cardiac hypertrophy in which the individual myocyte increases in length as well as in width serving to increase cardiac output (CO) and to reduce ventricular wall tension (Heineke and Molkentin 2006). This cardiac hypertrophy leads to an increased

myocardial oxygen consumption, impaired subendocardial blood flow, abnormal myocardial bioenergetics and an increased risk of ventricular arrhythmias (Cohn 1995). The CO can only be stabilized for a limited amount of time and decreases subsequently. This insufficient cardiac output (CO) in HF has multiple effects. The renin-angiotensin-aldosterone system (RAAS) as well as the sympathetic nervous system (SNS) are activated. This in turn leads to a systemic vasoconstriction and volume retention. The venous return and therefore the preload is increased, which is designed to maintain CO. Additionally the increased vasoconstriction leads to an increased afterload. Though these mechanisms help to perpetuate a sufficient blood supply at the time being, all these effects are detrimental in the long run. The increased mechanical stretch of the myocardium leads to further cardiac hypertrophy and remodeling, both being additionally modified by several factors including hormones, ischemia and vasoactive peptides (Swynghedauw 1999). This usually leads to a further decrease in CO and therefore what seems beneficial in the beginning is detrimental in the long run.

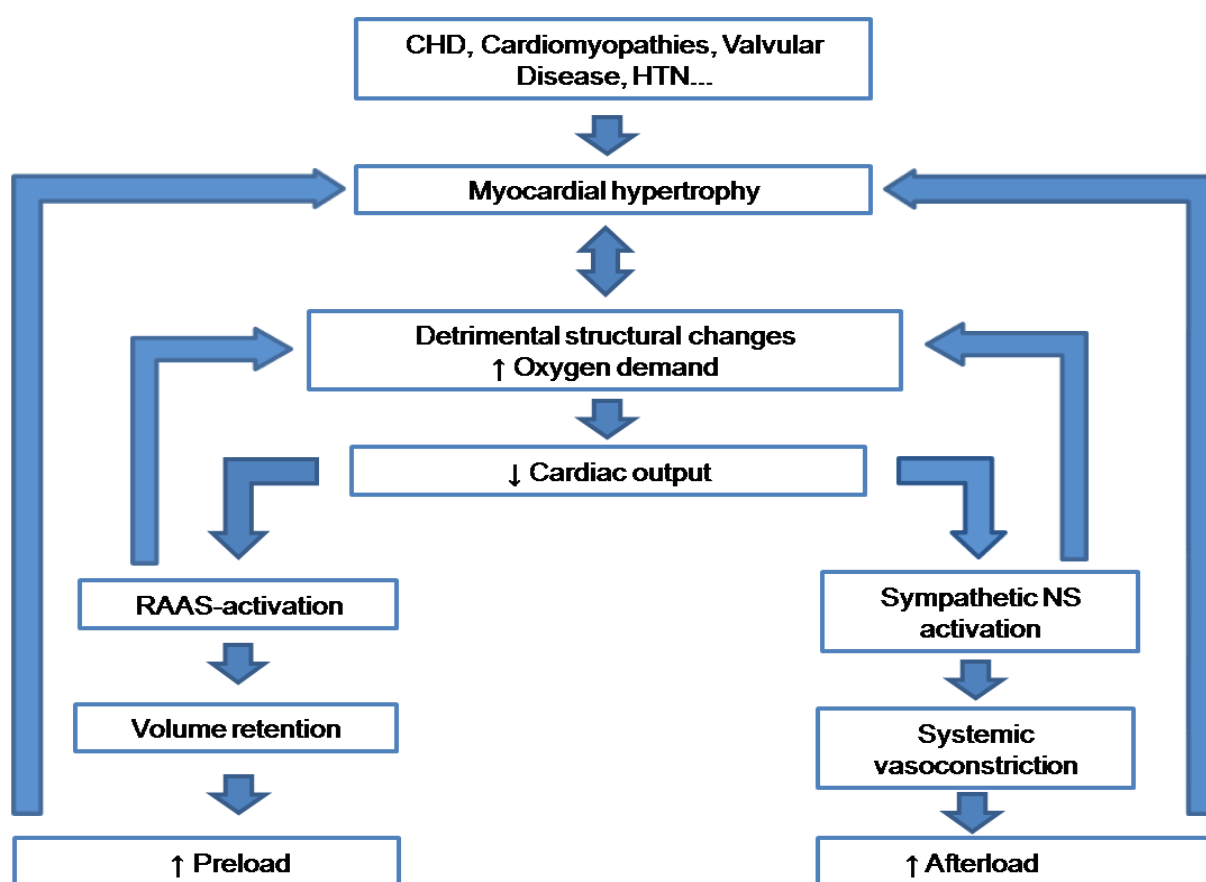


Figure 1: Pathogenesis of heart failure, emphasizing the chronic negative effects of cardiac output adaption, which leads to a perpetuation of detrimental influences.

1.3 Clinical features and therapy of heart failure

Two main groups of HF are distinguished in the clinical routine: (1) right- and (2) left-sided HF. Symptoms of right-sided HF are due to a congestion of blood in the venous system and presents with pitting edema, nocturia, jugular venous distention, hepatomegaly, which might cause cirrhosis of the liver (*cirrhose cardiaque*), and ascites. Right-sided HF might also be referred to as backward-failure. Left-sided HF on the other hand is also called forward-failure, although one main symptom, the pulmonary congestion, is not in accordance to this concept. Besides pulmonary congestion acute left-sided HF can present with symptoms of insufficient blood supply to virtually any organ, e.g. confusion and memory impairment, renal failure and acute or chronic mesenteric ischemia. Often symptoms of right- and left-sided HF appear simultaneously. A more recent classification for HF distinguishes systolic and diastolic HF. Systolic dysfunction simply describes the disability of the heart muscle cell to adequately contract, therefore rendering the heart's global contraction ineffective, which leads to diminished forward flow with subsequent backward congestion. Diastolic dysfunction on the other hand is a more controversially discussed topic. In the end, it focuses more on the filling aspect of the heart, which might be impaired by various mechanisms. Ischemia is discussed to impair ATP generation in heart muscles, which leads to an impairment of relaxation and therefore insufficient influx. Fibrosis or hypertrophy might also impair the ventricle's compliance and impair influx. With all mechanisms, there are increased end-diastolic filling pressures, which might lead to dyspnea by an increased pulmonary capillary pressure.

HF is classified in the clinical routine using the New York Heart Association (NYHA) classification, which utilizes the incidence of dyspnea at certain levels of physical work (Jessup and Brozena 2003). HF is treated stage-adapted with diuretics, ACE-inhibitors, β -blockers, aldosteron-antagonists and digitalis when HF is not acute. The treatment of acute heart failure will not be discussed here.

1.4 The physiologic role of the β -adrenergic signaling cascade

The major part in the regulation of cardiac work (CW) is borne by the autonomic nervous system (ANS). An increase in cardiac work is mediated by an increased

activity of the SNS. This activity of the SNS is regulated by central and peripheral mechanisms, e.g. the baroreceptor-reflex. Upon activation, the SNS releases catecholamines, directly at the heart, but also at the medulla of the adrenal gland, which in turn para- and endocrinally stimulate cardiac β -adrenergic receptors (β -AR). This has positive ino-, chrono-, dromo- and lusitropic effects on the heart and in turn CO can be increased nearly 5-fold. The β_1 -AR is the receptor isoform that constitutes 75-80% of the heart's β -AR. The other β -ARs on the heart are mainly β_2 -AR. α -AR, which represent only 10% of total ARs on the heart, are of subsidiary importance (Rockman et al. 2002). The classical way of signal transduction via β -ARs is the activation of the membrane-bound adenylyl cyclase (AC) via a stimulating GTP-binding protein (G_s). The AC then transforms ATP into cAMP, which in turn activates the cAMP-dependent protein kinase A (PKA) (Lohse et al. 2003). PKA phosphorylates a variety of target proteins, which are responsible for mediating the catecholamines' effects on the heart. These proteins include cardiac troponin inhibitor (cTnI), the cardiac myosin-binding protein C (cMyBP-C), the L-type calcium channel, the ryanodine receptor II and phospholamban (PLB) which among others are responsible for the positive inotropic and lusitropic effects, and the HCN-channels of the sinus- and atrioventricular-node, which mediate the positive chronotropic effects (Lohse et al. 2003; Dorn and Molkentin, 2004; El-Armouche et Eschenhagen 2009).

The opponents of the PKA are the protein phosphatases (PP). Whereas in the past the protein kinases (PK) were thought to be the central regulatory element, today PPs have gained a similar significance, since inhibition of PPs might as well increase the phosphorylation of proteins (Oliver and Shenolikar 1998; Aggen et al. 2000; Herzig and Neumann 2000; Cohen 2002; El-Armouche et Eschenhagen 2009).

Pps remove the phosphate groups, which have previously been bound to amino acid residues (mainly to serine, threonine and tyrosine residues). The classification of the currently known PPs divides them into the following groups: Tyrosine-Pps, serine/threonine-Pps and dual-specificity PP, which dephosphorylate both tyrosine- and serine/threonine-residues (Cohen et al. 1989). The serine/threonine-Pps PP1, PP2A, PP2B and PP2C are responsible for the main part of serine/threonine-PP activity *in vivo* (Cohen et al. 1989; Mac Dougall et al. 1991). Their activity is controlled by further regulatory elements.

1.5 Regulation of cardiac protein phosphatase activity

Serine/threonine-kinases display a consensus-sequence selectivity, meaning they recognize their substrates by a common local motif (Pinna and Ruzzene 1996). Serine/threonine-PPs on the other hand do not display such a consensus sequence selectivity, instead they dephosphorylate multiple substrates, both *in vivo* and *in vitro* (Pinna and Donella-Deana 1994).

PP1's activity is on the one hand regulated by its interaction with many different protein subunits, which target its catalytic subunit (PP1c) to specific subcellular compartments. This serves two purposes, (a) it provides proximity of PP1c to its particular substrate and (b) it diminishes dephosphorylation of other potential substrates (Feng et al. 1991; Stuart et al. 1994).

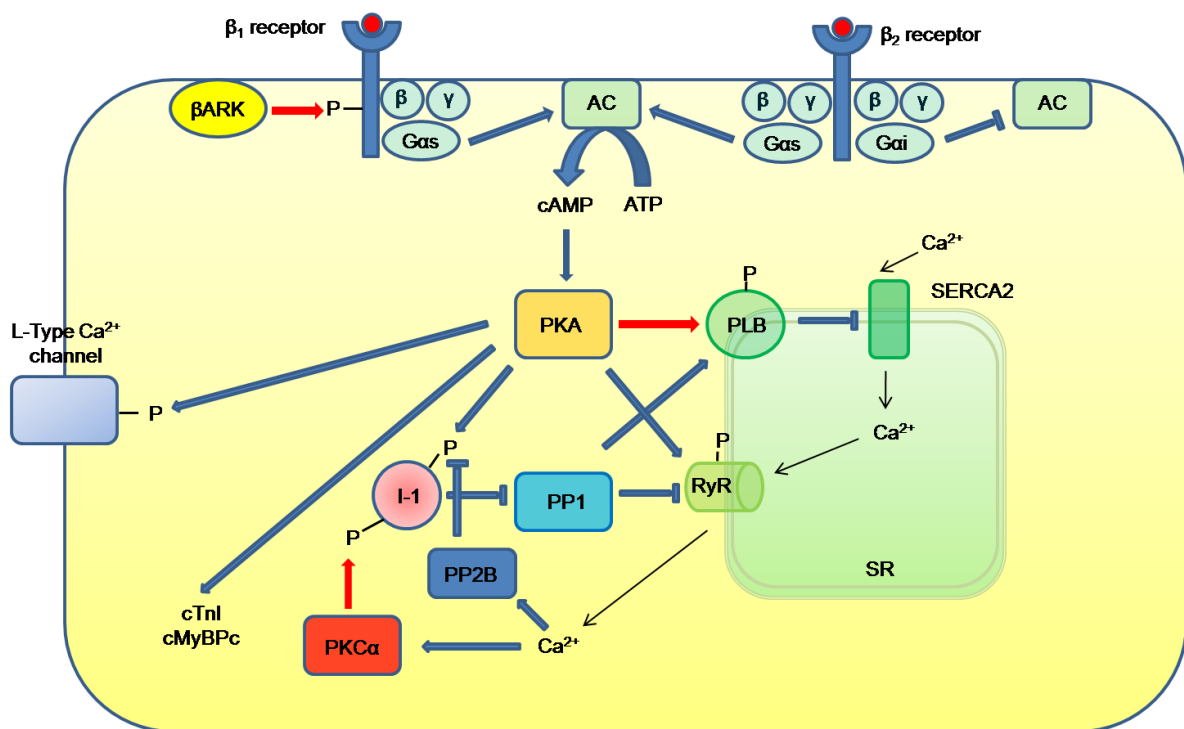


Figure 2: Simplified drawing of a cardiomyocyte, illustrating the interactions in the β -adrenergic pathway. Blue arrows indicate a stimulatory effect (whether by phosphorylation or not), whereas red arrows indicate an inhibitory effect caused by phosphorylation.

The other important regulatory mechanism of PP1 is the interaction with regulatory subunits, the so-called PP inhibitors, which leads to a formation of heterotrimeric complexes (Wera and Hemmings 1995). The most prominent regulator of PP1, which is the dominating cardiac PP, is the cytosolic inhibitor-1 (I-1).

I-1 can be phosphorylated at its Thr-35 residue by PKA and in this phosphorylated state it is an extremely potent inhibitor of PP1 (Cohen et al. 1989). Interestingly I-1 had already been described as a link between PP1 and PKA more than 30 years ago (Huang and Glinsmann 1976), but has only been viewed as a mechanism involved in the glycogen metabolism in liver and skeletal muscle for a long time (Cohen and Cohen 1989). It was assumed that the inhibition of PP1 would be decreased insulin-dependently, which would lead to an increased activity of the glycogen synthase. The decreased inhibition of PP1 was thought to be an effect of reduced phosphorylation of I-1. This theory was falsified by Srimegeour et al. (1999), which demonstrated that I-1 *knockout* mice had the same glycogen synthesis rate as *wildtype* mice.

The research about I-1's role in the heart started in 1991, when Neumann et al. (1991) found evidence for an activation of I-1 as a consequence of β -adrenergic stimulation *in vivo*. I-1 stabilizes the phosphorylated state of important cardiac regulatory proteins, so it could be said that its role is that of an amplifier of PKA-signaling (El-Armouche et al, 2003).

1.6 Regulation of I-1

Furthermore I-1 itself is regulated by a number of factors, which may vary between different tissues. In epithelial cells of the renal tubule I-1 can be dephosphorylated at Thr-35 and therefore deactivated by PP2A, but not by the calcium-dependent PP2B (Calcineurin; Higuchi et al. 2000). In neurons on the other hand dephosphorylation is mainly dependent on PP2B (Mukey et al. 1994). In the heart dephosphorylation of I-1 is dependent on both PP2A and PP2B. It was shown that in cardiac myocytes a specific blockade of both, PP2A as well as PP2B, leads to an increased PKA-dependent phosphorylation of I-1 and subsequently of PLB (El-Armouche et al. 2006). Additionally to its PKA phosphorylation site at Thr-35 I-1 exhibits two other possible sites of phosphorylation at Ser-67 (Braz et al. 2004) and Thr-75 (Sahin et al. 2006). The protein kinase phosphorylating these sites is protein kinase C α (PKC- α), which's activity is calcium-dependent (Allen and Katz 1996). A phosphorylation on one of these sites has an opposite effect of one of Thr-35 and leads to a decreased activity of I-1. This was shown when *knockout* mice for PKC- α analyzed, which exhibited a hypercontractility. This phenotype was caused by a increased activity of I-

1 due to the decreased phosphorylation of its Ser-67 residue. The activity of PP1 was therefore diminished, which in turn led to an increased phosphorylation of PLB (Braz et al. 2004).

Recapitulating this one could say that I-1 plays a central role in connecting the two most important signaling ways of the heart, whereas its activity is modulated by both these signaling pathways. On the one side there is the activating influence by PKA, which is mediated by cAMP. On the other side there are calcium-dependent processes, the dephosphorylation by PP2B at Thr-35 and the phosphorylation at Ser-67 by PKC- α , which decrease the activity of I-1.

Since PKA, PKC- α and PP2B all play vital roles in the pathophysiology of HF (Molkentin and Dorn 2001), I-1 appears to be an interesting protein concerning the pathophysiology and pharmacological therapy of HF.

1.7 The role of the β -adrenergic signaling cascade in heart failure

Increased cardiac work load physiologically leads to a cardiac hypertrophy. Since myocardial cells are terminally differentiated and therefore lost their ability to respond by cell division, myocardial hypertrophy is mostly caused by an increase in the size of the individual cell (Chien 1999). This myocyte growth is thought to be regulated by stretch-sensitive mechanisms, whose exact molecular mechanisms remain elusive, and by membrane-bound G-Protein-coupled receptors (GPCRs). These receptors possess intracellular protein-kinase domains or gp130-linked receptors (Heineke and Molkentin 2006). These GPCRs mediate myocyte growth via a complex network of interacting pathways, involving key effector molecules like *ras* and MAPKs as well as phosphatidylinositol-3-OH- and calcineurin-dependent pathways (Rockman et al. 2002; Heineke and Molkentin 2006). From the adrenergic receptors, α_1 -AR are the pivotal receptors in cardiomyocyte hypertrophy. Together with other GPCRs like the receptors for angiotensin II and endothelin-1 they activate hypertrophic MAP-Kinase pathways (Clerk and Sugden 1999). But β -ARs also play a role in the moderation of hypertrophy, there are thought to exert their role via $G_{\beta\gamma}$ -subunits of GPCRs (Heineke and Molkentin 2006) and a recent study has proven that the ablation of beta-adrenergic receptors diminishes hypertrophy in a pressure overload model, indicating a cross-link to hypertrophic pathways (Kiriazis et al. 2008).

This emphasizes the crucial role β -ARs play in HF. Previously it was mentioned that a decrease in CO leads to an activation of the SNS, which accelerates the progression of HF. Upon this stimulation of β -adrenergic signaling various pathways exhibit abnormalities on multiple levels. A chronic increase in catecholamine levels leads to a desensitization and downregulation of β -ARs. The process of downregulation, which seems to affect only β_1 -ARs, is caused by an internalization of these receptors. This internalization is regulated by a complex cascade which involves β -AR kinase-1 (β ARK1), β -arrestin and the phosphoinositide 3-kinase (PI(3)K) (Sathyamangla et al. 2005). Since β_2 -ARs are also desensitized, other mechanisms also play a role, here G-Protein receptor kinases (GRK) as well as $G\alpha_{i2}$ seem to be involved (Bristow 1998).

The question, which has not been answered yet, though it has been extensively studied, is whether the downregulation of β -ARs is beneficial or detrimental in HF (El-Armouche and Eschenhagen, 2009). Several studies have been conducted overexpressing either β_1 -ARs or β_2 -ARs. They have clearly demonstrated that an overexpression of β_1 -ARs leads to a dilated cardiomyopathy even in young mice (Engelhardt et al. 1999), while a moderate (~ 60- fold) overexpression of β_2 -ARs enhances *in vivo* cardiac function. Overexpression (> 100-fold) of β_2 -ARs at high levels on the other hand does result in a rapid and progressive cardiomyopathic phenotype (Milano et al. 1994; Ligett et al. 2000). The antiapoptotic effects of β_2 -ARs are attributed to signaling pathways which are not mediated by a stimulatory G-Protein (Pönicke et al. 2003) and will not be discussed in detail here. Concluding this, β_1 -selective blocking agents might reveal advantages over unselective agents, but this hasn't been proven yet, and a regulative mild upregulation of β_2 -ARs might provide benefits in HF.

Another interesting model which might help to clarify the question is the overexpression of an inhibitor (β ARKct) of the β ARK1. The inhibition of β ARK1 by β ARKct in several animal models prevented biochemical abnormalities in the β -AR system, delayed the onset of HF and even reversed the onset of HF after myocardial infarction (Akther et al. 1997; White et al. 2000; Shah et al. 2001). Tachibana et al. (2005) even showed that the extent of inhibition of β ARK1 by β ARKct determines the degree of cardiac dysfunction. These studies support the hypothesis that

enhancement of contractility by maintenance of β -AR signaling might guard against secondary hypertrophy and fibrotic remodeling.

Other studies conducted with β ARKct- and β 2-AR-overexpression did not yield such positive results. β ₂-overexpression led to an increase in myocardial injury after myocardial infarction (Cross et al. 1999) and transgenic mice exhibited a greater functional deterioration and higher death rates after aortic stenosis (Du et al. 2000). In a severe model of HF, caused by overexpression of a dominant-negative CREB protein (Eckhart et al. 2002), β ARKct overexpression did not exhibit any effect on survival. These and other studies therefore suggest that an enhanced contractility might not be beneficial in every situation or model. Additionally some authors (Lohse et al. 2003) criticize the conclusions drawn from β ARKct-overexpression studies and suggest the increase in β ARK1 is actually a part of the protective downregulation response of the β -AR signaling, whereas the positive effects of β ARKct were exerted on pathways unrelated to the β -AR signaling cascade, but instead by binding of G β γ , which is supported by the fact that similar findings as seen with β ARKct have been made with truncated phosducin (Li Z et al. 2003), which also binds G β γ (Bauer et al. 1992). The synergism of β ARKct with β -blockers (Harding et al. 2001) is regarded as an argument that β ARKct exerts its effects independently from β -adrenergic signaling by some (Lohse et al. 2003, Eschenhagen 2008k, El-Armouche and Eschenhagen 2009), while others (Rockman et al. 2002) argue that β ARKct shares many characteristics with β -AR blockade, e.g. both should resensitize the response to catecholamines.

A recent knockout of AC5-isotype also seemed to have beneficial effects in a chronic isoprenaline infusion model (Okumura et al. 2007), which also supports the hypothesis that downregulation of β -AR signaling might be protective, but for the *knockout* of isotype 6 deleterious effects were reported (Tang et al. 2008).

Lately, a GRK5 polymorphism, which downregulates beta-adrenergic signaling, has shown to be protective in HF, in a murine model as well as in a retrospective clinical trial (Liggett et al. 2008).

In the light of this controversy, it is unfortunate that even two clinically proven facts, which are (a) the poor outcome of inotropic therapy in the chronic treatment of HF (Warner-Stevenson 2003) and (b) the positive effects of β -blockers in HF, which have

been reported first in the 1970s (e.g. Swedberg et al. 1979) and made them a standard medication in the treatment of HF today (ACC/AHA 2005), do not cause enlightenment.

The molecular mechanisms by which β -blockers exert their positive effects in HF have not been clarified yet. The question remains whether it is a blocking or indeed a resensitization of the β -adrenergic signaling cascade. Dorn and Molkentin (2004) suggest a dichotomous role of β -adrenergic signaling in the heart, whereas the augmentation of ventricular performance has a long-term benefit, while the recruitment of secondary signaling pathways is detrimental.

The targets of the β -adrenergic signaling cascade, as PLB, RyR2, or the L-type Calcium-channel, are important proteins in the regulatory process of intracellular calcium content, which also regulates the activity of PKC- α . An increased expression and activity of PKC- α has been reported in human HF and murine HF models (Bowling et al. 1999; Bayer et al. 2003; Wang et al. 2003). Recent murine models report that an inhibition of PKC- α enhances cardiac contractility and can effectively alleviate the progression or development of HF (Braz et al. 2004; Hambleton et al. 2007).

1.8 The particular role of PP1 and I-1 in HF

In consensus with the downregulation of PKA-activity in human HF an increased expression and activity of PP1 has been reported (Neumann et al. 1997; Netticadan et al. 2000). In a murine model a three-fold overexpression of PP1c resulted in a stage resembling HF presenting with depressed cardiac function, dilated cardiomyopathy and premature mortality (Carr et al. 2002). Consistent with the increased activity of PP1 a decrease of phosphorylation, activity and expression of I-1 has been reported (El-Armouche et al. 2003). Murine models suggest an impairment of cardiac contractility (FS reduced by 23%) in I-1 *knockout* mice and a beneficial influence of overexpressed truncated I-1 in a pressure-induced HF model (Carr et al. 2002; Pathak et al. 2005). Increased inhibition of PP1 by I-2 has also been reported to ameliorate HF progression (Yamada et al. 2005, Brüchert et al. 2008), but has as well been reported to cause an exacerbated progression of HF in a pressure overload model (Grote-Wessels et al. 2008). Additionally it has to be taken

into consideration that at least parts of the beneficial action of PKC- α inhibition are attributed to a decreased inhibition of I-1 (Braz et al. 2004). To complicate this matter, a study published by our group showed detrimental effects of I-1 overexpression and beneficial effects of I-1 KO in a chronic isoprenaline infusion model (El-Armouche et al. 2008).

This data obtained on the role of PP1, I-1 and PKC- α in murine models does not clearly seem to support either thesis, neither that decreased contractility and abnormal β -AR signaling are detrimental in HF nor that the opposite is true, but magnificently illustrates the complexity of the issue.

1.9 Goals and composition of this study

The data which has been reported up to this date does not allow clear conclusions as to the role of I-1 in HF, its role is as controversial as that of β -adrenergic signaling itself. This study aimed at illuminating the role of I-1 in more detail by investigating the role of I-1 KO in HF and to follow on findings made in the chronic isoprenaline study model (El-Armouche et al. 2008).

In the study of Carr et al. 2002 the KO mice's contractility seemed to be impaired at baseline compared to wildtype mice and the authors concluded this would lead to an even more marked negative effect if challenged. This hypothesis was not reproduced by our group (El-Armouche et al. 2003) and this led to the wish to test this hypothesis in a HF model. The isoprenaline infusion model had previously been tested and showed a beneficial effect of I-1 KO. The model chosen for this study was the transverse aortic constriction model (TAC), which, on the one hand, was chosen to complement the observations made in the chronic isoprenaline infusion model and on the other hand, was modeled as a counterpart to the study overexpressing truncated I-1 (Pathak et al. 2005) and aimed to illuminate the role of I-1 in HF more closely. Therefore, this study compared I-1 KO mice with normal WT mice, hoping to demonstrate differences in various parameters, ranging from survival to phosphorylation of key elements of the beta-adrenergic signaling cascade and thereby add further aspects to the role of I-1 in HF.

2 Material and Methods

2.1 Origin and handling of mice

The genomic engineering of the I-1 KO mice was not included in this project, but had already been conducted by the lab of Dr. P Greengard, whose lab conducted used these mice on studies of long term potentiation in the CNS (Allen et al. 2000). The first study which used them to study the role of I-1 in the cardiac muscle was conducted by Carr et al. (2002) and will be discussed later. Dr. Greengard kindly donated the mice to this laboratory. The mice were created on a C57Bl/6J background, which was used as the WT control.

The further breeding of the mice used in this project was conducted under the supervision and directions of the author by the animal care facility of the University medical center Hamburg (UKE). For breeding causes, it was mandatory that the mice's genetic identity was permanently controlled by genotyping, which is described here:

Tail tips were acquired either from the animal facility or directly in the sacrifice process. The DNA was extracted using the DirectPCR® Lysis Reagent (Peqlab Biotechnologie GmbH, Erlangen, Germany) as described by the manufacturer.

Adjacently, it was used as a template for polymerase chain reaction (PCR). This was designed as a multiplex PCR using a common reverse primer lying in Intron 1 and two different forward primers, one lying in the NEO-cassette and one in Exon 1. The NEO-cassette primer bound to the DNA of knockout mice, resulting in a product of 380 bp, while the Exon 1 primer bound to wildtype DNA, resulting in a product of 280 bp. The primers were synthesized by MWG Biotech (Ebersberg, Germany).

PCR-reaction mixture:

dNTPs	0.2 mM
10x Buffer	1x
MgCl ₂	3 mM
Forward Exon 1	0.3 µM
Forward Neo	0.1 µM
Reverse Intron 1	0.05 µM
Taqpolymerase	0.1 U/µl
Template	5 ng - 500 ng

Step	Temperature [C°]	Duration	Number of cycles
Preincubation	94	10'	1
Denaturing	94	30''	35
Annealing	56	45''	35
Synthesis	72	45''	35
Extinktion	72	10'	1

Table 1: PCR-programme used for genotyping

Genotyping primers:

Exon 1 forward	5' CCCACGGAAGATCAAGTTTA 3'	T _m 57.3 °C
Intron 1 revers	5' CACTTAGCCGGGAAACTCTG 3'	T _m 59.4 °C
NEO-cassette forward	5' TAAAGCGCATGCTCCAGACT 3'	T _m 57.3 °C

Afterwards, the PCR-product was applied on an agarose gel, which was made out of 2% of Agarose (Sigma, Munich, Germany) soluted in TAE-buffer. 0.03% of Ethidiumbromide was added, which intercalates DNA and allows subsequent visulazation by emitting an orange glow when illuminated by UV-light.

20% of loading dye was added to the PCR-product before the running process and then the gel was electrophorized for about one hour at 80 V. The standard used was the GeneRuler 100 bp DNA Ladder (Fermentas, St. Leon-Rot, Switzerland). The gel

was visualized and a picture was taken using the ChemiGenius2 (Syngene, Cambridge, Great Britain).

TAE-buffer:

0.1 M EDTA
2 M TRIS
1 M acetic acid
diluted in H₂O

Loading dye:

75 mg Bromphenylblue
25 mg Xyclencyanol
100 ml Glycerol

2.2 Echocardiographic assessment of cardiac parameters

Before assessing echocardiographic parameters in mice it had to be decided whether the mice should be anesthetized or should remain conscious during the examination. Although, in principle, the conscious examination of mice is possible and has been conducted in several studies (e.g. Suehiro et al. 2001), for reasons of standardization and handling it was decided to anesthetize the mice for examination. The anesthetic used was isoflourane (isf; Baxter, Vienna, Austria), because it was shown that it causes only slight cardiac depression on the one hand, which is an advantage in the handling of already cardially depressed TAC-mice, and on the other hand allows the repeated assessment of cardiac function (Roth et al. 2002).

Isoflourane was brought into a gaseous form by a thermal vaporizer (Dräger, Lübeck, Germany). For the actual examination, mice were first placed in a plexiglass box filled with Isf for the induction of anesthesia. After a sufficient depth of anesthesia was achieved, mice were placed in a supine position on an auto-regulative heating pad stabilizing the body temperature at 37° C. Subsequently, the mouse's left hemithorax was depilated using a depilatory cream (Pilca®, ASID BONZ GmbH, Böblingen, Germany) to avoid interference of echocardiography. Finally preheated ultrasound gel (Sonogel, Bad Camberg, Germany) was applied. Anesthesia was maintained by Isf supplied via a hose which had been placed directly over the mouse's mouth. The heating pad contained four electrodes on which the mouse's pads were placed which allowed the registration of an electrocardiogram (ECG), which was, amongst other things, used to adjust the depth of anesthesia, aiming for a heart rate of above 500 bpm, which corresponded to approximately 2.0% of Isf in 95% oxygen and 5%CO₂.

The following procedure was performed as standardized as possible. First, the probe was placed in an angle which allowed the visualization of the long axis of the left ventricle. When visualized, it was adjusted in a fashion that simultaneously allowed the view on the aortic valve and the apex demonstrating a minimal wall thickness. Three B-mode films were acquired in this position in a 30 Mhz, 60 Mhz and in a so-called EKV-mode, which assembled many ECG triggered beats to appear as one.

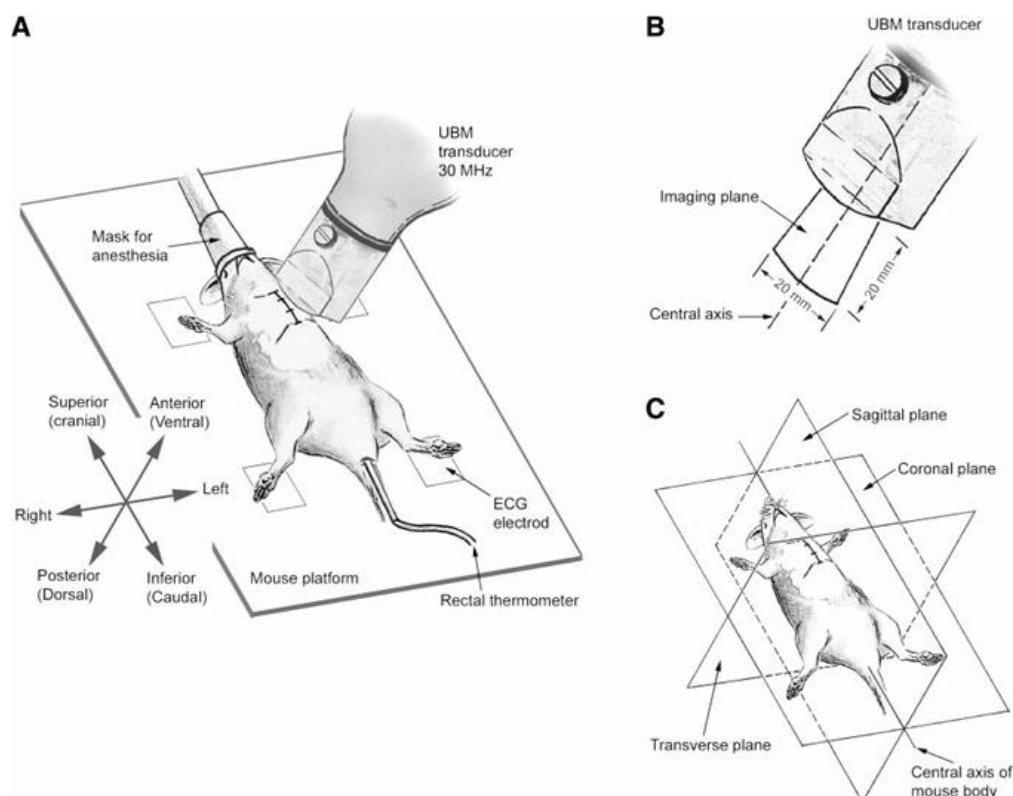


Figure 3: Placement of mouse for echocardiography (Zhou et al. 2004)

After the acquisition of those films, the mouse was moved slightly downwards below the probe without changing the probe's angle to visualize the right pulmonary artery crossing the ascending aorta. Here, a 30 MHz B-Mode recording of the right pulmonary artery and a continuous wave (CW)-doppler recording were acquired.

Following this, the probe was tilted by 90° to the right to allow a short axis view. The plain in which this was acquired allowed visualization of the papillary muscles. Here again, the recordings were made as described above. Additionally, an M-Mode recording was made. Afterwards, the mouse was injected a maximal effective dose of 20 µg/g dobutamine (Carinopharm, Gronau, Germany) intraperitoneally and the

process was carried out in reverse omitting the acquisition of the EKV®-recordings. The echocardiography machines used were the Vevo 660™ and Vevo 770™ High Resolution Imaging system (Visual Sonics, Toronto, Canada).

The acquired recordings were subsequently evaluated with the computer program belonging to the Vevo 660™ and 770™ and measurements of several parameters both in diastole and systole were made, if possible from the EKV recordings.

Long axis view:

- Left ventricular diameter in length (long diam d/s)
- Left ventricular diameter in width (short diam d/s)

Short Axis view:

- Inner left ventricular area (area endo d/s)
- Outer left ventricular area (area epi d/s)
- Anterior left ventricular wall thickness (both B- and M- mode) (AwTh d/s)
- Posterior left ventricular wall thickness (both B- and M- mode) (PwTh d/s)
- Left ventricular diameter in width (both B- and M- mode) (LVEDD / LVESD)

Right pulmonary artery:

- Pulmonary artery diameter (DPA)
- Heart rate (HR)
- Velocity time integral (VTI)

The acquired measurements were used to calculate several parameters: The mass of the left ventricle (LV) was calculated using the 2D area-length method, which has been shown to be of sufficient accuracy (Collins et al. 2003):

$LV\ mass = (1.05 * (5/6 * area\ epi * (long\ diam + (PwTh + AwTh)/2)) - 5/6 * area\ epi * long\ diam)$. 1.05 is the specific gravity of the muscle.

The left ventricular enddiastolic and endsystolic volumes were calculated as:

$LVEDV = 5/6 * long\ diam\ d * area\ epi\ d$ and $LVESV = 5/6 * Long\ diam\ s * area\ epi\ s$

The fractional area shortening (FAS) was calculated:

$\%FAS = ((area\ epi\ d - area\ epi\ s) / area\ epi\ d) * 100$

The fractional shortening was calculated accordingly with area being replaced by diameter:

$$\%FS = ((\text{diameter } epi\ d - \text{diameter } epi\ s) / \text{diameter } epi\ d) \times 100$$

Cardiac index (CI) was calculated as:

$$CI = (\pi \times DPA^2 \times VTI \times HR / 100) BW * 1000$$

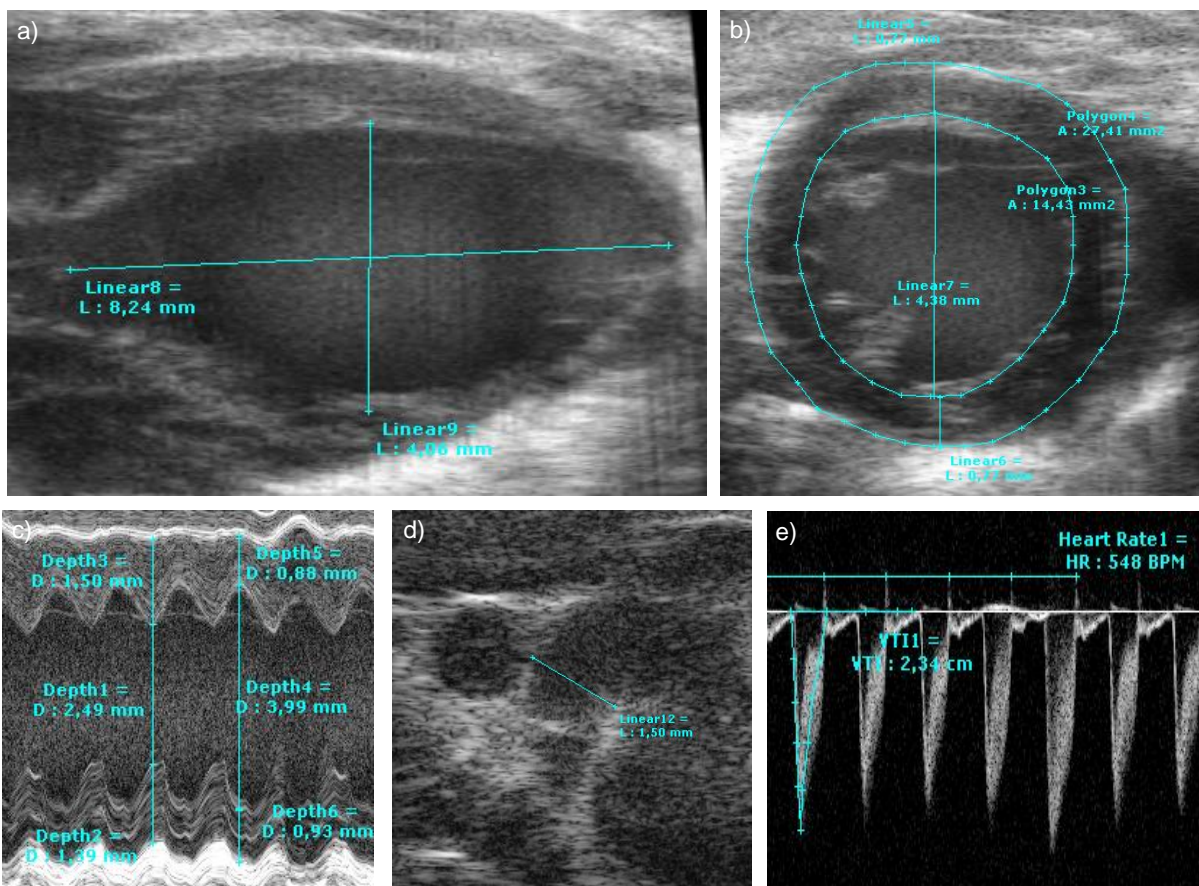


Figure 4: Excerpts from the acquired echocardiography recordings: **(a)** Long axis diastole; **(b)** Short axis diastole; **(c)** M-Mode; **(d)** Right pulmonary artery; **(e)** Pulsed wave Doppler of right pulmonary artery.

2.3 Transverse aortic constriction

The transverse aortic constriction as a model for pressure induced hypertrophy was introduced in the early 90s (Rockman et al. 1991). It used the open chest approach, which is still the most commonly used approach. The approach used in this project

was introduced about 10 years later (Hu et al. 2003), using the suprasternal approach, having the advantage of rendering intubation superfluous.

The anesthesia was acquired using a mixture of 90 mg/kg Ketamin S (Pfizer, Zürich, Switzerland) and 10 mg/kg Xylazine (Bayer AG, Leverkusen, Germany) which was injected intraperitoneally. The mouse was allowed to fall into sufficiently deep anesthesia. Then it was depilated suprasternally in the same manner as for echocardiography. It was subsequently taped to a Styrofoam pad in a supine position and a loop was placed behind the upper front teeth to extend the head backwards.

Thus prepared an about 1.0 cm long horizontal cut was made suprasternally. This allowed the visualization of the thyroid, which was then retracted cranially. The pretracheal muscles were medially dissected and a 2-3 mm long medial cut was made in the superior sternum. Then a forceps was used to retract the sternum caudally exhibiting the aortic arch. This was underridden with a blunted, 90° angled 27G cannula (BBraun, Melsungen, Germany) to create a sufficiently big opening for the following: a 5.0 Polyviolene suture (Harvard Apparatus, Holliston, USA) was placed under the aortic arch using a 25G permanent venous catheter (BBraun, Melsungen, Germany), which was consecutively tied against a 25G (0.5 mm diameter) or 27G (0.4 mm) blunted, and 90° angled cannula, creating a stenosis of approximately 50% or 65% respectively. Then the pretracheal muscles and thyroid were moved into their previous positions and the skin was closed using 6.0 Prolene® suture (Ethicon, Norderstedt, Germany). In principle, the same method was applied at the Sham operated animals, but no suture was applied. The whole process was carried out under x16 magnification using a microscope (Zeiss, Oberkochen, Germany).

Afterwards, the mice were placed on a heating mat (Gaymar Industries, Orchard Park, NY, USA) until they were fully awake. Postoperative analgesia was achieved by adding metamizol (Rathiofarm, Ulm, Germany) to their drinking water. To minimize post-operative weight loss, the mice received their food munched.

2.4 Animal sacrifice

The sacrifice of mice followed a standard protocol. The mouse was weighed on a precision scale and afterwards placed in a container which had previously been filled

with CO₂, in which it remained until it was unconscious; thereafter the mouse was beheaded using scissors of an appropriate size. The corpse was placed in a supine position on a cork mat and its extremities were fixated with needles. The thorax was quickly opened with a left parasternal cut and the heart was removed, cleansed in isotonic sodium-chloride solution and subsequently dried and weighed. Then the atria were dissected and the heart was transversely cut into three slices. Atria, apex and base were quickly frozen in liquid nitrogen while the medial slice was stored in 4% formaldehyde. Subsequently, the lungs were removed and weighed and the right tibia was removed as well and measured with a sliding calliper (Mettler-Toledo, Giessen, Germany). Finally the tip of the tail was removed to be used for genotyping. The heart tissue and tail tip were stored at -80 °C until further use.

2.5 Quantification of mRNA levels

2.5.1 Preparation of cDNA

The tissue used for the quantification of mRNA expression was the apex of the heart, which was chosen because this minimized the risk of a contamination by atrial tissue. This tissue was powdered in a metal mortar which was continually cooled in liquid nitrogen. 40 mg of the obtained powder was used for RNA extraction using the SV Total RNA Isolation System (Promega, Madison, USA), a spin basket based approach including an RNase digestion step. In the final step of this process, the RNA was taken up in water and stored at -80 °C.

For quantification, the RNA was 1:50 diluted in water and the absorption was photometrically measured at 260 nm and 280 nm using a spectrometer (Smart Spec® 3000 photometer, Bio Rad, Munich, Germany). The A260/A280 ratio was supposed to be between 1.8 and 2.0.

500 ng of RNA were used for reverse transcription into cDNA. For this, the Super Script First Strand Synthesis System for RT-PCR (Invitrogen, Carlsbad, USA) was used as described by the manufacturer. The primers were chosen to be Oligo-dTs for a more specific transcription of mRNA due to their property of binding the poly-adenylated tail of mRNA.

2.5.2 Principle and design of qPCR

The cDNA obtained was subsequently quantified using real time quantification based on dual-labelled probes, the so called TaqmanTM technology, first described by Lee et al. (Lee et al, 1993). The probes used in this method have their 5'-end labelled with a reporter dye (6-Carbofluorescein; FAM) and their 3'-end labelled with a quencher dye (6-Carboxy-tetramethylrhodamin; TAMRA), whereas the quencher dye alters the emitting frequency of the reporter dye upon excitation by UV-light. In the PCR process, the probe, which is placed behind the forward primer, becomes hydrolyzed by a 5' exonuclease-activity of the DNA-polymerase. This leads to a diverging of the two dyes altering the emitted sequence. This altered emission is increasing in the course of the PCR process, ideally it would reduplicate with each PCR-cycle. The increase of emission would therefore be directly proportional to the expression of the gene.

The design of the primers and probes was supported by the use of the software "ABI Primer Express" (Applied Biosystems, Foster City, USA), which considers melting temperature, base pair matching and secondary structure. The length of the amplicon was chosen to be smaller than 250 bp if possible and the probe's distance from the forward primer to be smaller than 50 bp for optimal reaction conditions. Additionally, the amplicon was designed to be exon-spanning, meaning that the forward and backward primer were placed on different exons and the probe on both these exons, which should have prevented emission if the cDNA had been contaminated by genomic DNA. The primers were checked for specificity by a normal PCR before the probes were ordered (MWG Biotech, Ebersberg, Germany).

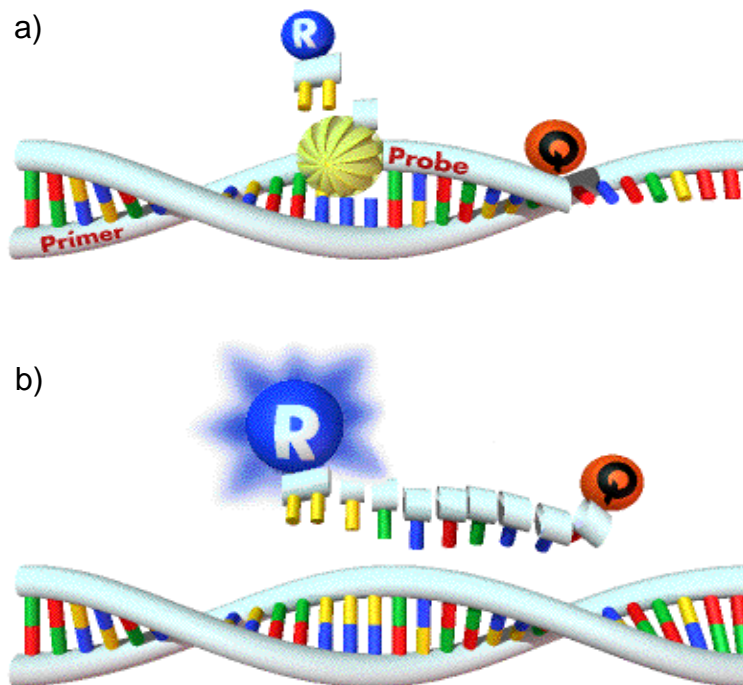


Figure 5: Principle of Taqman™-PCR: a) DNA-Polymerase hydrolyzing the dual-labelled probe; b) Reporter dye emitting after spatial separation from quencher dye. (7700 SDS Workshop, Thomas A. Schild)

Primers and probes used for qPCR:

Inhibitor 1a

Forward	5' GGCAACGGAAGAAGATGACAA 3'	T_m 63 °C
Probe	5' CACACCCACCATGAAAGACCTCCAGA	T_m 66.4 °C
Reverse	5' GCCCTAGGTGATGTTCAACAA 3'	T_m 64.6 °C

Inhibitor 1b

Forward	5' CCACGGAAGATCCAGTTTACG 3'	T_m 59.8 °C
Reverse	5' GACTGATCACTGGTCAGCACAA 3'	T_m 60.3 °C

ANP

Forward	5' GTGCGGTGTCCAACACAGAT 3'	T_m 59.4 °C
Probe	5' TGATGGATTTCAAGAACCTGCTAGACCACCTG 3'	T_m 68.2 °C
Reverse	5' GCTTCCTCAGTCTGCTCACTCA 3'	T_m 62.1 °C

BNP

Forward	5' CCAGTCTCCAGAGCAATTCAA 3'	T_m 57.9 °C
Probe	5' TGCAGAAGCTGCTGGAGCTGATAAGAGA 3'	T_m 66.6 °C
Reverse	5' AGCTGTCTCTGGGCCATTTTC 3'	T_m 59.4 °C

GAPDH

Forward	5' ATGTTCCAGTATGACTCCACTGACG 3'	T_m 57.9 °C
Probe	5' AAGCCCATCTTCCAGGAGCGAGAGCGAGA 3'	T_m 66.6 °C
Reverse	5' GAAGACACCAGTAGACTCCACGAC 3'	T_m 59.4 °C

2.5.3 qPCR procedure

The components of the reaction mixture are listed in table 2. The running protocol did not differ for the different genes and is displayed in table 3. The annealing and the extension step were combined into one common step. It is a property of the Taq-Polymerase to stabilize the binding of the primer to the reading strand. Since the probe is not stabilized in this way, the melting temperature of the probe was chosen to be at least 5 °C above that of the primer. This was to ensure the binding of the probe before replication started. The omission of the elongation step had the same reason, since the temperature would have reached values at which a separation of the probe from the reading strand had been eminent and a secure hydrolyzation had not been assured. For quantification, a small volume from each sample was used to create a common pool which was used to create a standard curve spanning five log-levels for each gene. The relative concentrations were normalized to GAPDH as an internal control. Each run included a no template control (NTC) to detect eventual contamination. ROX was added to the reaction mixture as a passive reference to balance minimal variances in pipetting. ROX is, like FAM and TAMRA, excited at 488 nm, but emits at 602 nm. The emission remains constant during the run and is only dependent on the amount of ROX used. ROX was acquired as “Standard Dye for Quantitative PCR” (Sigma, Munich, Germany) and was ready for use. All other reagents including the 384 well – plate were acquired from Applied Biosystems (Applied Biosystems, Foster City, USA). The PCR buffer and the 25 mM MgCl₂ were delivered along with the “AmpliTaq” Gold polymerase. 1 µl of cDNA was included in the reaction of 10 µl totally.

	GAPDH	I-1	ANP	BNP
10x PCR buffer	1 x	1 x	1 x	1 x
MgCl ₂	3 mM	3 mM	3 mM	3 mM
dNTPs (per nucleotide)	0.2 mM	0.2 mM	0.2 mM	0.2 mM
ROX	1%	1%	1%	1%
Taq – Polymerase	0.05 U/μl	0.05 U/μl	0.05 U/μl	0.05 U/μl
I-1 for		0.3 μM		
I-1 rev		0.9 μM		
I-1 probe		0.2 μM		
ANF for			0.6 μM	
ANF rev			0.4 μM	
ANF probe			0.2 μM	
BNP for				0.45 μM
BNP rev				0.45 μM
BNP probe				0.2 μM
GAPDH for	0.6 μM			
GAPDH rev	0.4 μM			
GAPDH probe	0.2 μM			
cDNA	10%	10%	10%	10%

Table 2: Components of the reaction mixture for qPCR

The reaction was performed on the “Abi Prism 7900HT Sequence Detection System” (Applied Biosystems, Foster City, USA). The subsequent evaluation was conducted with the “SDS 2.2” software.

Temperature	Time	Number of cycles
95 °C	10'	1
94 °C	15''	40
60 °C	1'	

Table 3: PCR-program for qPCR

2.6 Proteinbiochemistry

2.6.1 Protein extraction

The tissue used for the extraction of proteins was the basis of the heart. The tissue was powdered using a metal mortar which was continually cooled in liquid nitrogen. 40 mg of powder was taken up in eight times its weight of lysis buffer was subsequently homogenized. For this procedure the Tissue Lyser™ (Qiagen, Hilden, Germany) was used, in which the samples were shaken two times for 1 minute at 30 Hz after adding a small metal bead. Afterwards, the samples were centrifuged at 2000 rpm for two minutes.

Lysis buffer:

Tris	30 mM
EDTA	50 mM
NaF	30 mM
SDS	3%
Glycerol	10%

2.6.2 Quantification of protein using Bradford's method (Bradford. 1976)

Bradford's method is based on the principle of Coomassie brilliant blue shifting its absorption maximum in the presence of protein from 465 nm to 595 nm. The increase of absorption at 595 nm is linear to the increase of protein in the measured solution. The reagent used for the assay was Nanoquant (Roth, Karlsruhe, Germany). The standard curve was established using IgG as a standard protein. Therefore 10 mg of standard were diluted in 2.94 ml of distilled water, creating a solution with a protein concentration of 3.4 mg/ml. This standard was diluted 1:10 in 0.1 M sodium hydroxide. From this 7 different dilutions were generated (Table 4). The samples were mixed with 795 µl of 0.1 M sodium hydroxide, 5 µl of sample previously diluted 1:10 in 0.1 M sodium hydroxide, and 200 µl of reagent. All samples were incubated for 10 minutes before the absorption was measured in disposable cuvettes (Sarstedt, Nürnberg, Germany) with a spectrometer (Smart Spec® 3000, Bio Rad, Munich, Germany). The measured absorption allowed calculation of protein concentration using the Lambert-Beer law.

Standard Diluted 1:10	0 µl	5 µl	10 µl	20 µl	30 µl	40 µl	50 µl	60 µl
0.1 M NaOH	800 µl	795 µl	790 µl	780 µl	770 µl	760 µl	750 µl	740 µl
Bradford-reagent	200 µl	200 µl	200 µl	200 µl	200 µl	200 µl	200 µl	200 µl
Expected protein concentration	0 mg/ml	85 mg/ml	170 mg/ml	340 mg/ml	510 mg/ml	680 mg/ml	850 mg/ml	1020 mg/ml

Table 4: Bradford standard curve

2.6.3 SDS polyacrylamide gel electrophoresis

The electrophoresis is used to separate proteins according to their size. Principally electrophoresis would separate proteins according to their charge, but here it is different, because before the proteins are electrophorised, they are reacting with sodium dodecyl sulfate (SDS), which leads to a denaturation of the proteins' secondary and tertiary structures and a coating of these proteins with negative charges in proportion to the proteins' mass. Therefore, all proteins are theoretically affected by the same force, which renders the separation caused by the polyacrylamide gel the only remaining separation mechanism, therefore allowing the separation by size only.

One fifth of the volume of proteins homogenized in lysis buffer or loading buffer (Lämmli, 1970) was added and this mixture was heated at 95 °C for 5 min to achieve an additional destruction of secondary and tertiary structures.

Loading buffer according to Lämmli:

SDS	0.4 M
Bromphenolblue	1 mM
Glycerol	6.5 M
TRIS	0.6 M
DTT	0.6 M

A polyacrylamide gel is created utilizing the polymerization of acrylamide by free radicals, which in our case were delivered by ammonium persulfate. This reaction was catalyzed by TEMED (Bio Rad, Munich, Germany).

The gel electrophoresis method used was introduced by Lämmli (1970). It features a gel which consists of two parts having different properties. The lower part is the resolving gel. This may contain different acrylamide concentrations, whereas a higher concentration leads to smaller pores and a therefore slower electrophoresis. Resolving gels with different acrylamide concentrations were used according to protein size to provide an optimal separation.

Protein	Acrylamide
PLB	2.1 M
CSQ, GSK, PP1, PP2a	1.7 M
SERCA, cMyBP-C	1.4 M
RyR	0.8 M

Table 5: Acrylamide concentration of resolving gel for specific proteins

Resolving gel:

Tris	0.375 M pH 8.8
Acrylamide	see table 5
SDS	3.5 mM
Ammonium persulfate	4.4 mM
TEMED	2.4 μ M

After finally adding TEMED the solution was stirred and then uninterruptedly given into the prepared gel chambers, leaving a 2 cm margin at the upper part. To achieve a smooth and straight upper border, the gel was subsequently covered by a small amount of isopropanol.

After the resolving gel had been allowed to polymerize thoroughly the isopropanol was removed and the remaining space in the chamber was filled with stacking gel. A spacer was placed in the stacking gel to create slots for the subsequent loading of protein.

Stacking gel:

Tris	1.25 M pH 6.8
Acrylamide	0.73 M
SDS	3.5 mM
Ammonium persulfate	4.4 mM
TEMED	6 μ M

Electrophoresis Buffer:

Tris	125 mM
Glycin	192 mM
SDS	10 nM

The electrophoresis was carried out in electrophoresis module (Bio Rad, Munich, Germany), which was filled with electrophoresis buffer. 30-120 μ g of protein was loaded in its designated slot. One slot was loaded with 5 μ g of a protein standard (Bio Rad, Munich, Germany), which produced colored bands of a defined size on the gel. This was important, because it allowed to evaluate the protein's size later on. After the loading process was finished, the electrophoresis was started by application of 80 V for 10 min and subsequently 120 V for about 2 h, varying with the electrophorized protein and the resolving gel used.

The principle of discontinuing gel electrophoresis is based on the different properties of resolving and stacking gel. The lower pH stacking gel causes the glycine ion to be present as a dipolar ion, which is therefore running markedly slower than the proteins. The chloride ions of the Tris-buffer on the other hand run much faster due to their small size and negative charge. These two different ions form to running fronts between which a potential difference is created, leading to a trapping and accumulation of proteins in between both fronts. Additionally all proteins are running at the same speed in the stacking gel. In the resolving gel the glycine ion is transformed into a negatively charged ion, which runs faster than the proteins. This leads to a breakdown of the potential difference and the proteins are released from their "trap", being adjacently separated according to their size.

2.6.4 Transfer of proteins

After the proteins had been separated in the SDS polyacrylamide gel, they were blotted to either a nitrocellulose membrane (Protran®, Schleicher & Schüll, Dassel,

Germany; Towbin et al. 1978) or to a polyvinylidendifluorid membrane (Amersham Biosciences, Pittsburgh, PA, USA; Gültekin et al. 1988) in the case of PLB. A swelling of the gel was inhibited by methanol included in the transfer buffer. For blotting, the gel had to be positioned on the cathode's side and the membrane on the anode's side. The blotting chamber (Bio Rad, Munich, Germany) was filled with the appropriate, 4 °C cold transfer buffer.

Transfer buffer I was used for proteins smaller than 75 kD. The transfer was usually conducted at 0.4 A for 75 min, just in case of RyR it was conducted at 45 V for 16 h.

Transfer buffer I:

Tris	25 mM
Glycine	192 mM
Methanol	12.5 M

Transfer buffer II:

Tris	50 mM
Glycine	360 mM
SDS	0.1%
Methanol	6.5 M

2.6.5 Further handling of the membrane

To visualize the transferred proteins, the membrane was stained with Ponceau S and the colored bands of the protein standard were permanently marked for further use. After incubation of the membrane with Ponceau S for 5 min, the membrane was washed with distilled water, which removes unbound dye but does not affect dye bound to proteins. After using the colored membrane (e.g. to take a picture), the dye was removed by washing the membrane with TBS including TWEEN 20 (Sigma, Munich, Germany; TBST).

TBST 0.1% (pH 7.5)

Tris	0.1 M
NaCl	0.15 M
Tween 20	0.9 mM

Ponceau S solution

Ponceau S	26 mM
TCA	30 mM

The blocking was conducted to prevent interactions between the membrane and the antibody used for detection of the target protein. Blocking of non-specific binding was achieved by placing the membrane in a 5% non-fat dry milk (Roth, Karlsruhe,

Germany) in TBST solution, where the protein of the milk attached to the non-specific binding sites. The membrane remained in this blocking solution for 1 h at room temperature while being softly shaken continually. Subsequently, the membrane was washed in TBST 4 times for 5 min each.

The incubation with the primary, protein-specific antibody was usually carried out overnight at 4 °C while being softly shaken. Then the membrane was washed in TBST 4 times for 5 min each and the incubation with the secondary was carried out at room temperature for 1 h. The secondary antibody, which was soluted in 5% non-fat dry milk in TBST, was directed against the primary antibody, which was, varying with the primary antibody, either anti-mouse, -goat or -rabbit, and was labeled with horseradish peroxidase. Finally, the membrane was again washed in TBST 4 times for 5 min each.

The membrane was incubated with the Western blot detection kit ECL or ECL-Dura (both Pierce Biotechnology, Rockford, IL, USA) for 5 min, which contains a substrate for the peroxidase, creating a chemoluminescence. For visualization, films (Hyperfilm ECL, Amersham Pharmacia Biotech, Freiburg, Germany) were illuminated for 1-30 min and subsequently developed. All total protein levels were normalized to the CSQ protein level, while the phosphorylated proteins were normalized to their total protein with the exception of TnI-Ser23/24 and RyR-Ser2809, which were also normalized to CSQ, since no adequate quantification of the total protein could be obtained due to technical difficulties.

	Dilution	Size of Protein (kD)	2 nd Antibody	Manufacturer
Phospholamban total	1:5000	7	Anti-Mouse 1:10000	Badrilla
PLB-Ser16	1:5000	7	Anti-Rabbit 1:5000	Badrilla
Calsequestrin	1:2500	53	Anti-Rabbit 1:10000	Dianova
Serca2a	1:500	100	Anti-Goat 1:10000	Santa Cruz
Protein phosphatase 1	1:500	30	Anti-Rabbit 1:5000	Upstate
GSK-3 β Ser9	1:2500	46	Anti-Rabbit 1:5000	Cell Signaling
GSK-3 β total	1:2500	46	Anti-Mouse 1:5000	BD Transduction Labs
cTnl-Ser22/23	1:1000	30	Anti-Rabbit 1:10000	Cell Signaling
cMyBP-C	1:1000	150	Anti-Rabbit 1:5000	Kind gift Dr. Linke
cMyBP-C phospho	1:2000	150	Anti-Rabbit 1:5000	Kind gift Dr. Carrier

Table 6: Antibodies used for Immunoblotting

2.7 Histological Analysis

As previously described, the central of three transversal slices of the ventricle was used for histological purposes. Therefore the cuts were fixed in 4% of formalin for one night, subsequently washed in PBS for one night and then they were dehydrated in ascending concentrations of isopropanol. After dehydration they were embedded in paraffin.

PBS:

NaCl	13.7 mM
Na ₂ HPO ₄	652 µM
KH ₂ PO ₄	147 µM
KCL	268 µM

Medium	Time	Temperature
70% Isopropanol	2 – 3 hours	Room temperature
80% Isopropanol	2 – 3 hours	Room temperature
96% Isopropanol I	2 – 3 hours	Room temperature
96% Isopropanol II	2 – 3 hours	Room temperature
100% Isopropanol I	2 – 3 hours	Room temperature
100% Isopropanol II	2 – 3 hours	Room temperature
100% Isopropanol III	1 hour	60 °C
Paraffin/Isopropanol	1 hour	60 °C
Paraffin I	2 hours	60 °C
Paraffin II	2 hours	60 °C
Paraffin III	2 hours	60 °C
Embedding in Paraffin		60 °C

Table 7: Protocol of tissue embedding

Medium	Time	Medium(continued)	Time
Xylol I	15 min	Tab water, running	10 min
Xylol II	15 min	Aqua dest.	rinse
100% Ethanol I	5 min	Eosin	10 min
100% Ethanol II	5 min	Aqua dest.	rinse briefly
96% Ethanol I	5 min	96% Ethanol I	rinse briefly
96% Ethanol II	5 min	96% Ethanol II	rinse briefly
80% Ethanol	5 min	100% Ethanol I	rinse briefly
70% Ethanol	5 min	100% Ethanol II	rinse briefly
Aqua dest.	5 min	Xylol	3 – 5 min
Hemalaun (Mayer)	20 min		

Table 8: Staining procedures of histology slices

Hemalaun – solution:

Hematoxylin	1%
NaJO ₃	0.2%
KAl(SO ₄) ₂	50%
Chloral hydrate	50%
Citric Acid	1%

Eosin – solution:

Eosin Y	1%
---------	----

After the paraffin had hardened the blocks were cut into 4 µm thick slices parallel to the heart's base using a rotary microtome (Leica, Wetzlar, Germany). The slices were stretched in an about 45 °C warm water bath before placing them on object plates (HistoBond®, Marienfeld, Lauda-Königshofen, Germany).

The tissue slices were freed from paraffin using xylol and hydrated in descending concentrations of ethanol, stained either with hematoxylin-eosin (HE) and repeatedly dehydrated in xylol and covered using Eukitt (O. Kindler, Freiburg, Germany).

For the determination of cell area the HE stained slices were used, which were made in the following fashion: 4 consecutive slices of 4 µm thickness were made, then a distance of 50 µm was cut and discarded, thereby assessing different bundles of cardiac myocytes. This was repeated twice so that 4 slices from 3 different heights, 12 slices altogether, were used for analysis. For this the slices were examined at x320 magnification with a light microscope (Zeiss-Axioplan IM-35, Oberkochen, Germany). Cells from the left ventricle which had a round nucleus and were as round as possible, meaning they had been cut in the horizontal plane, were identified and a picture was taken (Zeiss-Axiocam, Oberkochen, Germany). The cell area was measured using the program Axiovison.

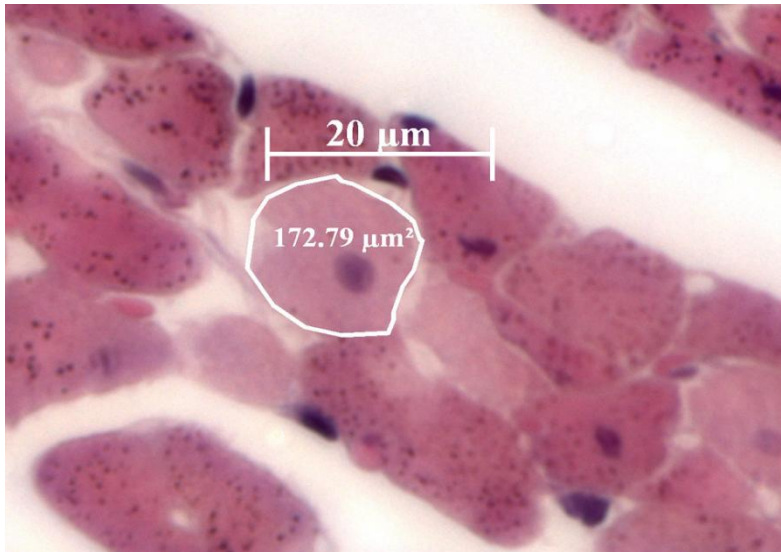


Figure 6: Example of cell used for area measurement

2.8 Statistic analysis

Data are reported as mean \pm S.E.M. Statistical differences between the groups of mice (WT^{Sham} , WT^{TAC} , KO^{Sham} , KO^{TAC}) were either calculated by Student's T-Test or Two-way ANOVA. Survival analysis of WT^{TAC} versus KO^{TAC} was calculated by the Kaplan-Meier method. Correlations were calculated using the Pearson product-moment correlation coefficient. $P < 0.05$ was considered to be significant.

3 Results

3.1 Baseline cardiac function and morphology assessed by echocardiography

All mice (age and sex-matched, WT n=21, KO n=21, unless indicated otherwise) were subjected to echocardiography before any manipulations were undertaken therefore allowing a comparison of baseline parameters. Selected findings are illustrated in figure 7.

Left ventricular mass (LVM) was comparable with a medium size of 126 ± 6 mg in WT and 122 ± 5 mg in KO. A correlation to the actually measured HW showed a significant correlation ($r^2 = 0.91$; $p < 0.0001$), therewith validating the quality of the echocardiographic measurements also for other parameters.

The FAS and FS were determined as parameters for contractility. The FAS was $52\pm 1\%$ in WT and $50\pm 2\%$ in KO. FS measured from B-Mode recordings was $31\pm 1\%$ in WT and $29\pm 1\%$ in KO, while FS measured from M-Mode recordings was $33\pm 2\%$ in WT and $33\pm 1\%$ in KO. The differences between the groups were not significant, indicating that the knockout of inhibitor does not affect baseline contractility. Additionally it could be observed that the measurement of FS by M-Mode recordings yielded significantly higher results ($p < 0.05$) than FS calculated by B-Mode recordings, where FS from B-Mode recordings was $30\pm 1\%$ and from M-Mode was $33\pm 1\%$. The FS and FAS shown in this report have usually been evaluated from B-Mode recordings unless explicitly stated otherwise.

The LVEDV and LVESV were also determined, since these parameters might indicate possible diastolic or systolic dysfunctions. LVEDV was 100 ± 4 μ l in WT and 103 ± 4 μ l in KO. The LVESV was 41 ± 3 μ l in WT and 45 ± 3 μ l in KO, and the EF was $57\pm 2\%$ in WT and $56\pm 1\%$ in KO. None of these values varied significantly.

The cardiac index indicating CO was also determined to assess possible differences, but with 768 ± 47 ml/min/kg in WT mice and 824 ± 55 ml/min/kg in KO mice no significant differences were detected.

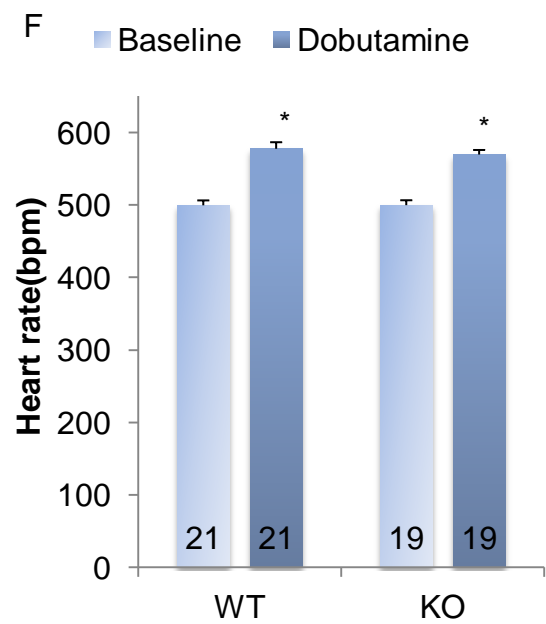
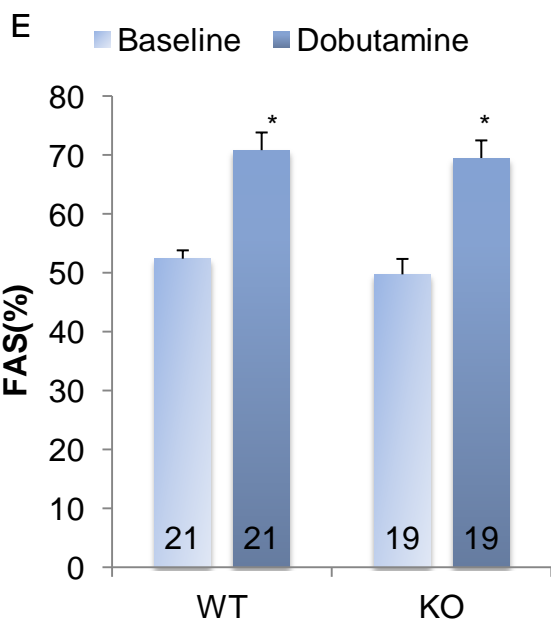
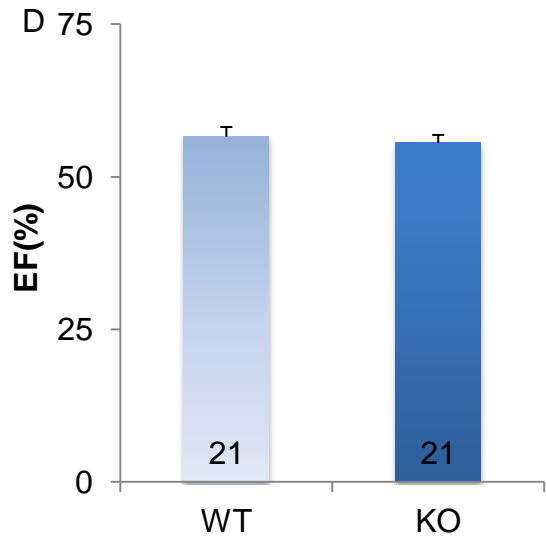
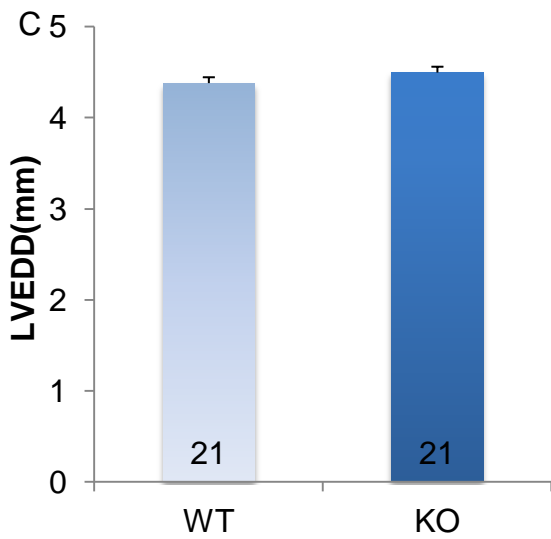
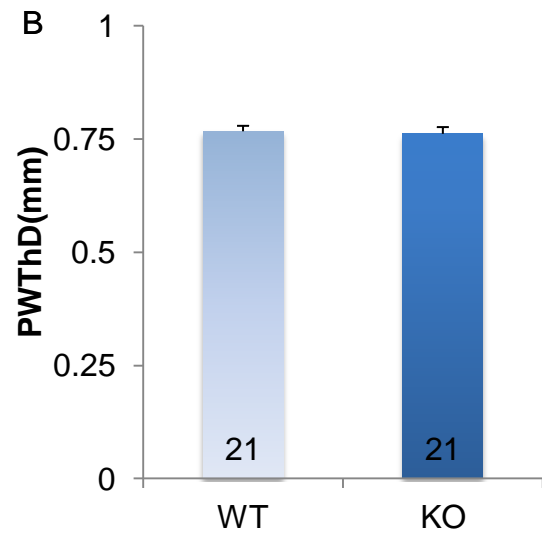
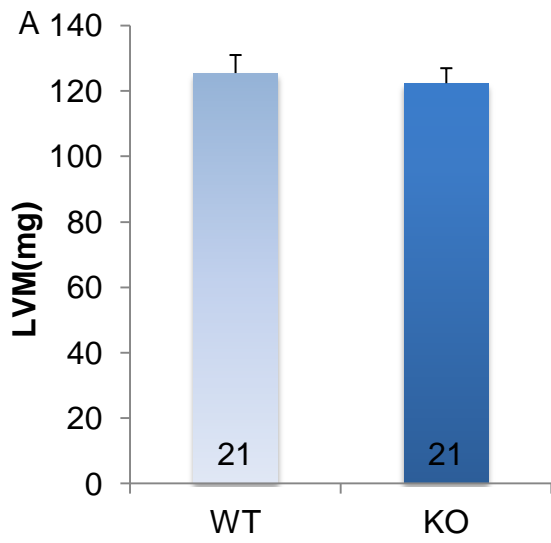
For a further morphologic analysis posterior wall thickness in diastole (PWThd) and left ventricular end-diastolic diameter (LVEDD) were evaluated. The PWThd was

0.77±0.01 mm in WT and 0.76±0.01 mm in KO. The LVEDD was 4.4±0.1 mm in WT and 4.5±0.1 mm in the KO, also revealing no difference.

Taken together, echocardiography revealed neither functional nor morphological differences between WT and KO at baseline.

To assess whether the *knockout* of I-1 as an element of the β -adrenergic signaling cascade might have an influence during the stimulation of this cascade, mice were injected dobutamine for this very purpose. Dobutamine increased heart rate similarly in both lines by a comparable amount from i.e. 500±7 bpm to 578±9 bpm in WT and from 500±7 bpm to 570±6 bpm in KO, with the increase itself being highly significant ($p < 0.001$). FAS rose about 56% to 71±3% in WT and 70±3% in KO, FS from about 33% to 46±2% in WT and 43±3% in KO, which indicates a comparable, in itself highly significant increase.

To sum these results up, a difference between WT and KO mice was not detectable neither at baseline nor in dobutamine-stimulated healthy mice.



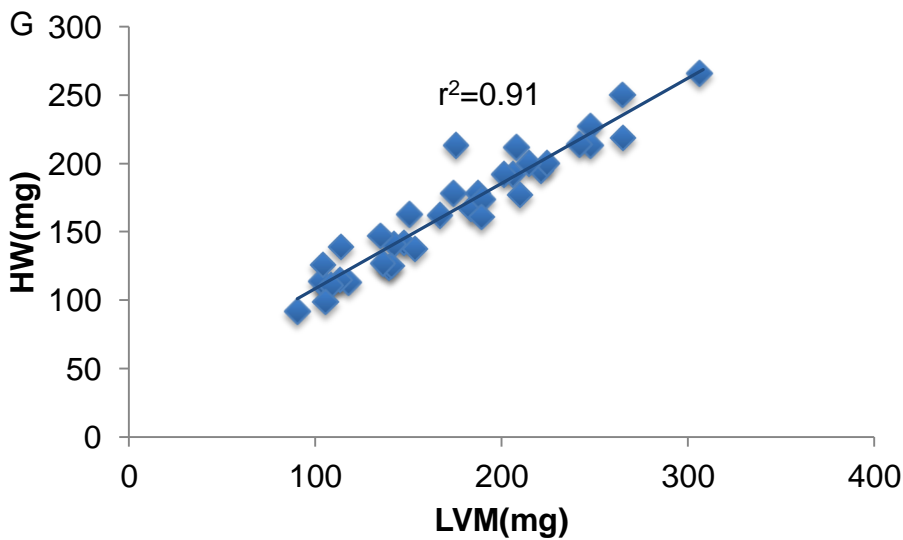


Figure 7: Cardiac morphology and function assessed by echocardiography detected no major differences between WT and KO in morphological parameters as **(A)** LVW, **(B)** PWThd and **(C)** LVEDD as well as in functional parameters like **(D)** EF, **(E)** FAS native and dobutamine stimulated and **(F)** heart rate native and dobutamine stimulated. **(G)** Illustrates the good correlation between LVM assessed by echocardiography and HW assessed by autopsy. * $P < 0.05$ Dobutamine compared to native.

3.2 Baseline cardiac function assessed by left heart catheter

To further investigate cardiac function in WT and I-1 KO mice, selected mice were subjected to a left heart catheter study. The results of this study have been published previous to the completion of this thesis by El-Armouche et al. (2008). 7 WT and 7 KO age- and sex-matched mice were used for this study. Left heart catheterization allowed both the control of the accuracy of measurements made by echocardiography as well as the assessment of parameters not measurable by echocardiography.

Heart rate was 611 ± 16 bpm in WT mice and 639 ± 11 bpm in I-1 KO mice. Left ventricular volume in diastole was 18 ± 2 μ l in WT and 18 ± 2 μ l in I-1 KO mice whereas left ventricular systolic volume was 9 ± 2 μ l in WT and 8 ± 1 μ l in KO mice. All differences were non-significant ($p > 0.05$).

Functional parameters were also assessed. CO as a parameter for work revealed an output of 7361 ± 670 μ l \cdot min $^{-1}$ in WT mice and 7447 ± 799 μ l \cdot min $^{-1}$ in KO mice and was

therefore not significantly different as was dp/dt_{max} as a parameter for contractility with values of 10841 ± 747 mmHg*s⁻¹ in WT mice and 10710 ± 702 mmHg*s⁻¹. No significant difference could also be seen in relaxation, dp/dt_{min} being -9351 ± 507 mmHg*s⁻¹ in WT mice and -9936 ± 236 mmHg*s⁻¹ in KO mice.

Heart catheterization therefore supported the findings made by echocardiography, pointing to a lack of differences in cardiac morphology or function at baseline.

3.3 Transverse aortic constriction using a 25G needle

The baseline analysis revealed results which already were in discordance to the results shown by another group (Carr et al. 2002). This made the comparison of *wildtype* and *knockout* mice even more compelling. In a first approach mice were subjected to a TAC procedure using a 25G needle, which leads to an aortic constriction of 40-50%. This method has previously been used by Rogers et al. (1999) and resulted in less acute mortality, which was seen as an advantage at the beginning of this study. Following the intervention mice were subjected to repeated echocardiographic controls on the 7th, 17th and immediately before sacrifice on the 25th day after the intervention.

3.3.1 Survival

In this first series a difference in the mortality rates between the groups was not observed, since mortality itself was extremely low. Only one KO^{TAC} mouse died on day 6 after the intervention (data not shown). The intended low mortality rate had therefore been reached.

3.3.2 Comparable development of a minor cardiac hypertrophy

After the intervention a slight increase in LVM/BW-ratio was observed in both groups, amounting to 29.1% in the WT^{TAC} and 17.9% in the KO^{TAC} group on day 7 (see Figure 8A). The LVM stagnated on this level since the increase on day 17 was 21.9% in WT and 17.2% in KO and on day 25 was 29.3% in WT and 22.5% in KO. Despite the relatively small differences and the small number of subjects (n=5 in WT^{Sham} and KO^{TAC}, n = 3 WT^{TAC} and KO^{Sham}) a significant difference was observed between the WT^{Sham} and WT^{TAC} group (p = 0.03) and an almost significant difference was seen between KO^{Sham} and KO^{TAC} (p=0.05). The LVM/TL-ratio exhibited a similar trend

showing a non-significant increase in both TAC groups on day 25 (data not shown). Since the hypertrophy did not progress any further after day 7, it was decided to sacrifice the mice on day 25.

The autopsy results confirmed, as expected, the findings made by echocardiography (see Figure 8B). The WT^{TAC} group exhibited a HW/BW-ratio of 5.6 ± 0.2 mg/g opposed to 4.8 ± 0.1 mg/g in WT Sham ($p < 0.01$, see above for n). Similar results were seen in the KO group, where HW/BW ratio in TAC was 5.8 ± 0.6 mg/g and 4.8 ± 0.6 mg/g in Sham ($p < 0.05$). Taken together the HW/TL-ratio showed a similar trend, but the differences were not significant. The intervention with a 25G needle caused a significant hypertrophy of about 20% in both groups but revealed no differences between WT and KO.

Besides this it was remarkable that the amount of hypertrophy massively differed between the individual animals of identical groups. This might have been caused by slight differences in the stenosis-diameter, which unfortunately had not been assessed in this study. One might suspect that a certain degree of stenosis might not lead to a significant hypertrophy and that this threshold value of stenosis had not been reached in all mice.

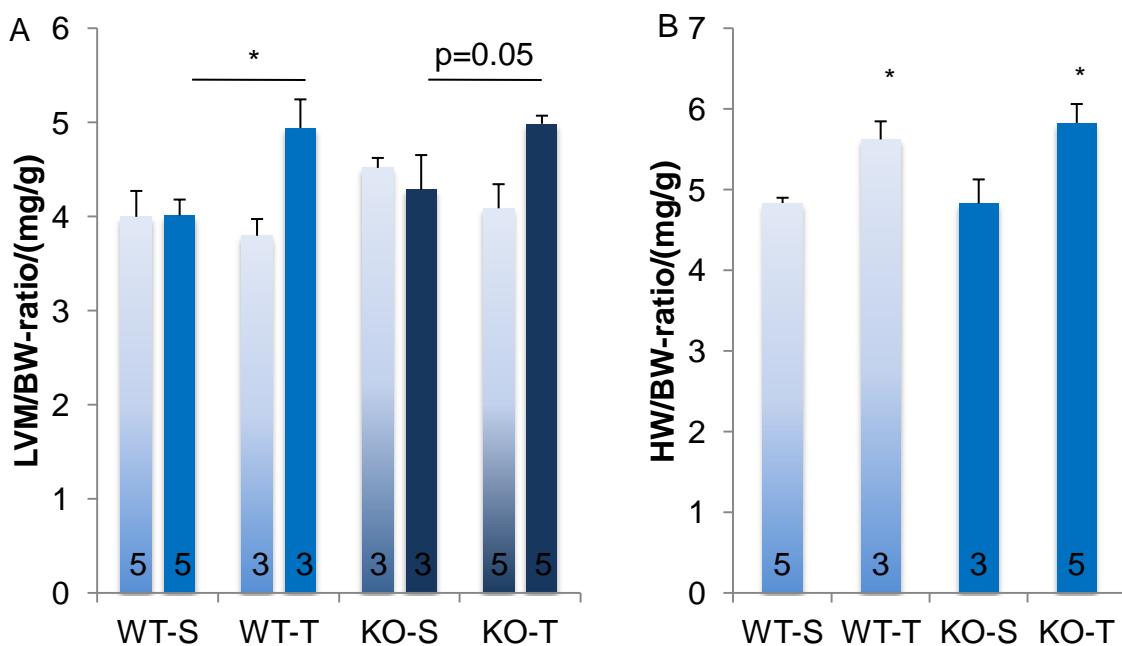


Figure 8: (A) LVM/BW-ratio recorded before TAC and on day 25 after TAC with a 25G needle; (B) HW/BW-ratio measured determined by autopsy. * $P < 0.05$ TAC compared to WT.

3.3.3 I-1 KO mice exhibited worse recovery of cardiac function

Apart from morphological parameters, functional consequences were of high interest. FAS dropped in both TAC groups had dropped by a comparable degree by day 7. In the WT^{TAC} group FAS decreased from 47.8±4.5% before intervention to 41.7±2.8% on day 7 ($p = 0.31$), in the KO^{TAC} group from 44.8±2.6% to 35.9±3.0% ($p = 0.05$; data not shown). This finding remained almost identical on day 17, up to which no recovery of cardiac function was observed. On day 25 however, FAS in the WT^{TAC} group was 50.5±3.3% and had therefore recovered to baseline level, while in the KO^{TAC} group FAS remained low with a value of 38.0±2.5% compared to the timepoint before intervention but did not reach statistical significance. A comparison between the WT^{TAC} and KO^{TAC} groups conducted with 2-way ANOVA did not yield any significant differences (see Figure 9A). The assessment of lung weight showed comparable results in all groups (data not shown), which argued against a massive cardiac failure in either subgroup, since no pulmonary congestion was observed.

The dobutamine response was not determined on day 7 and 17, therefore preventing an evaluation of the course and only allowing an endpoint analysis. The dobutamine-stimulated FAS before TAC intervention was 63.1±1.1% in WT^{TAC} and 71.2±2.8% in KO^{TAC}. The WT^{TAC} group exhibited a comparable value of 65.8±2.7% on day 25, while the KO^{TAC} group still seemed to show a depressed dobutamine response, the FAS being 58.6±5.6%. The difference was not being significant though ($p = 0.12$). Regarding that the baseline FAS was still diminished in KO^{TAC}, an analysis of the gain of contractility in response to dobutamine was used, revealing no major differences ($p=0.34$) (see Figure 9B).

Summing this up a comparable decrease in contractility was observed in both groups up to day 17. After this a recovery of the contractility was seen in the WT^{TAC} mice, and such a recovery has been previously reported (Nakamura et al. 2001), while the KO^{TAC} mice seemed to remain depressed in their baseline contractility but not in their dobutamine response. At the time of sacrifice mice were not in a state of acute HF, but in a state of balanced hypertrophy.

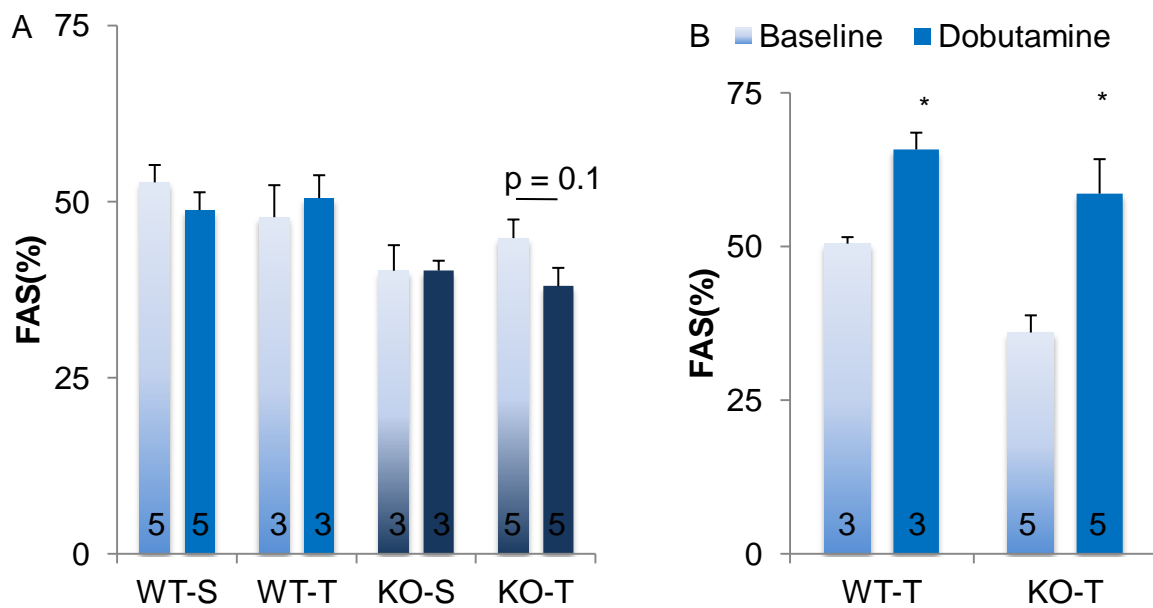


Figure 9: No recovery of FAS was seen in KO^{TAC} on day 25 after TAC (A), but an equally strong response to Dobutamine stimulation was seen at this time (B). * $P < 0.05$ WT^{TAC} vs. KO^{TAC} .

3.3.4 Induction of hypertrophy was confirmed on a molecular level

For the identification of non-physiologic hypertrophy on a molecular level the ventricular expression of atrial natriuretic factor (ANF) and brain natriuretic peptide (BNP) mRNA was analyzed. These genes, along with others like β -MHC i.e., have been reported to be overexpressed in the ventricle in the course of a return to a fetal genetic programme in HF (Mercadier et al. 1989; Rockman et al. 1991; Nishigaki et al. 1996).

The levels of ANF mRNA approximately increased by a factor of two in both WT^{TAC} and KO^{TAC} mice ($p < 0.05$). The KO^{TAC} group had a slightly lower baseline level (see Figure 10A). This was quite low and in accordance to the mild hypertrophy observed. BNP baseline levels were almost identical in both groups, and the increase in both groups was also significant, but the relative increase tended to be higher in the WT group after TAC ($p = 0.08$) (see figure 10B).

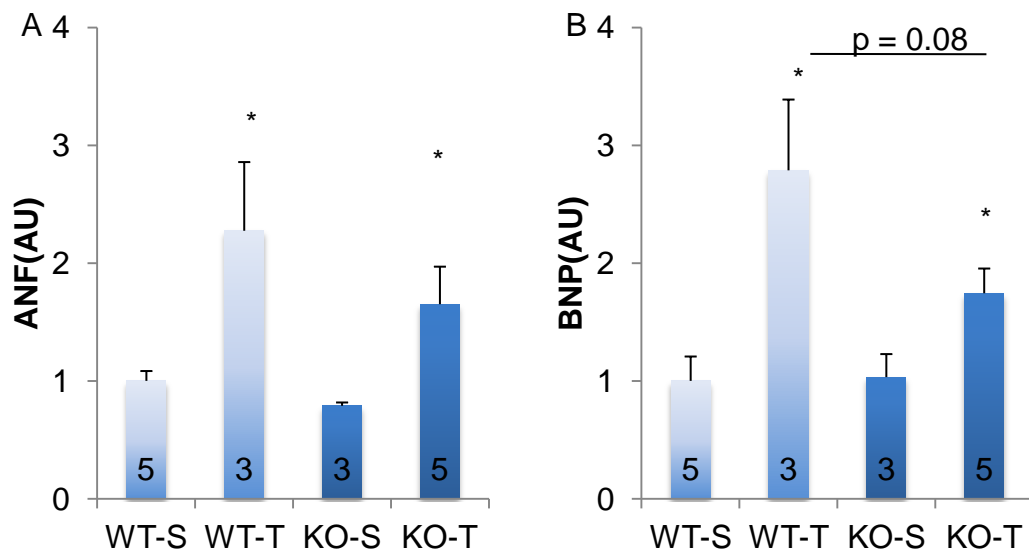


Figure 10: Higher levels of **(A)** ANP and **(B)** BNP were observed in both TAC groups. * P < 0.05 TAC vs. Sham.

3.3.5 mRNA assessment of I-1 revealed higher levels of I-1 mRNA

Transcript levels of I-1 in WT tended to be upregulated by 40% ($p = 0.24$; see Figure 11). This was an unexpected finding, since numerous reports (e.g. El-Armouche et al. 2008) showed a decrease of I-1 mRNA in HF. This probably indicates on another level that these mice with the 25G TAC intervention had not reached HF. Instead these mice had probably reached a state of compensated hypertrophy at the time point of sacrifice. In this setting, I-1 mRNA levels were at either unaltered or elevated, which by itself is an interesting finding and could be a matter of investigation in the future.

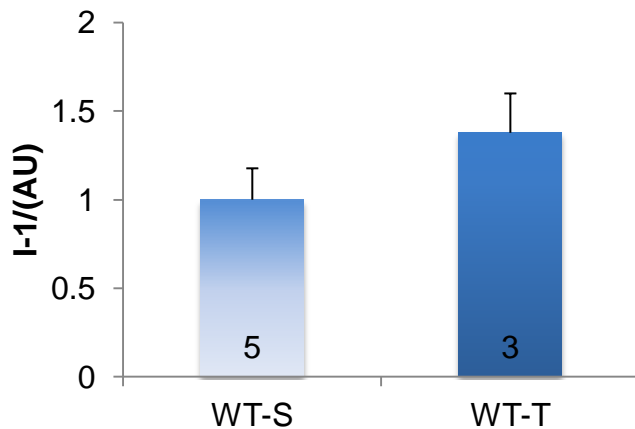


Figure 11: I-1 mRNA levels after 25G intervention in WT mice. In a state of balanced hypertrophy, I-1 mRNA levels are at least stable.

3.3.6 Transverse aortic constriction using a 27G needle

Due to the small effects observed when using a 25G needle, it was decided to conduct further series with a more marked stenosis which was achieved by using a 27G needle, which caused a stenosis to 0.4 mm in diameter, which was 0.1 mm more than in the 25G experiment. This would possibly result in an increased pressure gradient over the stenosis, since the stenosis expected with a 27G was about 60-70%, and supposedly bring the mice into a stage of HF and not compensated hypertrophy as previously seen. A further advantage of using the 27G needle is the better comparability to the previously mentioned report by Pathak et al. (2005).

3.3.7 Higher mortality rate in I-1 KO^{TAC} mice

Previous studies reported mortality rates of 20-25% after the TAC procedure, omitting intra-operative casualties and depending on the mouse strain, age, sex and amount of constriction (Rockman et al. 1991; Nakamura et al. 2001; Zhou et al. 2004) A comparable mortality rate was, to some extent, aimed for in this experiment, since this served as an indicator for a sufficient amount of stenosis.

For the C57BL6/J mice (WT), this was principally achieved, at least in male mice. Here the postoperative mortality over 8 days was 4 out of 15, resulting in a survival of 73.5%, which principally reflects the known data (see Figure 14B). Two of the mice died on the first and third postoperative day respectively. From the operated female WT mice only 4 out of 7 operated animals survived up to day 8 (see Figure 14C). Two mice died on the first and one on the third day. This difference in survival

between the sexes was significant ($p = 0.03$). This was especially surprising since the amount of stenosis in female mice was relatively smaller, as their aortic diameter is smaller and therefore the decrease in diameter was less pronounced. Due to the significant difference in mortality, it was decided to assess further parameters in a gender-specific way.

A similar result was expected in the I-1 knockout (KO) mice group. Nevertheless only 5 out of 15 operated male KO mice survived up to day 8, resulting in a survival percentage of 33.3% (see Figure 14B). From the 10 mice which died six died on the first, two on the third, one on the sixth and one on the seventh day. In the females, 6 out of 9 operated mice survived, with two casualties occurring on the first and one on the seventh day (see Figure 14C), but from the surviving mice 3 were in a disastrous nutritional status having lost more than 20% of their preoperative weight and it is likely that they would not have survived much longer (exclusion criteria are listed later). The difference between the sexes in the KO group was therefore non-significant.

Overall, this projects into a survival rate of 63.6% in the WT and of 45.8% in the KO group. The difference in itself was not significant ($p=0.10$) (see Figure 14A). What was interesting was the time point of deaths. No WT mouse, female or male, died after the third postoperative day, while the KO mice died even beyond that time point. Therefore, the survival up to the third postoperative day between both groups was absolutely comparable ($p=0.42$), while survival after the third postoperative day showed a significant difference with a survival advantage for the WT group ($p=0.03$).

A subgroup analysis according to gender revealed quite interesting findings. In the female subgroup a rather similar mortality rate was observed while in the male subgroup a significantly larger mortality was seen in KO^{TAC} mice ($p=0.03$). This might contribute to a better comparability of the surviving female mice, since one could suspect a slight bias toward a better cardiac function in the male KO^{TAC} mice.

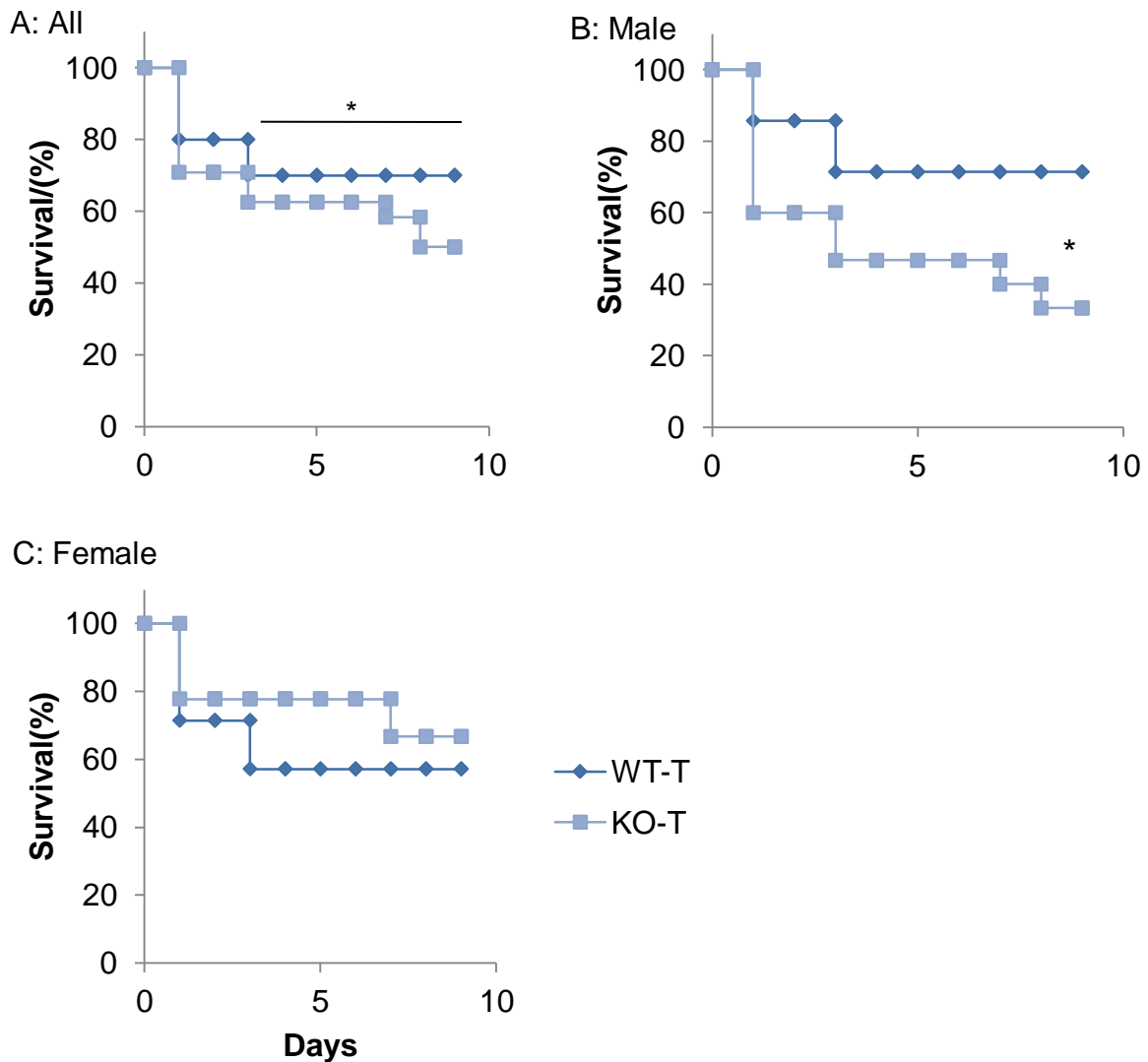


Figure 14: Survival curves after TAC with a 27G needle: **(A)** All, **(B)** male and **(C)** female mice. In **(A)**, a significant difference in survival after day three was seen. * $P < 0.05$ between KO and WT.

3.3.8 All mice exhibited a massive heart failure on day 8 after intervention

The first echocardiographic assessment of mice was conducted on day 8 after the intervention. The mice which had been subjected to TAC showed a massive decrease in contractility. Considering the massive mortality in the KO group it was decided to terminate the study at this point for ethical reasons and because even more mice were expected to die, which would have been useless for the study.

3.3.9 Hypertrophy was attenuated in male KO^{TAC} mice

The autopsy results revealed a massive increase of heart weight in WT^{TAC} as well as in KO^{TAC} mice, exactly like it was predicted by echocardiographic assessment. The HW/TL-ratio in the WT^{TAC} group was 11.8±0.4 mg/mm, compared with 7.7±0.3 mg/mm in WT^{Sham} mice. In the KO^{TAC} group it was 11.4±0.2 mg/mm compared to 8.0±0.3 mg/mm in KO^{Sham} mice. Therefore the increase in each group was highly significant ($p < 0.001$; see Figure 15A). As previously mentioned it has to be noted that three female mice from the KO^{TAC} group had been excluded from the analysis due to a postoperative weight loss of more than 25%, which was decided to be the cut off point for postoperative weight loss. A difference between WT^{TAC} and KO^{TAC} in the amount of hypertrophy was not seen. These findings were in accordance to LVM calculated from the echocardiographic findings recorded (see Figure 15B).

A subdivision into female and male mice revealed an interesting finding. In male mice the HW/TL-ratio in TAC mice reached 13.8±0.8 mg/mm (n=9) in WT^{TAC} but only 11.6±0.5 mg/mm (n=6) in KO^{TAC} (see Figure 16A), revealing a significantly smaller ratio in KO^{TAC} mice ($p < 0.05$). These findings were principally supported by echocardiography (data not shown).

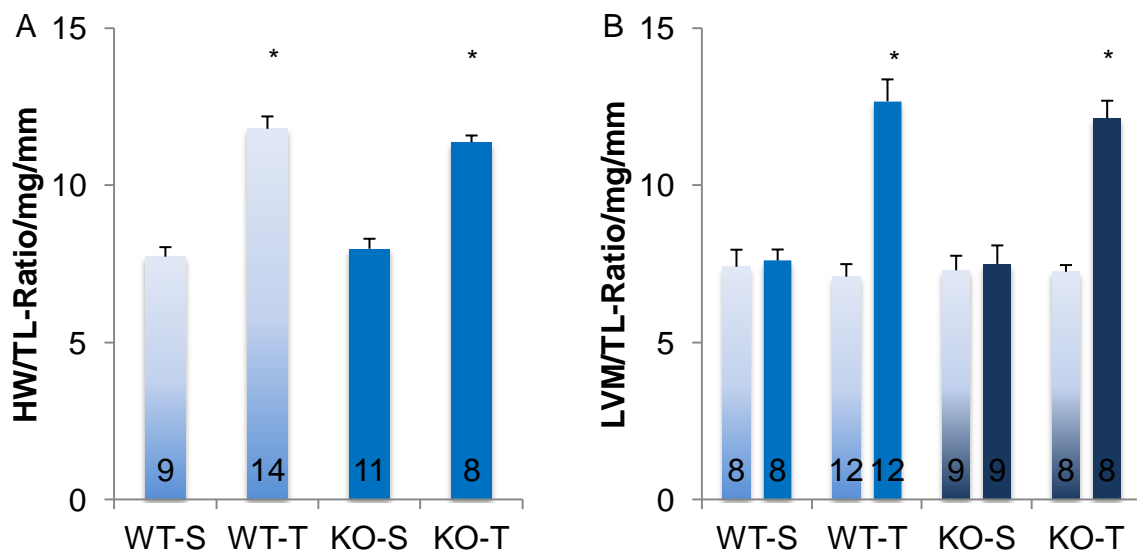


Figure 15: (A): HW/TL-ratio in all mice sacrificed on day 8 after TAC with a 27G needle; **(B):** LVM/TL-ratio of the same animals determined by echocardiography before TAC and briefly before sacrifice. * $P < 0.001$ TAC vs. Sham.

In female mice, where no difference in survival was observed, no significant differences were observed. If anything, a minor trend for less hypertrophy in WT^{TAC}

was seen, HW/TL-ratio being 10.4 ± 0.3 mg/mm in WT^{TAC} (n=4) and 11.1 ± 0.3 (n=3) in KO^{TAC} (p=0.16; see Figure 16B).

Another observation made was that HW/TL-ratio in male WT^{TAC} mice was significantly higher than in female WT^{TAC} mice (p < 0.05), which was not the case for KO^{TAC} mice.

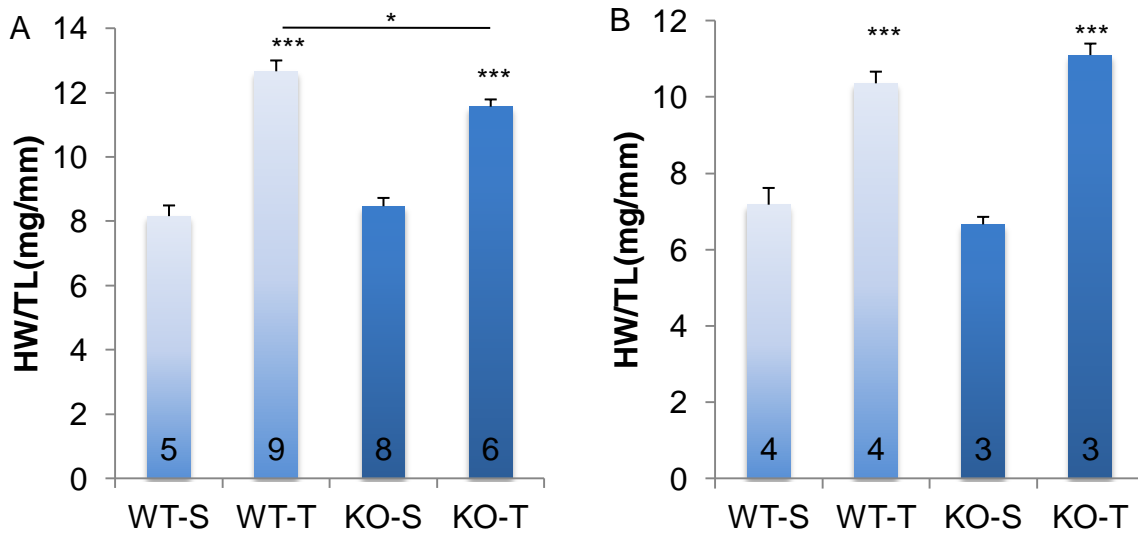


Figure 16: HW/TL-ratio in male (A) and female (B) mice after TAC. *** P < 0.001 Sham vs. TAC; * P < 0.05 WT^{TAC} vs. KO^{TAC} .

Echocardiographic parameters were also used to illustrate the development of hypertrophy and the form of hypertrophy. The anterior and posterior wall thicknesses as well as the left ventricular end-diastolic diameter were evaluated to determine the form of hypertrophy. The increase in AWThd and PWThd was distinct in both groups undergoing TAC, being about 45%, but there was neither a difference between the groups, nor between the sexes (see Figure 17). A significant, although small increase in LVEDD was detected in the WT^{TAC} group, but the credibility of this finding was reduced by the fact that a similar increase was also seen in the WT^{Sham} group. No differences were seen between the sexes. Taken together, the hypertrophy after 27G TAC appeared to be of a concentric, non-dilated type.

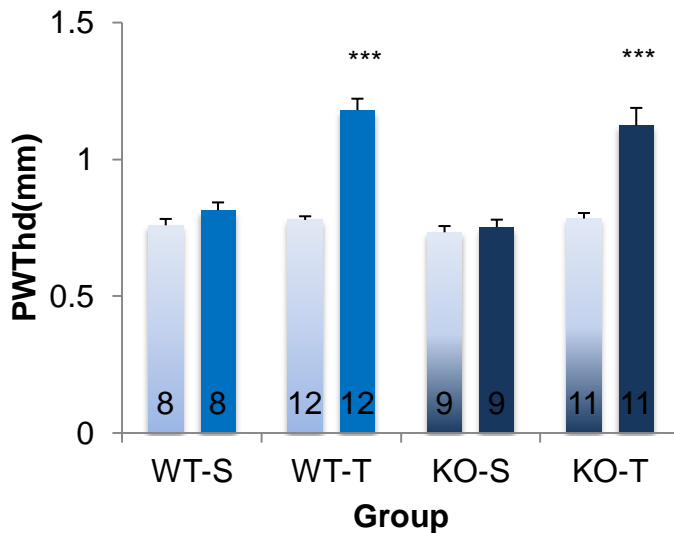


Figure 17: PWThd was assessed, indicating a symmetrical, non-dilated hypertrophy. *** P < 0.001 before vs. after TAC.

3.3.10 Contractility was equally diminished in WT^{TAC} and KO^{TAC} , while dobutamine response seemed to be slightly attenuated in KO^{TAC}

As described above a massive decrease in contractility was observed in both groups which underwent the TAC procedure. While FAS remained unchanged in both Sham groups, FAS in WT^{TAC} decreased from $52.0 \pm 1.8\%$ before TAC to $25.5 \pm 2.3\%$ (n=12) on day 8 (see Figure 18). A comparable drop in FAS was seen in KO^{TAC} , here it dropped from $50.5 \pm 2.7\%$ to $22.3 \pm 1.9\%$ (n=8). Similar values were obtained in FS measurements (data not shown). A sex-separated analysis did not reveal differences.

The EF was used as another parameter to assess contractility, since it additionally takes the contraction in the long axis into account. As in FAS no major differences, despite a massive reduction after the intervention, were observed between the groups in the overall evaluation. The EF in WT^{TAC} mice dropped to $30.7 \pm 2.3\%$ from previously $56.6 \pm 1.8\%$, (n=12) and in KO^{TAC} it dropped to $27.2 \pm 1.8\%$ (n=8) from $54.8 \pm 2.5\%$ (p=0.6). No major differences were seen between the sexes, but EF tended to drop even stronger in female KO^{TAC} than in male.

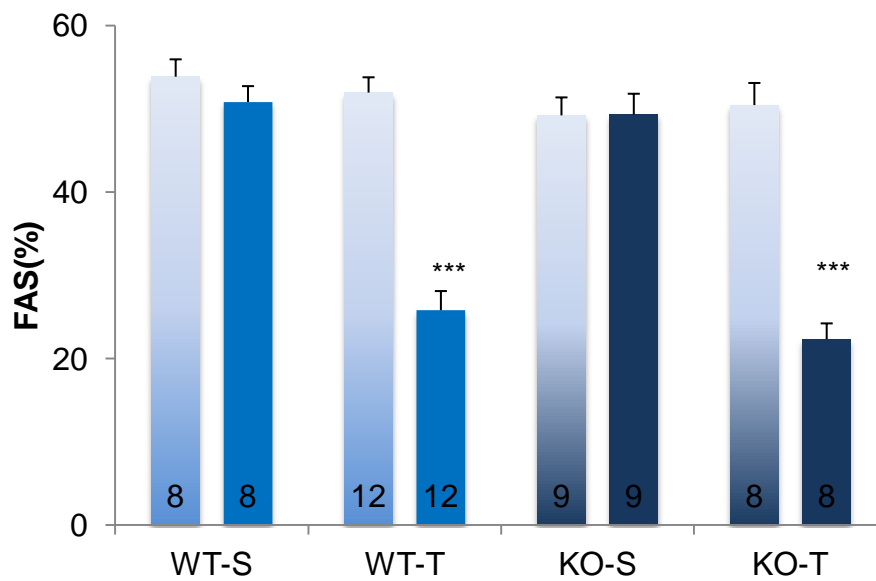


Figure 18: FAS decreased massively in all TAC groups *** P < 0.001 TAC groups before vs. after TAC.

A parameter assessing cardiac function which was not obtained from echocardiography was pulmonary congestion. Both groups, WT^{TAC} as well as KO^{TAC}, exhibited massive pulmonary congestion displayed by a significant increase in the LW/BW-ratio (see Figure 19).

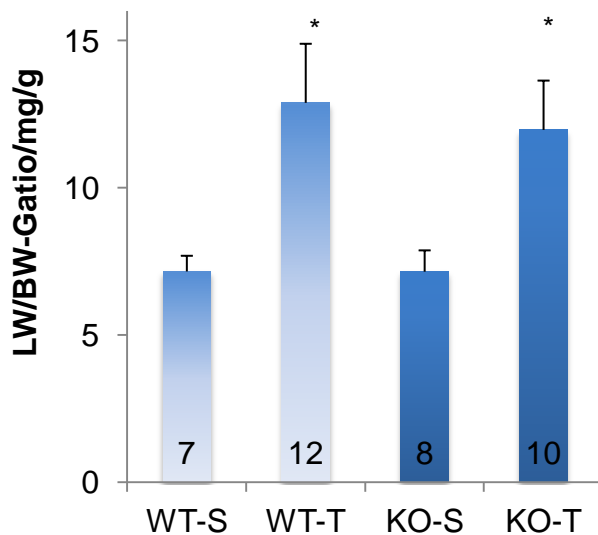


Figure 19: A massive pulmonary congestion was detected in both TAC groups. * P < 0.05 TAC vs. Sham groups.

The dobutamine response was partially preserved in the WT^{TAC} group, which showed an increase in FAS from 25.4±2.4% (n=11) to 33.0±3.9%, resembling an increase of

about 30% (see Figure 21A). In KO^{TAC} mice a dobutamine response was hardly present, the FAS only increased from a baseline value of 22.3±1.9% (n=7) to a stimulated value of 23.6±3.9%, which only represents an increase by 5%, this increase not being in the least significant. The difference in relative response almost reached significance (p=0.08).

Again, a sex-separated analysis was performed and showed an interesting result. Both male TAC groups showed basically no response (see Figure 21C). WT^{TAC} mice showed a small, not quite significant increase (p=0.10). KO^{TAC} mice revealed an almost unnoticeable, non-significant increase (p=0.77). A difference between the groups was not distinguishable (p=0.57).

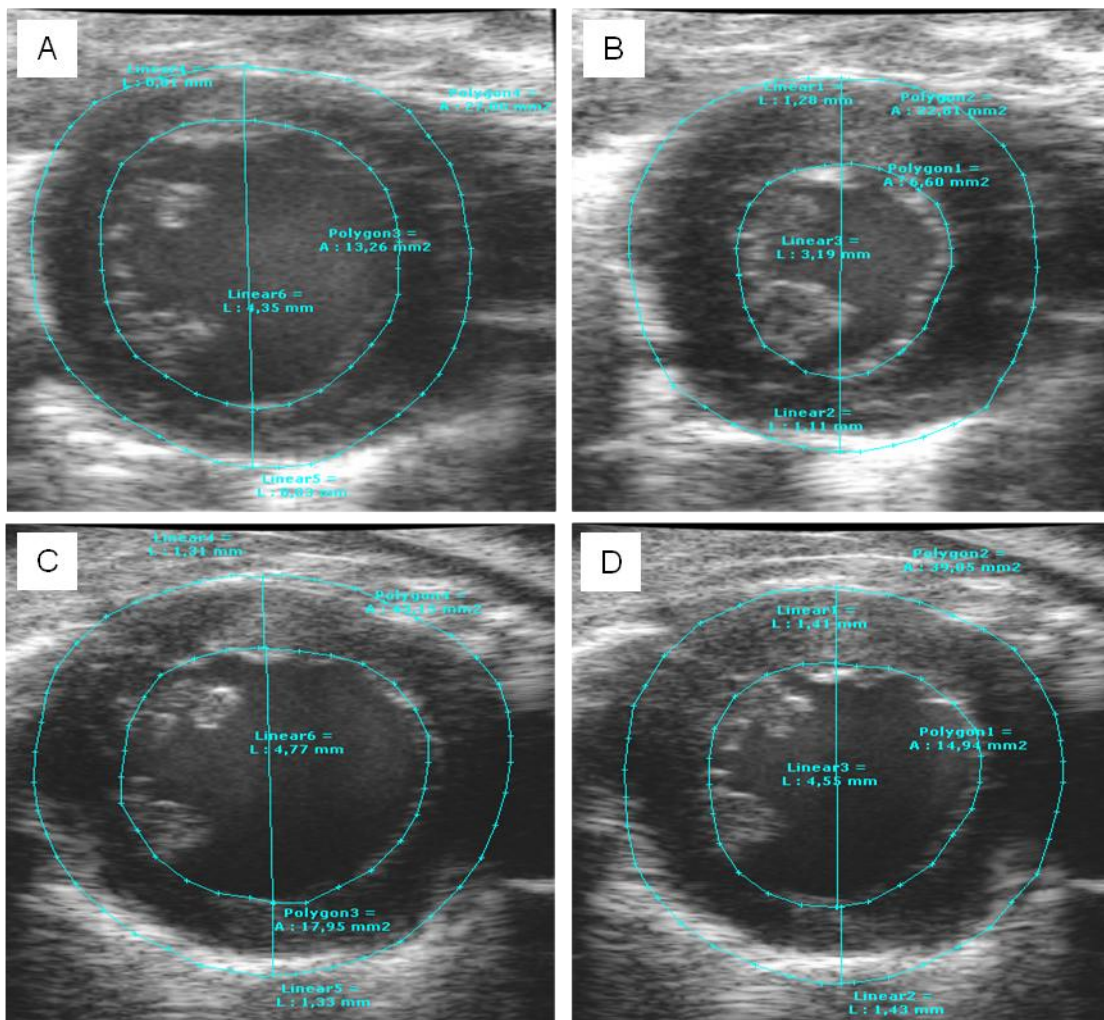
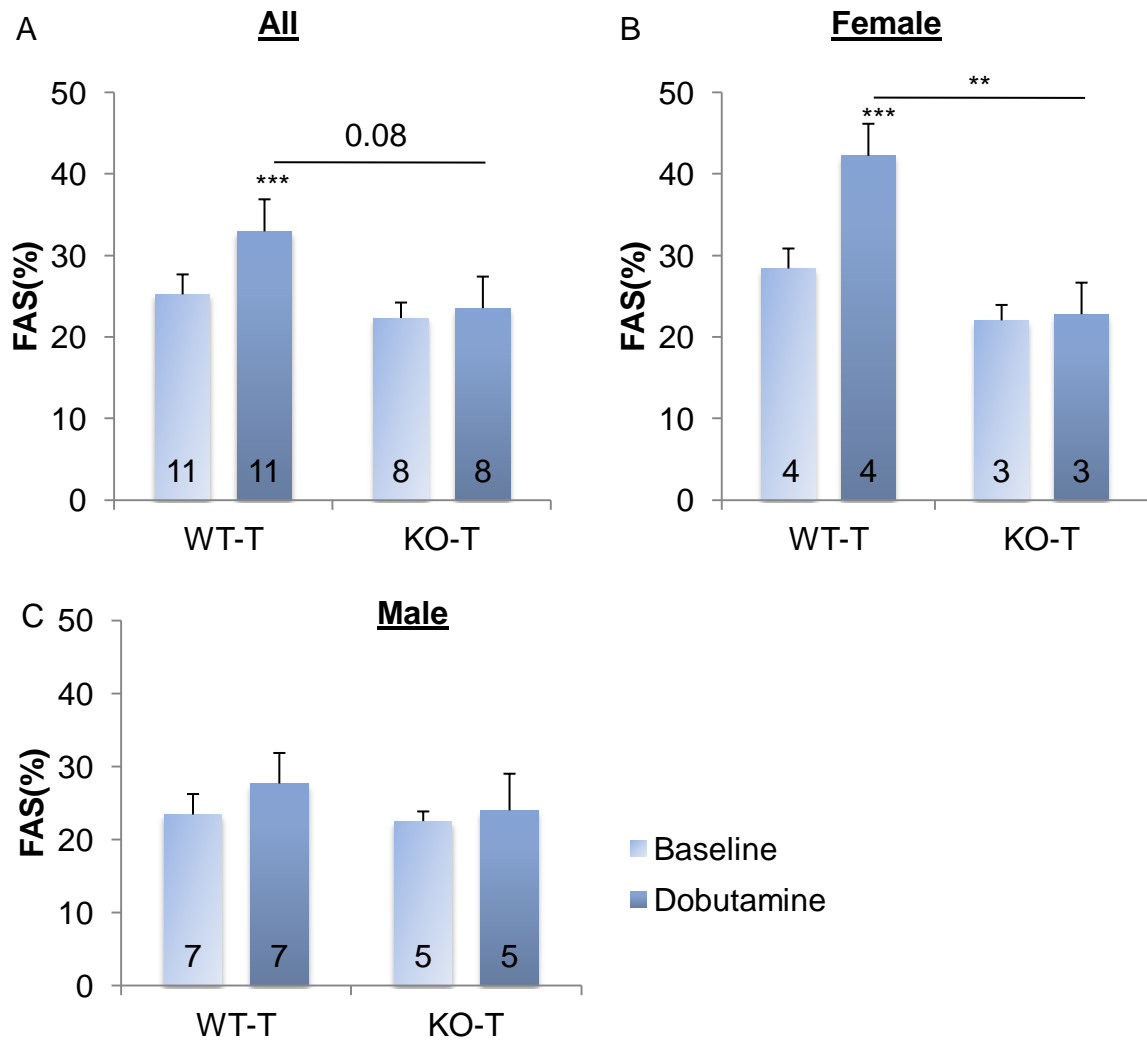


Figure 20: Echocardiographic images of a WT mouse, showing a heart in short axis view in diastole (A) and systole (B) before TAC intervention, where a clear contraction can be perceived. Diastole (C) and systole (D) after TAC intervention on the other hand are almost identical, illustrating the massive decrease in contractility after TAC.

In the female subgroup however, the WT^{TAC} group revealed exhibited a marked, statistically significant increase ($p < 0.001$), whereas the KO^{TAC} showed almost no response. The difference between both groups was as well a significant ($p < 0.01$). It had to be concluded that the significant differences to dobutamine stimulation were mostly carried by the female WT^{TAC} subgroup (see Figure 21B).



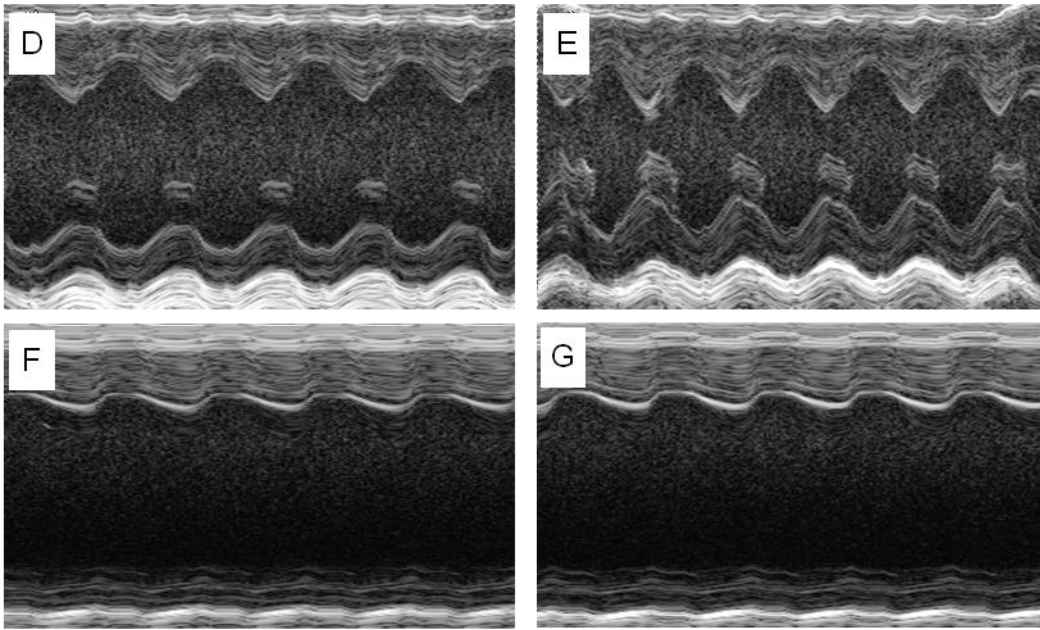


Figure 21: A trend for a more strongly decreased dobutamine response is seen in KO^{TAC} (A), especially in female mice (B), not so much in male mice (C). *** $P < 0.01$ WT^{TAC} before vs. after TAC; ** $P < 0.01$ KO^{TAC} vs. WT^{TAC} . (D-G) demonstrate a M-Mode recording, (D) a mouse in an basal state before TAC, (E) after the stimulation with dobutamine revealing a massive response, which is diminished if not absent after TAC, (F) showing a basal and (G) a dobutamine stimulated TAC animal.

In conclusion it can be said that the differences in contractility at baseline after intervention were only marginal, where only a really small trend might have been observed arguing for a stronger FAS in WT^{TAC} , especially in female WT^{TAC} mice. The evidence for a stronger response to dobutamine in WT^{TAC} is better, but it has to be kept in mind that this is effect almost exclusively exerted by the female WT^{TAC} subgroup.

3.3.11 I-1 mRNA levels were clearly downregulated after TAC

The echocardiographic data suggested that the mice which underwent the TAC procedure were in a stage of HF when they were sacrificed on day eight.

The levels of I-1 were clearly downregulated by over 50% in WT^{TAC} compared to its control group, which is consistent with previous reports of I-1 in HF (El-Armouche et al. 2004), and was therefore an expected finding (see Figure 22A). Additionally we could observe a correlation to the HW/BW-ratio ($r^2=0.80$) (see Figure 22B). Interestingly, a recently published report (Grote-Wessels et al. 2008) detected no change in I-1 levels after TAC, whereas it has to be noted that mice were kept alive

for 28d and could therefore potentially again be in a state of a more compensated hypertrophy, as it was also observed in our 25G TAC study. This topic will be further discussed later.

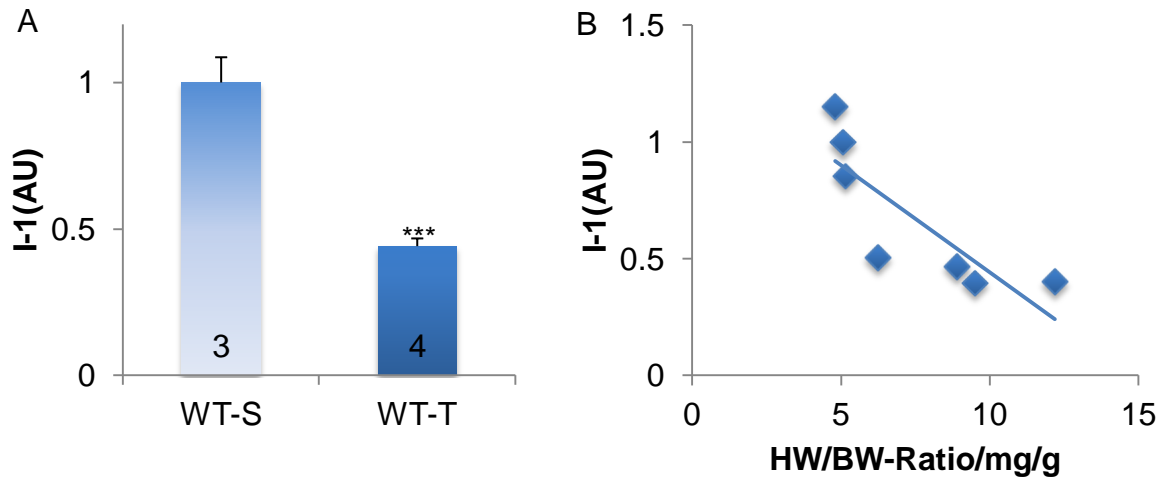


Figure 22: I-1 is clearly downregulated in after TAC **(A)** and reveals a correlation to the HW/BW-ratio **(B)**. *** $P < 0.001$ WT^{Sham} vs. WT^{TAC} .

3.3.12 Pathological hypertrophy markers were massively elevated after TAC

ANP increased by a factor of 9.5 in WT^{TAC} compared to WT^{Sham} and by a factor of 11.9 in KO^{TAC} compared with KO^{Sham} (shown in Figure 23A). The increase in the individual group was highly significant, but the difference between the groups was not ($p=0.25$). A correlation of the ANP values to the HW/BW-ratio was undertaken. In itself the ANP values correlated very well with the HW/BW-ratio in the individual groups. An almost significant difference between the two groups could be seen, indicating a higher ANP value in KO^{TAC} at the same HW/BW-ratio ($p=0.09$; see Figure 23B).

This trend was even stronger in male mice, were a correlation of HW/BW-ratio with the mRNA levels of ANP yielded significantly higher ANP values at the same body weight ($p<0.05$). This difference was not observed in female mice, the increase of ANP with increasing HW/BW-ratio was identical between KO^{TAC} and WT^{TAC} (data not shown).

The induction of BNP was not as profound as that of ANP. In WT^{TAC} BNP increased by the factor 2.2, and by the factor 2.3 in KO^{TAC}. The correlation between HW/BW-ratio and BNP values yielded a similar result as for ANP, here a higher BNP value per HW/BW-ratio was seen in KO^{TAC} mice, the result here was as well almost significant (p=0.09). The sex separated analysis was comparable with that of ANP (data not shown).

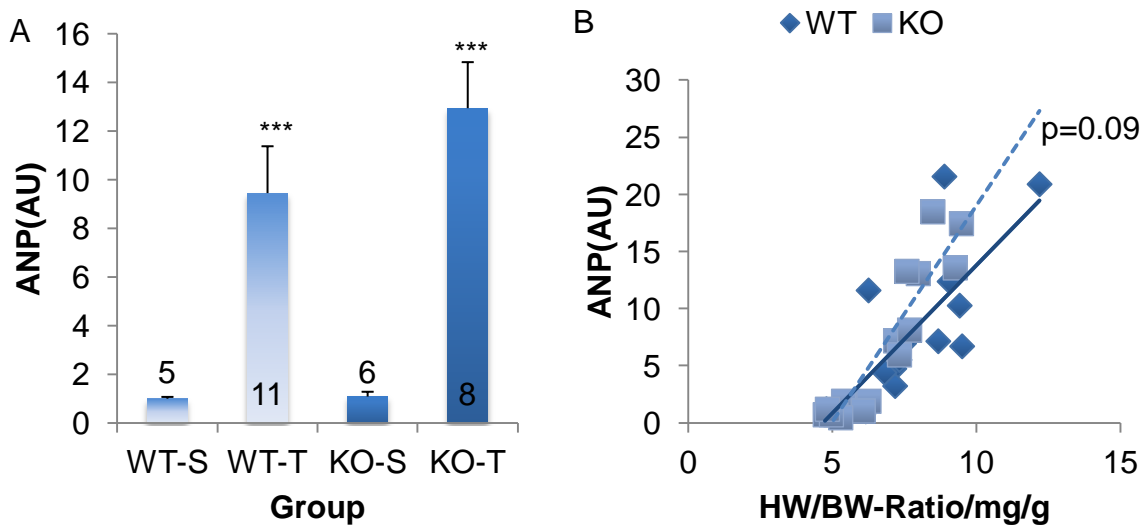


Figure 23: The massive induction of ANP was seen in both TAC groups (A), whereas KO^{TAC} mice seem to exhibit higher levels of ANP at identical HW/BW-ratios (B). ***p < 0.001 Sham vs. TAC

3.3.13 Immunoblotting showed an increase of PP1 levels after TAC

An immunoblot analysis exhibited comparable protein levels of PP1 in the Sham animals. In the TAC mice an increase by 34.6% in WT^{TAC} and by 33.3% in KO^{TAC} was observed (see figure 24). This increase in both groups was highly significant, but no significant difference between the groups was observed (p=0.87). A subgroup analysis by sexes yielded similar results, whereas the level in female mice in both groups was elevated slightly stronger (data not shown).

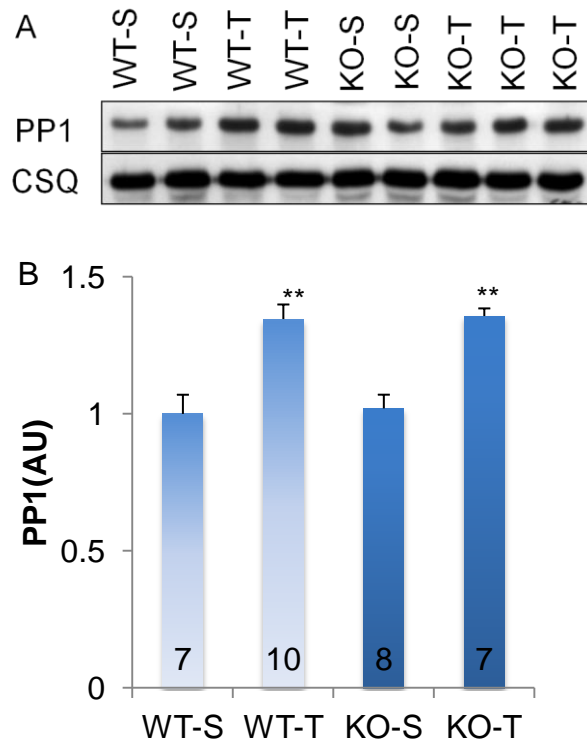


Figure 24: Uniform elevation of PP1 in both TAC groups (**B**) illustrated by a sample immunoblot (**A**). ** P < 0.01 Sham vs. TAC groups.

3.3.14 PKA substrates differed in phosphorylation, but results were inconclusive

3.3.14.1 *cTnl*-phosphorylation was selectively decreased in KO^{TAC}

The level of Tnl-Ser23/24 phosphorylation did not differ between WT^{Sham} and KO^{Sham} . WT^{TAC} mice exhibited no or only a minimal decrease in the level of phosphorylation compared to WT^{Sham} . In contrast KO^{TAC} mice revealed an about 38% lower phosphorylation level compared to KO^{Sham} (see Figure 25). While this finding was significant, the difference in the phosphorylation level to WT^{TAC} was not quite significant ($p=0.07$). The analysis of male and female mice did not yield different results (data not shown).

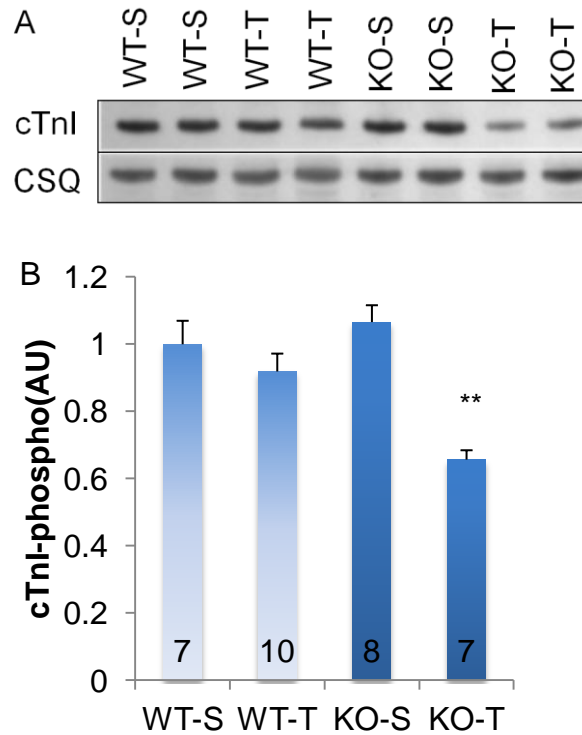


Figure 25: cTnI-phosphorylation was significantly downregulated in KO^{TAC} , whereas WT^{TAC} only exhibited a mild downregulation (**A + B**). ** $P < 0.01$ KO^{Sham} vs KO^{TAC} .

3.3.14.2 *cMyBP-C* exhibited a comparable phosphorylation pattern to *cTnI*

Total *cMyBP-C* levels did not vary significantly between the groups. The level of phosphorylation was not significantly different between WT^{Sham} and WT^{TAC} groups, but on the other hand a significant reduction in KO^{TAC} phosphorylation of about 30% was observed compared to KO^{Sham} (see Figure 26). Therefore the phosphorylation level in KO^{TAC} appears to exhibit a similar trend as *cTnI* phosphorylation. A sex-separated subgroup analysis was not performed.

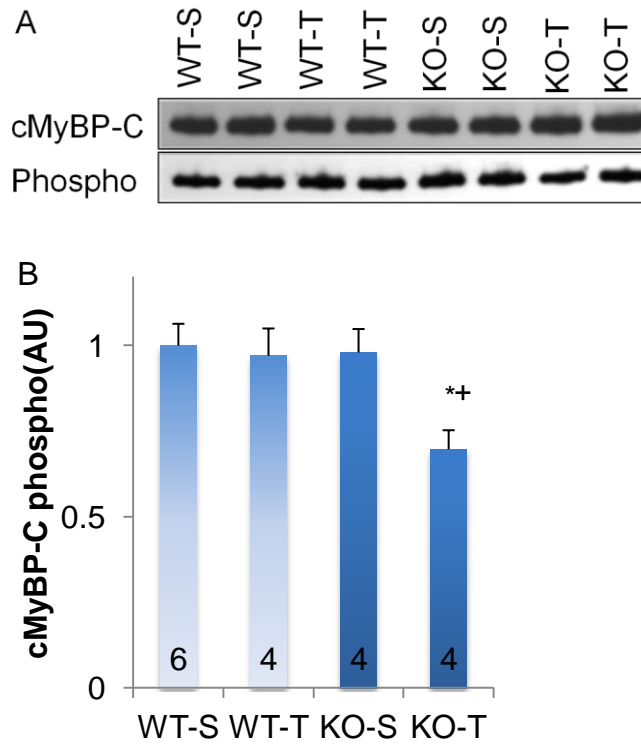


Figure 26: cMyBP-C pattern of dephosphorylation is comparable to cTnl's (**A+B**).
 * $P < 0.05$ KO^{Sham} vs KO^{TAC} ; + < 0.05 WT^{TAC} vs. KO^{TAC} .

3.3.14.3 PLB phosphorylation levels after TAC were equally diminished

Total Plb levels did not differ between WT and KO or Sham and TAC. In contrast, Plb-Ser16 phosphorylation tended to be lower in KO^{Sham} than in WT^{Sham} and both TAC groups showed significantly (WT) or non-significantly (KO) lower Plb-Ser16 phosphorylation levels when compared to Sham (see Figure 27).

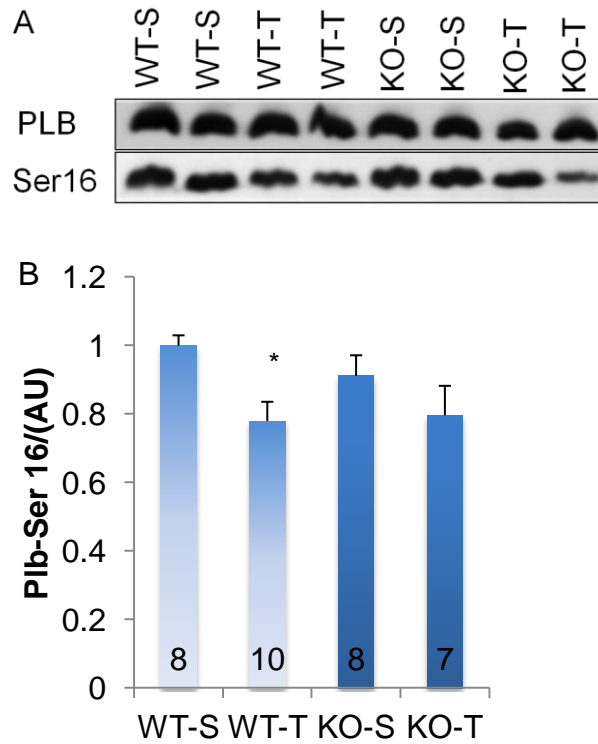


Figure 27: Phosphorylation of the PLB-Ser16 site did not differ significantly in both TAC groups. A statistically significant decrease was only seen in WT^{TAC} animals though **(A+B)**. * $P < 0.05$ WT^{Sham} vs. WT^{TAC}.

3.3.15 Serca2 levels exhibited a significant decrease in WT^{TAC} only

Serca2 levels of seemed to be slightly decreased in KO^{Sham} when compared to WT^{Sham} ($p=0.15$; see Figure 28). WT^{TAC} animals revealed significantly lower protein levels than WT^{Sham}, whereas between KO Sham and TAC mice, this difference was only almost significant ($p=0.09$). Male and female subgroups exhibited an identical trend.

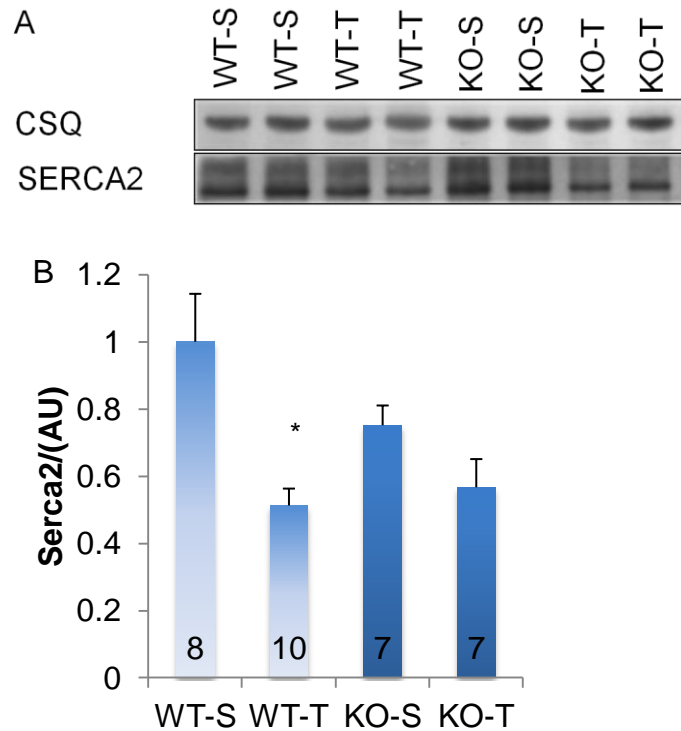


Figure 28: The SERCA2 levels were almost identical in both TAC groups, a significantly lower level was seen in WT^{TAC} compared with WT^{Sham} due to the higher levels of SERCA2 in WT^{Sham} (**A+B**). * P < 0.05 Sham vs. TAC.

3.3.16 GSK-3 β protein levels conformably increase after TAC

Hypertrophy in HF is mediated by numerous ways (Molkentin 2006), GSK-3 β representing one of them. It was selected to be examined in this study because it is linked with PP1 in an interesting way. It was reported that GSK-3 β phosphorylates Inhibitor-2, which leads to a decreased inhibition of PP1, which in turn leads to a dephosphorylation of GSK-3 β at the Ser-9 residue and therefore, since GSK-3 β is active in the non-phosphorylated state, to a higher activity of GSK-3 β (Zhang et al. 2003). One of GSK-3 β effects is a phosphorylation of NFAT, which cannot enter the nucleus in the phosphorylated form and therefore not mediate hypertrophy.

The protein levels of GSK-3 β did not differ between WT^{Sham} and KO^{Sham} (see figure 29B). In both TAC groups, the protein level was elevated by a little more than 20%. This difference was significant in between the WT groups and almost significant between the KO groups, while the levels of both TAC groups were almost identical. Male and female mice did not exhibit prominent differences. The phosphorylation of

the Ser-9 residue also showed almost identical level in both WT^{Sham} and KO^{Sham}. WT^{TAC} mice's phosphorylation level was slightly (about 10%), but by no means significantly, lower than in WT^{Sham}. In KO^{TAC} mice the phosphorylation level was about 35% lower than in KO^{Sham} (see figure 29C), this finding being significant. Comparing directly the phosphorylation levels of WT^{TAC} and KO^{TAC}, phosphorylation was roughly 30% lower in KO^{TAC}, but this difference was not significant (p=0.14). The sexes did not vary significantly.

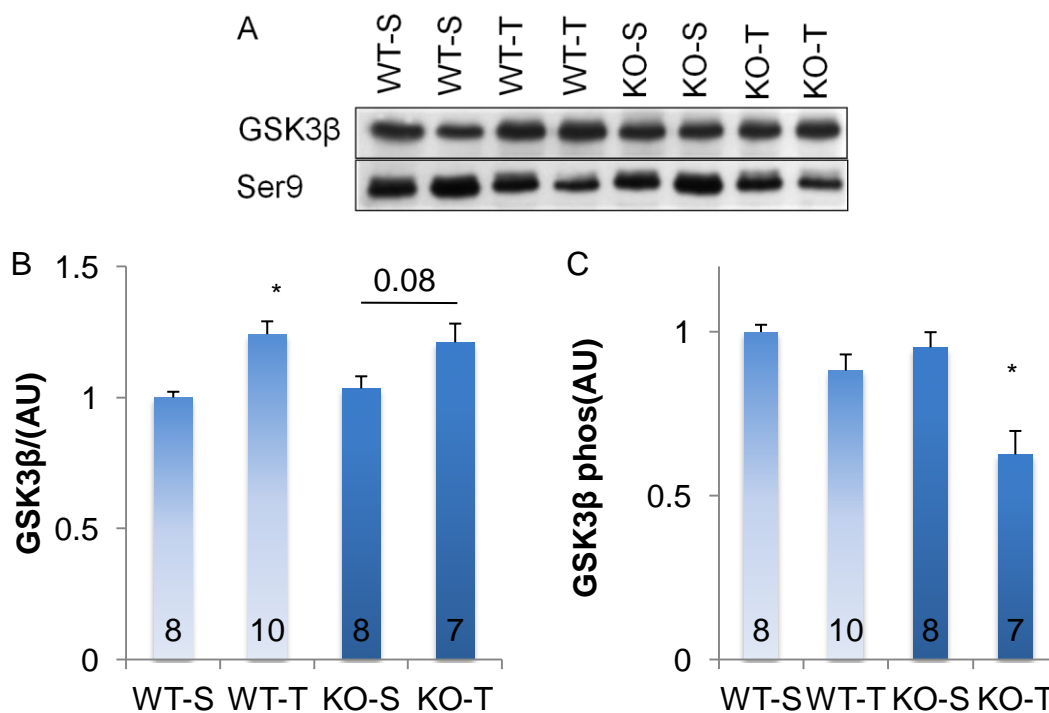


Figure 29: Total GSK3β values appear to increase after TAC (**A+B**), whereas phosphorylation decreases, especially in KO^{TAC} (**A+C**). * P < 0.05 Sham vs TAC.

3.3.17 Slightly larger cell area in WT^{TAC} mice

When assessed by histology, no basal difference in cell area was seen between the WT and the KO group (Sham). After the TAC procedure, there was a non significant trend towards a smaller increase in cell area in the KO^{TAC} group (see Figure 30).

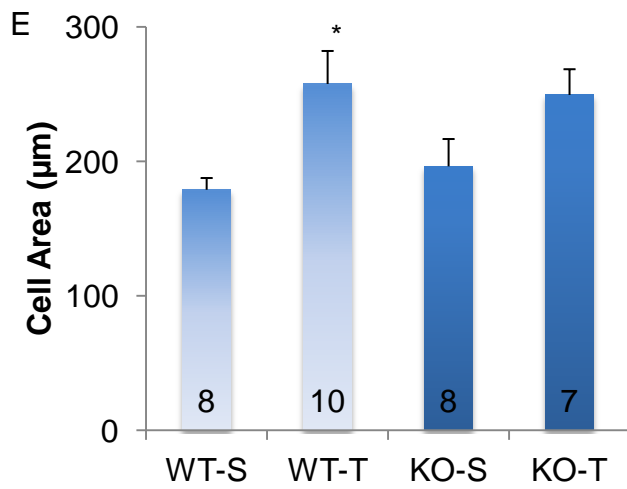
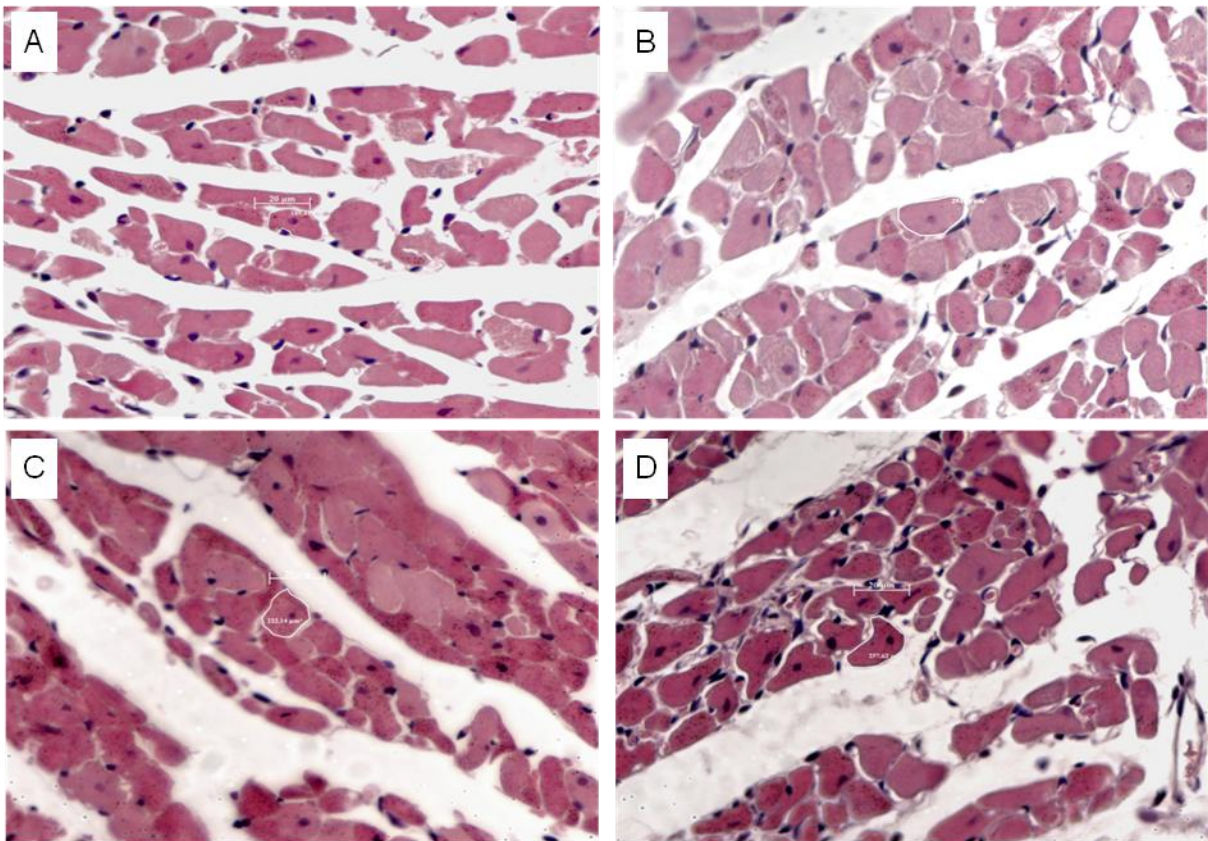


Figure 30: HE stained slices of WT-S (A), WT-T (B), KO-S (C) and KO-T (D). The cell size is comparable between both TAC groups (E). * P < 0.05 Sham vs. TAC.

4 Discussion

This study aimed at characterizing the role of I-1 in a murine model of pressure overload-induced hypertrophy and HF by comparing I-1 KO with WT mice at baseline and after TAC. A brief summary of the results is given at the beginning of the discussion.

At baseline WT and KO mice between eight to eleven weeks of age did not differ, neither in morphological nor in functional parameters. Subjected to a TAC model with moderate stenosis (25G), KO^{TAC} mice revealed no significant differences compared with WT^{TAC} mice in functional or morphological parameters. A more pronounced stenosis (27G) resulted in a drastic impairment of cardiac function in both WT and KO. The most striking finding was the increased mortality in KO^{TAC} mice, which was restricted to male KO mice. Female mice of both TAC groups revealed a comparable mortality. Excess mortality in male KO^{TAC} mice might have caused a bias of the results obtained in this particular subgroup, since the most impaired mice had probably already died at the point of sacrifice.

Contractility was massively and comparably diminished in both TAC groups. The KO^{TAC} subgroup exhibited a trend towards an attenuated dobutamine response. The difference to WT^{TAC} was significant in the female subgroup. The male KO^{TAC} subgroup exhibited significantly less hypertrophy.

Relatively higher levels of ANP and BNP were detected in KO^{TAC} mice, especially in the male subgroup. Dephosphorylation of some PKA substrates in KO^{TAC} was more pronounced. These substrates were cTnI Ser23/24 and cMyBP-C. PLB-Ser16 on the other hand seemed more strongly dephosphorylated in WT^{TAC} mice.

4.1 Absence of functional differences at baseline is contradictory to earlier reports

The KO mice used for this study had been previously examined by Carr et al (2002), who detected a decrease of 25% in baseline contractility compared to WT. This was attributed to a decreased PLB-Ser-16 phosphorylation. This study could not detect functional impairments at baseline in KO mice (see below). Another report which has been published by our group (El-Armouche et al. 2008) also did not report a decrease in baseline contractility, but decreased responsiveness to isoprenaline in

vitro, which is well compatible with the amplifier role of I-1 in normal physiology. Discrepancies between the studies could be related to differences in the depth of anesthesia during echocardiography and/or the degree of catecholaminergic stimulation.

4.2 Assessment of the 25G-TAC-Series

The transverse aortic constriction using a 25G needle produced only mild effects on heart weight and had no significant effect on cardiac function in both TAC groups. No significant difference between the groups was observed. Due to the small sample size of both groups this is not unanticipated, since only major effects would have been distinguishable. We therefore decided to evaluate a second series on animals with a higher degree of stenosis because this study sought to evaluate I-1's role in HF.

4.3 Increased mortality in KO^{TAC} mice unexpected

In the light of an absence in functional and morphological differences at baseline and protective effects in another stress model (El-Armouche et al. 2008) the worse survival in KO^{TAC} mice was unexpected. KO^{TAC} mice kept dying even though the event of acute stress induced by the TAC procedure was probably already ameliorating. Other studies showed recovery of LV function on day three after TAC (e.g. Nakamura et al. 2001). Although most mice certainly died within the first three days after the procedure, a significant difference in survival was still observed after day three.

Additionally it has to be considered that the TAC procedure performed in this study resulted in a drastic and extremely unphysiological increase in afterload and equally drastic impairments of cardiac function, i.e., in decompensated HF. Its effects were much stronger than in the study cited above (Nakamura et al. 2001). Few studies concerning the beta-adrenergic signaling cascade report survival data, which renders an in detail discussion useless.

4.4 Stronger impairment of cardiac function in KO^{TAC} mice resembles survival data

Loss of contractility was striking in both WT^{TAC} and KO^{TAC} after the 27G intervention and KO^{TAC} exhibited a trend towards even worse contractility. Furthermore KO^{TAC} mice subjected to the 27G TAC approach showed no response to dobutamine at all, whereupon in WT^{TAC} mice a response was clearly discernible. This response was comparable to Sham groups when regarding not absolute but relative values. This effect of an I-1 KO would be supported by many reports. All these have in common that the loss of I-1 affects the β -adrenergic signaling downstream from the PKA, either directly via transgenic expression of I-1, which maintained hypercontractile cardiac function and prevented decompensation (Pathak et al. 2005) or indirectly, e.g. *via* increased activity of PP1, either by overexpression of PP1 itself, which led to depressed cardiac function, dilated cardiomyopathy, and premature mortality (Carr et al. 2002). On the other hand, lately published reports postulated a positive effect of a stronger PP1 action, e.g. caused by ablation of I-1, where I-1-KO had normal heart structure with mildly reduced sensitivity, but unchanged maximal contractile responses to beta-adrenergic stimulation (El-Armouche et al. 2008), or constitutively active I-2 mice showing development of focal fibrosis, impaired fractional shortening and diastolic function (Grote-Wessels et al. 2008).

4.4.1 Diminished phosphorylation of cardiac troponin I and C protein might play a pivotal role

An interesting question is which mechanisms are involved on a molecular level in worsening cardiac function. First, a comparable decrease in PLB Ser-16 phosphorylation and absolute protein levels of SERCA2 was observed, which has been previously reported in human HF and experimental HF models (Hasenfuss et al. 1994; Movsesian et al. 1994, Schwinger et al. 1999). These changes certainly account for an essential part of the worsened cardiac function of TAC vs. Sham mice of both WT and KO mice.

Since PLB-Ser 16 dephosphorylation and reduction of SERCA2 levels were comparable, a possible mechanism for differences in contractility and dobutamine response still needs to be identified. cTnI and Protein-C might contribute to this mechanism.

cTnI is phosphorylated by PKA at its Ser-22/23 in mice (respectively Ser-23/24 in human). It is also a key regulatory protein of cardiac muscle contraction, since it links Ca^{2+} -TnC binding to the thin filament. Altered thin filament function is suggested to act as a crucial factor in human HF. Dephosphorylation of the Ser23/24-site has been found in human HF (Zakhary et al. 1999; van der Velden et al. 2003). Especially interesting in the context of this study is the fact that cTnI-phosphorylation at PKA plays a crucial role in situations involving an increased afterload, since it serves to reduce afterload-induced delay in relaxation (Layland et al. 2005). Besides PLB-Ser16 and cTnI-Ser22/23 another protein which is PKA-phosphorylated is c-MyBP-C, which has also been reported to be dephosphorylated in HF (El-Armouche et al. 2007). The role of c-MyBP-C appears to consist in the acceleration of force development kinetics (Stelzer et al. 2007).

The difference in phosphorylation of cTnI's Ser22/23-residue and of C-MyBP-C in 27G TAC mice was pronounced. While no significant decrease in phosphorylation was seen in WT^{TAC} , a massive dephosphorylation of both proteins was detected in KO^{TAC} . This might indeed explain the differences in contractility and dobutamine response between KO^{TAC} and WT^{TAC} mice.

4.5 Comparable hypertrophy response in KO^{TAC} and WT^{TAC}

The hypertrophy response in both groups was very pronounced. Differences in extent and form of hypertrophy between WT^{TAC} and KO^{TAC} mice were relatively small and not significant. This finding is in accordance to the rather minor impact of the beta-adrenergic signaling cascade in hypertrophy (Heineke and Molkentin 2006). Apart from macro- and microscopic differences, this study also investigated molecular hypertrophy markers.

4.5.1 Stronger induction of fetal gene program in KO^{TAC}

ANP and BNP seemed to be more markedly elevated in KO^{TAC} mice when normalized to BW. Higher levels of ANP and BNP in HF along with other proteins like β -myosin heavy chain or α -actin are often considered markers of pathological hypertrophy (van Bilsen and Chien 1993). Both natriuretic peptides, especially BNP, are also known biomarkers of cardiac hemodynamic stress (Braunwald 2008). Considering this, the trend towards higher levels of natriuretic peptides in KO^{TAC} mice

could indicate a worse hypertrophy response as well as a failure to adapt to hemodynamic stress caused by TAC.

4.6 Gender specific analysis reveals significant differences

Response to TAC was different between male and female mice. Most importantly, the overall mortality was higher in female mice, whereas there was no difference between female WT^{TAC} and KO^{TAC} groups. Overall, female mice in the WT^{TAC} group exhibited less hypertrophy than male mice. Moreover, male KO^{TAC} mice exhibited less hypertrophy response than WT^{TAC}. Furthermore, female KO^{TAC} mice had a worse dobutamine response than WT^{TAC}.

These results are only in part reflected in literature. Overall mortality of about 25% in male WT^{TAC} mice is in accordance with known data (Rockman et al. 1991; Nakamura et al. 2001; Zhou et al. 2004). Why female mice of the WT^{TAC} and KO^{TAC} group revealed excess mortality cannot be explained by this study and has not yet been addressed by similar studies.

The larger hypertrophy response in male than in female WT^{TAC} mice has previously been described (Skavdahl et al. 2005; Fliegner et al. 2010). This gender difference was not seen in the KO^{TAC} group and might serve as an explanation for the worse survival in the male KO^{TAC} subgroup.

The absence of a dobutamine recruitable contractile reserve in the male TAC group has also been described previously (Weinberg et al. 1999). Female WT mice subjected to TAC had a preserved contractile reserve and this was not the case in the female KO^{TAC} group. This effect may also be explained by the I-1 KO.

Overall, the sex-specific analysis is in accordance with the general picture that I-1 KO mice performed worse than their WT counterparts. But one has to keep in mind that numbers in each subgroup were low and statistical effects might be disproportionate. The high mortality in female WT^{TAC} mice is also not represented in the literature, since female mice generally show a better outcome after TAC (Weinberg et al. 1999; Skavdahl et al. 2005; Fliegner et al. 2010).

4.7 Does failure to adapt cause worse outcome in KO^{TAC} group?

Overall, KO^{TAC} mice revealed a worse outcome in this study. This is in contrast with the study by El-Armouche et al. (2008), which used a chronic isoprenaline infusion model of seven days duration. It showed a decreased HW/BW-ratio, less marked dilatation and a relatively sustained catecholamine response in I-1 KO mice compared to WT. Hypophosphorylation of PLB-Ser16 and RyR-Ser2815 was observed, whereas the phosphorylation of cTnI-Ser22/23 and cMyBPc was unaltered.

A study by Pathak et al. (2005) subjected truncated I-1 transgenic mice to TAC with a 27G needle and sacrificed these mice after six weeks. The truncation of I-1 rendered it constitutively active. The transgenic mice revealed increased FAS, attenuated hypertrophy and better response to catecholaminergic stimulation. The authors therefore concluded that an augmentation of I-1 signaling is beneficial in pressure overload induced HF.

On the other hand, Grote-Wessels et al. conducted a study with transgenic mice for I-2, which should be comparable to transgenic I-1 mice. These mice were also subjected to TAC with a 27G needle, but these mice were sacrificed after 28 days. The outcomes were quite opposite to the findings made by Pathak et al. A detrimental effect of transgenic I-2 was observed. This study showed various remarkable observations in WT mice. As described above, I-1 mRNA levels increased, which would actually be expected to be decreased in HF. Additionally, SERCA levels were unaltered and PLB-Ser16 phosphorylation levels were increased. All these findings are not in accordance to observations made by Pathak et al. (2005) and in this study.

The worse outcome of KO animals in the present study is hard to appraise. One possible explanation is that a decrease of beta-adrenergic signaling in KO mice leads to a failure to adapt to stress connected with an increased afterload. The decreased dobutamine response in KO as a sign of a decreased cardiac reserve indicates such a mechanism. Its molecular cause may be found in the decreased phosphorylation of cTnI und cMyBP-C. This explanation is in accordance to the findings made by Pathak et al. (2005) and not contradictory to the findings made by El-Armouche et al. (2008), since the isoprenaline infusion model does not stress cardiac function as much as

TAC does and actually reduces wall stress by markedly decreasing diastolic blood pressure.

The failure to adapt cannot be sought exclusively in a diminished response to catecholamines. A study by Rapacciuolo et al. (2001) showed a beneficial effect of abolition of catecholamines after TAC. Therefore, an imbalance of signaling pathways on the heart is more likely to cause the effects seen in this study.

The role of beta-adrenergic signaling in human can only be speculated about. A situation comparable to TAC does hardly occur in humans, with the exception of hypertensive emergency. No extensive studies of HF due to a hypertensive emergency have been performed. For a long time it was standard operating procedure to halt beta-blocker therapy in decompensated HF, but a recent study by Jondeau et al. (2009) showed non-inferiority of beta-blocker continuation. The uniqueness of the TAC situation of a massive increase in afterload with normal cardiac function certainly renders a comparison to disease mechanisms difficult. Moreover, it is possible that β -adrenergic support of the heart is beneficial under a certain degree of stress, but deleterious under another.

4.8 Conclusion and outlook

This experiment's aim was to evaluate the effects of an acute and sustained increase in afterload in KO mice for I-1, which was expected to gain clarity on the role of I-1 in HF in particular, and additionally add further insight to the role of β -adrenergic signaling in HF.

The higher mortality combined with slightly worse functional parameters in I-1 knockout mice might indicate a detrimental role of I-1 downregulation in the pathogenesis of pressure-induced HF in the initial period after TAC. This could in part be attributable to the decreased phosphorylation of cTnI and cMyBP-C. Since cTnI is supposed to play a crucial role in situations of increased afterload (Layland et al. 2005), the worse outcome in KO^{TAC} mice would be understandable and would also explain the beneficial outcome of overexpression of truncated constitutively active I-1 in the study by Pathak et al. (2005). This could possibly also explain the differences which were observed in contrast to the isoprenaline-infusion model also conducted in this lab (El-Armouche et al. 2008). The mechanism detected here might serve as an

additional mechanism for the understanding of β -adrenergic signaling in HF, but certainly demands further exploration.

The plethora of studies concerning beta-adrenergic signaling therefore foremost seem to illustrate the following: detrimental or beneficial effects of beta-adrenergic signaling are closely linked to intensity, duration and timing.

Considering this, one has to keep in mind that the TAC response was extremely pronounced in our hands, especially when regarding mortality data. The less marked hypertrophy in male KO^{TAC} could therefore be an early indicator that an I-1 KO might be beneficial in the long run, but might also hint at a failure to adapt.

A controversial finding of this study in concern is the fact that no difference in PLB-phosphorylation was detected. As previously said most studies which detected a beneficial influence of an augmentation of β -adrenergic signaling downstream of PKA explained this beneficial effect by an increase of PLB-phosphorylation, which this study fails to illustrate, but again, also this finding is controversial, as we can see by the results of the study of Grote-Wessels et al (2008). Therefore, this study cannot be seen as a strong support of this general principle.

One weakness is its relatively short survival after TAC. One might argue that a longer survival after TAC might lead to a better outcome of the KO^{TAC} subgroup, hinted at by the less pronounced hypertrophy.

I-1 remains an interesting research target in the pathomechanism of cardiac events. Evidence for a detrimental role of I-1 downregulation in HF is accumulating and probable mechanism for enhancing I-1 activity are interesting and already being evaluated (Braz et al. 2005; Pathak et al. 2005). The positive outcomes of PP1 inhibition in slightly different settings (El-Armouche et al. 2008, Grote-Wessels et al. 2008) seem to indicate that the method of investigation seems to play a major role.

A recently published paper by this group investigating the role of constitutively active I-1 (I-1c) found enhanced cardiac contractility but exaggerated contractile dysfunction and ventricular dilation upon catecholamine infusion in young mice. Older mice developed a phenotype dilated cardiomyopathy (Wittköpper et al. 2010). This hints at an additional role of I-1 in the development of arrhythmias, which was first illuminated by El-Armouche et al. (2008) and is therefore an interesting target for an

antiarrhythmic therapy. The augmentation of downstream β -adrenergic signaling, which's role is still controversial in HF, seems to have a proarrhythmogenic effect and since I-1 knockout mice show a normal longevity, a long-term medicinal inhibition of I-1 in arrhythmias appears possible.

5 Abstract

Aims

Phosphatase inhibitor-1 (I-1) is a conditional amplifier of beta-adrenergic signalling downstream of protein kinase A (PKA). PKA inhibits type-1 phosphatases (PP1) only in its PKA-phosphorylated form. I-1 is downregulated in failing hearts and thus contributes to beta-adrenergic desensitization. It is unclear whether this should be viewed as a predominantly adverse or protective response.

Methods and results

Mice with targeted disruption of the I-1 gene (KO) and their genetically unaltered littermates (WT) were subjected to transverse aortic constriction (TAC). Cardiac function and mass as well as molecular parameters were evaluated after 8 days.

I-1 KO and WT did not differ at baseline. When subjected to TAC, KO mice revealed a significantly higher mortality, especially in the male subgroup. The hypertrophy response in the total group was comparable, but significantly lower in male KO^{TAC} mice. Cardiac function was massively impaired in both groups, but even worse in KO, both at baseline and under catecholamine stimulation. Levels of cardiac natriuretic peptides tended to be more elevated in KO and a glycogen synthase kinase-3 β was less phosphorylated in KO than in WT. Phosphorylation of cardiac troponin I and cardiac myosin binding protein-C was uniformly diminished in KO also. Phospholamban-serin 16-phosphorylation was mildly diminished in both groups without differences.

Conclusion

In the initial phase after acute, severe TAC, the absence of I-1 had detrimental effects, both on mortality and cardiac function. This was associated and may be causally related to phosphorylation of regulatory proteins of the sarcomere and growth cascade. Hypertrophy on the other hand was less pronounced in male KO^{TAC} mice. Whether the detrimental effects, especially the higher mortality, would persist in the long term is hard to predict and would be an interesting subject of further investigation, especially since the reduced hypertrophy could argue for some long term protection result in the KO^{TAC} group.

6 Abbreviations

AC	Adenylate cyclase
ANP	Atrial natriuretic peptide
ANF	Atrial natriuretic factor
ANS	Autonomic nervous system
AwTh	Anterior wall thickness
BNP	Brain natriuretic peptide
Bp	Base pair
β -AR	Beta-adrenergic receptor
β ARK1	Beta-adrenergic receptor kinase-1
β ARKct	Inhibitor of beta-adrenergic receptor kinase-1
β -MHC	Beta myosin heavy chain
CHD	Coronary heart disease
cMyBP-C	Cardiac myosin binding protein C
CO	Cardiac output
CSQ	Calsequestrin
cTnI	Cardiac troponin I
CVD	Cardiovascular disease
CW	Cardiac work
Diam	Diameter
DNA	Desoxyribonucleinacid
DPA	Pulmonary artery diameter
ECG	Electrocardiogramm
EF	Ejection fraction
FAM	6-Carbofluorescein
FAS	Fractional area shortening
FS	Fractional shortening
G _s	Stimulatory G-Protein
GPCR	G-Protein-coupled receptor
GRK	G-Protein receptor kinase
GSK-3 β	Glycogen synthase kinase 3 beta
HE	Hematoxylin Eosin
HF	Heart failure
HR	Heart rate
HTN	Hypertension
HW	Heart weight
I-1	Inhibitor 1
IgG	Immunoglobulin G
Isf	Isoflourane
KO	Knockout
KO ^{Sham}	I-1 knockout mice subjected to Sham procedure
KO ^{TAC}	I-1 knockout mice subjected to TAC procedure
LV	Left ventricle
LVEDD	Left ventricular end-diastolic diameter
LVEDV	Left ventricular end-diastolic volume
LVESD	Left ventricular end-systolic diameter
LVESV	Left ventricular end-systolic volume
LVM	Left ventricular mass

Mhz	Megahertz
NTC	Non template control
PCR	Polymerase chain reaction
PI(3)K	Phosphoinositide 3-kinase
PK	Protein Kinase
PKA	Protein Kinase A
PKC- α	Protein Kinase C alpha
PLB	Phospholamban
PP	Protein phosphatase
PP1	Protein phosphatase 1
PP1c	Catalytic subunit of Protein Phosphatase 1
PP2A	Protein phosphatase 2A
PP2B	Protein phosphatase 2B
PP2C	Protein phosphatase 2C
PwTh	Posterior wall thickness
RAAS	Renin-Angiotension-Aldosteron-System
Rpm	Rounds per minute
RyR	Ryanodine Receptor
SDS	Sodium duodecyl sulfate
Ser	Serin
SERCA	Sarcoplasmatic calcium ATPase
SNS	Sympathetic nervous system
TAC	Transverse aortic constriction
TAMRA	6-Carboxy-tetramethylrhodamin
Thr	Threonin
TL	Tibia length
UKE	University medical center Hamburg-Eppendorf
VTI	Velocity time integral
WT	Wildtype
WT ^{Sham}	C57Bl6J mice subjected to Sham procedure
WT ^{TAC}	C57Bl6J mice subjected to TAC procedure

7 Literature

Allen BG, Katz S. Phosphorylation of cardiac junctional and free sarcoplasmic reticulum by PKC alpha, PKC beta, PKA and the Ca²⁺/calmodulin-dependent protein kinase. *Mol Cell Biochem.* 1996 Feb 23;155(2):91-103.

Allen PB, Hvalby O, Jensen V, Errington ML, Ramsay M, Chaudhry FA, Bliss TV, Storm-Mathisen J, Morris RG, Andersen P, Greengard P. Protein phosphatase-1 regulation in the induction of long-term potentiation: heterogeneous molecular mechanisms. *J Neurosci.* 2000 May 15;20(10):3537-43.

Antos CL, McKinsey TA, Frey N, Kutschke W, McAnally J, Shelton JM, Richardson JA, Hill JA, Olson EN. Activated glycogen synthase-3 beta suppresses cardiac hypertrophy in vivo. *Proc Natl Acad Sci U S A.* 2002 Jan 22;99(2):907-12.

Bauer PH, Müller S, Puzicha M, Pippig S, Obermaier B, Helmreich EJ, Lohse MJ. Phosducin is a protein kinase A-regulated G-protein regulator. *Nature.* 1992 Jul 2;358(6381):73-6.

Bayer AL, Heidkamp MC, Patel N, Porter M, Engman S, Samarel AM. Alterations in protein kinase C isoenzyme expression and autophosphorylation during the progression of pressure overload-induced left ventricular hypertrophy. *Mol Cell Biochem.* 2003 Jan;242(1-2):145-52.

van Bilsen M, Chien KR. Growth and hypertrophy of the heart: towards an understanding of cardiac specific and inducible gene expression. *Cardiovasc Res.* 1993 Jul;27(7):1140-9.

Bowling N, Walsh RA, Song G, Estridge T, Sandusky GE, Fouts RL, Mintze K, Pickard T, Roden R, Bristow MR, Sabbah HN, Mizrahi JL, Gromo G, King GL, Vlahos CJ. Increased protein kinase C activity and expression of Ca²⁺-sensitive isoforms in the failing human heart. *Circulation.* 1999 Jan 26;99(3):384-91.

Bradford MM. A rapid and sensitive method for the quantitation of microgram quantities of protein utilizing the principle of protein-dye binding. *Anal Biochem.* 1976 May 7;72:248-54.

Braunwald E. Biomarkers in heart failure. *N Engl J Med*. 2008 May 15;358(20):2148-59.

Braz JC, Gregory K, Pathak A, Zhao W, Sahin B, Klevitsky R, Kimball TF, Lorenz JN, Nairn AC, Liggett SB, Bodi I, Wang S, Schwartz A, Lakatta EG, DePaoli-Roach AA, Robbins J, Hewett TE, Bibb JA, Westfall MV, Kranias EG, Molkenstein JD. PKC- α regulates cardiac contractility and propensity toward heart failure. *Nat Med*. 2004 Mar;10(3):248-54.

Bristow MR. Why does the myocardium fail? Insights from basic science. *Lancet*. 1998 Aug;352 Suppl 1:S18-14.

Brüchert N, Mavila N, Boknik P, Baba HA, Fabritz L, Gergs U, Kirchhefer U, Kirchhof P, Matus M, Schmitz W, DePaoli-Roach AA, Neumann J. Inhibitor-2 prevents protein phosphatase 1-induced cardiac hypertrophy and mortality. *Am J Physiol Heart Circ Physiol*. 2008 Oct;295(4):H1539-46.

Carr AN, Schmidt AG, Suzuki Y, del Monte F, Sato Y, Lanner C, Breeden K, Jing SL, Allen PB, Greengard P, Yatani A, Hoit BD, Grupp IL, Hajjar RJ, DePaoli-Roach AA, Kranias EG. Type 1 phosphatase, a negative regulator of cardiac function. *Mol Cell Biol*. 2002 Jun;22(12):4124-35.

Chien KR. Stress pathways and heart failure. *Cell*. 1999 Sep 3;98(5):555-8.

Clerk A, Sugden PH. Activation of protein kinase cascades in the heart by hypertrophic G protein-coupled receptor agonists. *Am J Cardiol*. 1999 Jun 17;83(12A):64H-69H.

Cohn JN. Structural basis for heart failure. Ventricular remodeling and its pharmacological inhibition. *Circulation*. 1995 May 15;91(10):2504-7.

Cohen P. The structure and regulation of protein phosphatases. *Annu Rev Biochem*. 1989;58:453-508.

Cohen P, Cohen PT. Protein phosphatases come of age. *J Biol Chem*. 1989 Dec 25;264(36):21435-8.

Cohen P, Schelling DL, Stark MJ. Remarkable similarities between yeast and mammalian protein phosphatases. *FEBS Lett*. 1989 Jul 3;250(2):601-6.

Cohen PT. Protein phosphatase 1--targeted in many directions. *J Cell Sci.* 2002 Jan 15;115(Pt 2):241-56.

Collins KA, Korcarz CE, Lang RM. Use of echocardiography for the phenotypic assessment of genetically altered mice. *Physiol Genomics.* 2003 May 13;13(3):227-39.

Cross HR, Steenbergen C, Lefkowitz RJ, Koch WJ, Murphy E. Overexpression of the cardiac beta(2)-adrenergic receptor and expression of a beta-adrenergic receptor kinase-1 (betaARK1) inhibitor both increase myocardial contractility but have differential effects on susceptibility to ischemic injury. *Circ Res.* 1999 Nov 26;85(11):1077-84.

Dodge-Kafka KL, Langeberg L, Scott JD. Compartmentation of cyclic nucleotide signaling in the heart: the role of A-kinase anchoring proteins. *Circ Res.* 2006 Apr 28;98(8):993-1001.

Dorn GW 2nd, Molkentin JD. Manipulating cardiac contractility in heart failure: data from mice and men. *Circulation.* 2004 Jan 20;109(2):150-8.

Du XJ, Autelitano DJ, Dilley RJ, Wang B, Dart AM, Woodcock EA. beta(2)-adrenergic receptor overexpression exacerbates development of heart failure after aortic stenosis. *Circulation.* 2000 Jan 4-11;101(1):71-7.

Eckhart AD, Fentzke RC, Lepore J, Lang R, Lin H, Lefkowitz RJ, Koch WJ, Leiden JM. Inhibition of betaARK1 restores impaired biochemical beta-adrenergic receptor responsiveness but does not rescue CREB(A133) induced cardiomyopathy. *J Mol Cell Cardiol.* 2002 Jun;34(6):669-77.

El-Armouche A, Bednorz A, Pamminger T, Ditz D, Didié M, Dobrev D, Eschenhagen T. Role of calcineurin and protein phosphatase-2A in the regulation of phosphatase inhibitor-1 in cardiac myocytes. *Biochem Biophys Res Commun.* 2006 Aug 4;346(3):700-6.

El-Armouche A, Pamminger T, Ditz D, Zolk O, Eschenhagen T. Decreased protein and phosphorylation level of the protein phosphatase inhibitor-1 in failing human hearts. *Cardiovasc Res.* 2004 Jan 1;61(1):87-93.

El-Armouche A, Wittköpper K, Degenhardt F, Weinberger F, Didié M, Melnychenko I, Grimm M, Peeck M, Zimmermann WH, Unsöld B, Hasenfuss G, Dobrev D, Eschenhagen T. Phosphatase inhibitor-1-deficient mice are protected from catecholamine-induced arrhythmias and myocardial hypertrophy. *Cardiovasc Res.* 2008 Dec 1;80(3):396-406.

Engelhardt S, Hein L, Wiesmann F, Lohse MJ. Progressive hypertrophy and heart failure in beta1-adrenergic receptor transgenic mice. *Proc Natl Acad Sci U S A.* 1999 Jun 8;96(12):7059-64.

Esposito G, Rapacciuolo A, Naga Prasad SV, Takaoka H, Thomas SA, Koch WJ, Rockman HA. Genetic alterations that inhibit in vivo pressure-overload hypertrophy prevent cardiac dysfunction despite increased wall stress. *Circulation.* 2002 Jan 1;105(1):85-92.

Feng ZH, Wilson SE, Peng ZY, Schlender KK, Reimann EM, Trumbly RJ. The yeast GLC7 gene required for glycogen accumulation encodes a type 1 protein phosphatase. *J Biol Chem.* 1991 Dec 15;266(35):23796-801.

Fliegner D, Schubert C, Penkalla A, Witt H, Kararigas G, Dworatzek E, Staub E, Martus P, Ruiz Noppinger P, Kintscher U, Gustafsson JA, Regitz-Zagrosek V. Female sex and estrogen receptor-beta attenuate cardiac remodeling and apoptosis in pressure overload. *Am J Physiol Regul Integr Comp Physiol.* 2010 Jun;298(6):R1597-606.

Grote-Wessels S, Baba HA, Boknik P, El-Armouche A, Fabritz L, Gillmann HJ, Kucerova D, Matus M, Müller FU, Neumann J, Schmitz M, Stümpel F, Theilmeier G, Wohlschlaeger J, Schmitz W, Kirchhefer U. Inhibition of protein phosphatase 1 by inhibitor-2 exacerbates progression of cardiac failure in a model with pressure overload. *Cardiovasc Res.* 2008 Aug 1;79(3):464-71.

Haghighi K, Kolokathis F, Pater L, Lynch RA, Asahi M, Gramolini AO, Fan GC, Tsiapras D, Hahn HS, Adamopoulos S, Liggett SB, Dorn GW 2nd, MacLennan DH, Kremastinos DT, Kranias EG. Human phospholamban null results in lethal dilated cardiomyopathy revealing a critical difference between mouse and human. *J Clin Invest.* 2003 Mar;111(6):869-76.

Haq S, Choukroun G, Lim H, Tymitz KM, del Monte F, Gwathmey J, Grazette L, Michael A, Hajjar R, Force T, Molkentin JD. Differential activation of signal transduction pathways in human hearts with hypertrophy versus advanced heart failure. *Circulation*. 2001 Feb 6;103(5):670-7.

Hasenfuss G, Reinecke H, Studer R, Meyer M, Pieske B, Holtz J, Holubarsch C, Posival H, Just H, Drexler H. Relation between myocardial function and expression of sarcoplasmic reticulum Ca(2+)-ATPase in failing and nonfailing human myocardium. *Circ Res*. 1994 Sep;75(3):434-42.

Higuchi E, Nishi A, Higashi H, Ito Y, Kato H. Phosphorylation of protein phosphatase-1 inhibitors, inhibitor-1 and DARPP-32, in renal medulla. *Eur J Pharmacol*. 2000 Nov 17;408(2):107-16.

Huang FL, Glinemann WH. Inactivation of rabbit muscle phosphorylase phosphatase by cyclic AMP-dependent kinase. *Proc Natl Acad Sci U S A*. 1975 Aug;72(8):3004-8.

Huang Z, Somanath PR, Chakrabarti R, Eddy EM, Vijayaraghavan S. Changes in intracellular distribution and activity of protein phosphatase PP1 γ 2 and its regulating proteins in spermatozoa lacking AKAP4. *Biol Reprod*. 2005 Feb;72(2):384-92.

Jessup M, Brozena S. Heart failure. *N Engl J Med*. 2003 May 15;348(20):2007-18.

Jondeau G, Neuder Y, Eicher JC, Jourdain P, Fauveau E, Galinier M, Jegou A, Bauer F, Trochu JN, Bouzamondo A, Tanguy ML, Lechat P; B-CONVINCED Investigators. B-CONVINCED: Beta-blocker CONTinuation Vs. INTerruption in patients with Congestive heart failure hospitalizED for a decompensation episode. *Eur Heart J*. 2009 Sep;30(18):2186-92.

King TD, Gandy JC, Bijur GN. The protein phosphatase-1/inhibitor-2 complex differentially regulates GSK3 dephosphorylation and increases sarcoplasmic/endoplasmic reticulum calcium ATPase 2 levels. *Exp Cell Res*. 2006 Nov 1;312(18):3693-700.

Kiriazis H, Wang K, Xu Q, Gao XM, Ming Z, Su Y, Moore XL, Lambert G, Gibbs ME, Dart AM, Du XJ. Knockout of beta(1)- and beta(2)-adrenoceptors attenuates pressure overload-induced cardiac hypertrophy and fibrosis. *Br J Pharmacol*. 2008 Feb;153(4):684-92.

Laemmli UK. Cleavage of structural proteins during the assembly of the head of bacteriophage T4. *Nature*. 1970 Aug 15;227(5259):680-5.

Layland J, Solaro RJ, Shah AM. Regulation of cardiac contractile function by troponin I phosphorylation. *Cardiovasc Res*. 2005 Apr 1;66(1):12-21.

Lee LG, Connell CR, Bloch W. Allelic discrimination by nick-translation PCR with fluorogenic probes. *Nucleic Acids Res*. 1993 Aug 11;21(16):3761-6.

Levy D, Larson MG, Vasan RS, Kannel WB, Ho KK. The progression from hypertension to congestive heart failure. *JAMA*. 1996 May 22-29;275(20):1557-62.

Liggett SB, Cresci S, Kelly RJ, Syed FM, Matkovich SJ, Hahn HS, Diwan A, Martini JS, Sparks L, Parekh RR, Spertus JA, Koch WJ, Kardia SL, Dorn GW 2nd. A GRK5 polymorphism that inhibits beta-adrenergic receptor signaling is protective in heart failure. *Nat Med*. 2008 May;14(5):510-7.

Lloyd-Jones DM, Larson MG, Leip EP, Beiser A, D'Agostino RB, Kannel WB, Murabito JM, Vasan RS, Benjamin EJ, Levy D; Framingham Heart Study. Lifetime risk for developing congestive heart failure: the Framingham Heart Study. *Circulation*. 2002 Dec 10;106(24):3068-72.

Li Z, Laugwitz KL, Pinkernell K, Pragst I, Baumgartner C, Hoffmann E, Rosport K, Münch G, Moretti A, Humrich J, Lohse MJ, Ungerer M. Effects of two Gbetagamma-binding proteins--N-terminally truncated phosphodiesterase-3 and beta-adrenergic receptor kinase C terminus (betaARKct) in heart failure. *Gene Ther*. 2003 Aug;10(16):1354-61.

Marx SO, Reiken S, Hisamatsu Y, Jayaraman T, Burkhoff D, Rosembliit N, Marks AR. PKA phosphorylation dissociates FKBP12.6 from the calcium release channel (ryanodine receptor): defective regulation in failing hearts. *Cell*. 2000 May 12;101(4):365-76.

Meyer M, Schillinger W, Pieske B, Holubarsch C, Heilmann C, Posival H, Kuwajima G, Mikoshiba K, Just H, Hasenfuss G, et al. Alterations of sarcoplasmic reticulum proteins in failing human dilated cardiomyopathy. *Circulation*. 1995 Aug 15;92(4):778-84.

Milano CA, Allen LF, Rockman HA, Dolber PC, McMinn TR, Chien KR, Johnson TD, Bond RA, Lefkowitz RJ. Enhanced myocardial function in transgenic mice overexpressing the beta 2-adrenergic receptor. *Science*. 1994 Apr 22;264(5158):582-6.

Movsesian MA, Karimi M, Green K, Jones LR. Ca(2+)-transporting ATPase, phospholamban, and calsequestrin levels in nonfailing and failing human myocardium. *Circulation*. 1994 Aug;90(2):653-7.

Mulkey RM, Endo S, Shenolikar S, Malenka RC. Involvement of a calcineurin/inhibitor-1 phosphatase cascade in hippocampal long-term depression. *Nature*. 1994 Jun 9;369(6480):486-8.

Nakayama H, Chen X, Baines CP, Klevitsky R, Zhang X, Zhang H, Jaleel N, Chua BH, Hewett TE, Robbins J, Houser SR, Molkentin JD. Ca²⁺- and mitochondrial-dependent cardiomyocyte necrosis as a primary mediator of heart failure. *J Clin Invest*. 2007 Sep;117(9):2431-44.

Netticadan T, Temsah RM, Kawabata K, Dhalla NS. Sarcoplasmic reticulum Ca(2+)/Calmodulin-dependent protein kinase is altered in heart failure. *Circ Res*. 2000 Mar 17;86(5):596-605.

Neumann J, Eschenhagen T, Jones LR, Linck B, Schmitz W, Scholz H, Zimmermann N. Increased expression of cardiac phosphatases in patients with end-stage heart failure. *J Mol Cell Cardiol*. 1997 Jan;29(1):265-72.

Neumann J, Gupta RC, Schmitz W, Scholz H, Nairn AC, Watanabe AM. Evidence for isoproterenol-induced phosphorylation of phosphatase inhibitor-1 in the intact heart. *Circ Res*. 1991 Dec;69(6):1450-7.

Pinna LA, Donella-Deana A. Phosphorylated synthetic peptides as tools for studying protein phosphatases. *Biochim Biophys Acta*. 1994 Jul 21;1222(3):415-31.

Pönicke K, Heinroth-Hoffmann I, Brodde OE. Role of beta 1- and beta 2-adrenoceptors in hypertrophic and apoptotic effects of noradrenaline and adrenaline in adult rat ventricular cardiomyocytes. *Naunyn Schmiedebergs Arch Pharmacol*. 2003 Jun;367(6):592-9.

Rapacciuolo A, Esposito G, Caron K, Mao L, Thomas SA, Rockman HA. Important role of endogenous norepinephrine and epinephrine in the development of in vivo pressure-overload cardiac hypertrophy. *J Am Coll Cardiol*. 2001 Sep;38(3):876-82.

Rogers JH, Tamirisa P, Kovacs A, Weinheimer C, Courtois M, Blumer KJ, Kelly DP, Muslin AJ. RGS4 causes increased mortality and reduced cardiac hypertrophy in response to pressure overload. *J Clin Invest*. 1999 Sep;104(5):567-76.

Rockman HA, Koch WJ, Lefkowitz RJ. Seven-transmembrane-spanning receptors and heart function. *Nature*. 2002 Jan 10;415(6868):206-12.

Rockman HA, Ross RS, Harris AN, Knowlton KU, Steinhilber ME, Field LJ, Ross J Jr, Chien KR. Segregation of atrial-specific and inducible expression of an atrial natriuretic factor transgene in an in vivo murine model of cardiac hypertrophy. *Proc Natl Acad Sci U S A*. 1991 Sep 15;88(18):8277-81.

Roth DM, Swaney JS, Dalton ND, Gilpin EA, Ross J Jr. Impact of anesthesia on cardiac function during echocardiography in mice. *Am J Physiol Heart Circ Physiol*. 2002 Jun;282(6):H2134-40.

Sahin B, Shu H, Fernandez J, El-Armouche A, Molkentin JD, Nairn AC, Bibb JA. Phosphorylation of protein phosphatase inhibitor-1 by protein kinase C. *J Biol Chem*. 2006 Aug 25;281(34):24322-35.

Sato Y, Kiriazis H, Yatani A, Schmidt AG, Hahn H, Ferguson DG, Sako H, Mitarai S, Honda R, Mesnard-Rouiller L, Frank KF, Beyermann B, Wu G, Fujimori K, Dorn GW 2nd, Kranias EG. Rescue of contractile parameters and myocyte hypertrophy in caldesmon overexpressing myocardium by phospholamban ablation. *J Biol Chem*. 2001 Mar 23;276(12):9392-9.

Schwinger RH, Münch G, Bölck B, Karczewski P, Krause EG, Erdmann E. Reduced Ca²⁺-sensitivity of SERCA 2a in failing human myocardium due to reduced serin-16 phospholamban phosphorylation. *J Mol Cell Cardiol*. 1999 Mar;31(3):479-91.

Skavdahl M, Steenbergen C, Clark J, Myers P, Demianenko T, Mao L, Rockman HA, Korach KS, Murphy E. Estrogen receptor-beta mediates male-female differences in the development of pressure overload hypertrophy. *Am J Physiol Heart Circ Physiol*. 2005 Feb;288(2):H469-76.

Stewart S, MacIntyre K, Capewell S, McMurray JJ. Heart failure and the aging population: an increasing burden in the 21st century? *Heart*. 2003 Jan;89(1):49-53.

Stuart JS, Frederick DL, Varner CM, Tatchell K. The mutant type 1 protein phosphatase encoded by *glc7-1* from *Saccharomyces cerevisiae* fails to interact productively with the GAC1-encoded regulatory subunit. *Mol Cell Biol*. 1994 Feb;14(2):896-905.

Suehiro K, Takuma S, Shimizu J, Hozumi T, Yano H, Cardinale C, DiTullio MR, Wang J, Smith CR, Burkhoff D, Homma S. Assessment of left ventricular systolic function using contrast two-dimensional echocardiography with a high-frequency transducer in the awake murine model of myocardial infarction. *Jpn Circ J*. 2001 Nov;65(11):979-83.

Swedberg K, Hjalmarson A, Waagstein F, Wallentin I. Prolongation of survival in congestive cardiomyopathy by beta-receptor blockade. *Lancet*. 1979 Jun 30;1(8131):1374-6.

Swynghedauw B. Molecular mechanisms of myocardial remodeling. *Physiol Rev*. 1999 Jan;79(1):215-62.

Tang T, Gao MH, Lai NC, Firth AL, Takahashi T, Guo T, Yuan JX, Roth DM, Hammond HK. Adenylyl cyclase type 6 deletion decreases left ventricular function via impaired calcium handling. *Circulation*. 2008 Jan 1;117(1):61-9.

Towbin H, Staehelin T, Gordon J. Electrophoretic transfer of proteins from polyacrylamide gels to nitrocellulose sheets: procedure and some applications. *Proc Natl Acad Sci U S A*. 1979 Sep;76(9):4350-4.

van der Velden J, Papp Z, Zaremba R, Boontje NM, de Jong JW, Owen VJ, Burton PB, Goldmann P, Jaquet K, Stienen GJ. Increased Ca²⁺-sensitivity of the contractile apparatus in end-stage human heart failure results from altered phosphorylation of contractile proteins. *Cardiovasc Res*. 2003 Jan;57(1):37-47.

Wang J, Liu X, Sentex E, Takeda N, Dhalla NS. Increased expression of protein kinase C isoforms in heart failure due to myocardial infarction. *Am J Physiol Heart Circ Physiol*. 2003 Jun;284(6):H2277-87.

Weinberg EO, Thienelt CD, Katz SE, Bartunek J, Tajima M, Rohrbach S, Douglas PS, Lorell BH. Gender differences in molecular remodeling in pressure overload hypertrophy. *J Am Coll Cardiol*. 1999 Jul;34(1):264-73.

Wera S, Hemmings BA. Serine/threonine protein phosphatases. *Biochem J*. 1995 Oct 1;311 (Pt 1):17-29.

Wittköpper K, Fabritz L, Neef S, Ort KR, Grefe C, Unsöld B, Kirchhof P, Maier LS, Hasenfuss G, Dobrev D, Eschenhagen T, El-Armouche A. Constitutively active phosphatase inhibitor-1 improves cardiac contractility in young mice but is deleterious after catecholaminergic stress and with aging. *J Clin Invest*. 2010 Feb 1;120(2):617-26.

Xiao B, Zhong G, Obayashi M, Yang D, Chen K, Walsh MP, Shimoni Y, Cheng H, Ter Keurs H, Chen SR. Ser-2030, but not Ser-2808, is the major phosphorylation site in cardiac ryanodine receptors responding to protein kinase A activation upon beta-adrenergic stimulation in normal and failing hearts. *Biochem J*. 2006 May 15;396(1):7-16.

Yamada M, Ikeda Y, Yano M, Yoshimura K, Nishino S, Aoyama H, Wang L, Aoki H, Matsuzaki M. Inhibition of protein phosphatase 1 by inhibitor-2 gene delivery ameliorates heart failure progression in genetic cardiomyopathy. *FASEB J*. 2006 Jun;20(8):1197-9.

Zakhary DR, Moravec CS, Bond M. Regulation of PKA binding to AKAPs in the heart: alterations in human heart failure. *Circulation*. 2000 Mar 28;101(12):1459-64.

Zakhary DR, Moravec CS, Stewart RW, Bond M. Protein kinase A (PKA)-dependent troponin-I phosphorylation and PKA regulatory subunits are decreased in human dilated cardiomyopathy. *Circulation*. 1999 Feb 2;99(4):505-10.

Zhang F, Phiel CJ, Spece L, Gurvich N, Klein PS. Inhibitory phosphorylation of glycogen synthase kinase-3 (GSK-3) in response to lithium. Evidence for autoregulation of GSK-3. *J Biol Chem*. 2003 Aug 29;278(35):33067-77.

Zhao W, Yuan Q, Qian J, Waggoner JR, Pathak A, Chu G, Mitton B, Sun X, Jin J, Braz JC, Hahn HS, Marreez Y, Syed F, Pollesello P, Annala A, Wang HS, Schultz Jel J, Molckentin JD, Liggett SB, Dorn GW 2nd, Kranias EG. The presence of Lys27 instead of Asn27 in human phospholamban promotes sarcoplasmic reticulum Ca²⁺-

ATPase superinhibition and cardiac remodeling. *Circulation*. 2006 Feb 21;113(7):995-1004.

Zhou YQ, Foster FS, Nieman BJ, Davidson L, Chen XJ, Henkelman RM. Comprehensive transthoracic cardiac imaging in mice using ultrasound biomicroscopy with anatomical confirmation by magnetic resonance imaging. *Physiol Genomics*. 2004 Jul 8;18(2):232-44.

8 Acknowledgements

First of all I would like to thank Prof. Dr. med. Thomas Eschenhagen for the opportunity to earn my doctorate at the “Institut für experimentelle und klinische Pharmakologie und Toxikologie”. I greatly appreciated meticulous scientific education he provided, which I will always remember.

Second, I have to specially have to thank Prof. Dr. med. Ali El-Armouche for providing the subject of investigation and the outstanding supervision in the course of its execution. His door was always open and his input highly appreciated.

I would also like to thank Birgit Geertz for her invaluable help in acquiring the echocardiographs.

Additionally I would like to thank Dr. med. Nils Teucher for his support with the TAC procedure. Without him, this project would have been impossible to carry out.

Special thanks goes to Jutta Starbatty for her excellent technical support and for being the heart and soul of the laboratory.

Furthermore I´d like to thank all the other wonderful coworkers I was allowed to meet during my time at the “Institut für experimentelle und klinische Pharmakologie und Toxikologie” and whose warm and supportive manners have made it a joy to work there.

Last but certainly not last I would like to thank my parents who have always supported me to this day and without whom I would have never finished this project.

9 Curriculum vitae

Due to protection of privacy not published in the online version.

10 Eidesstattliche Versicherung:

Ich versichere ausdrücklich, dass ich die Arbeit selbständig und ohne fremde Hilfe verfasst, andere als die von mir angegebenen Quellen und Hilfsmittel nicht benutzt und die aus den benutzten Werken wörtlich oder inhaltlich entnommenen Stellen einzeln nach Ausgabe (Auflage und Jahr des Erscheinens), Band und Seite des benutzten Werkes kenntlich gemacht habe.

Ferner versichere ich, dass ich die Dissertation bisher nicht einem Fachvertreter an einer anderen Hochschule zur Überprüfung vorgelegt oder mich anderweitig um Zulassung zur Promotion beworben habe.

Micha Peeck

11 Addendum: Data from the 27G TAC series

All	Unit	WT ^{Sham}	WT ^{TAC}	KO ^{Sham}	KO ^{TAC}
FS B-Mode	%	32.2 (1.9) 29.6 (1.3)	28.4 (1.4) 11.7 (1.6)	28.7 (2.0) 28.7 (1.5)	28.9 (1.8) 9.9 (1.6)
FAS	%	53.9 (2.1) 50.8 (1.9)	52.0 (1.8) 25.8 (2.3)	49.2 (2.2) 49.3 (2.5)	50.5 (2.7) 22.3 (1.9)
EF	%	57.1 (3.1) 54.8 (2.1)	56.6 (1.8) 30.7 (2.2)	54.8 (1.9) 54.6 (2.4)	54.8 (2.5) 27.2 (1.8)
FAS-Dobu	%	68.6 (5.0) 70.4 (3.4)	72.5 (3.2) 33.0 (3.9)	70.7 (4.2) 68.6 (4.1)	68.3 (4.6) 23.6 (3.9)
LVM	mg	128.9 (10.2) 132.0 (6.2)	123.1 (7.2) 219.8 (12.1)	127.6 (7.9) 131.0 (9.7)	125.7 (4.6) 210.1 (10.2)
LVW/TL-ratio	mg/ mm	7.4 (0.5) 7.6 (0.4)	7.1 (0.4) 12.7 (0.7)	7.3 (0.5) 7.5 (0.6)	7.2 (0.2) 12.1 (0.6)
AWTh dias.	mm	0.76 (0.02) 0.83 (0.03)	0.79 (0.01) 1.17 (0.04)	0.73 (0.02) 0.76 (0.03)	0.78 (0.02) 1.12 (0.06)
PWTh dias.	mm	0.76 (0.02) 0.81 (0.03)	0.78 (0.01) 1.18 (0.04)	0.73 (0.02) 0.75 (0.03)	0.78 (0.02) 1.12 (0.07)
LVEDD	mm	4.3 (0.0) 4.5 (0.1)	4.4 (0.1) 4.6 (0.1)	4.7 (0.1) 4.6 (0.1)	4.4 (0.1) 4.4 (0.1)
Heart rate	bpm	488 (15) 516 (19)	490 (15) 498 (19)	472 (12) 528 (21)	505 (17) 537 (14)
Male					
FS B-Mode	%	30.3 (3.2) 27.2 (1.6)	29.2 (1.9) 11.1 (1.6)	28.5 (3.0) 29.4 (2.0)	26.4 (1.1) 9.5 (0.1)
FAS	%	52.5 (3.6) 47.3 (2.9)	51.7 (2.3) 24.5 (2.7)	48.7 (3.2) 49.5 (3.2)	46.8 (2.0) 22.5 (1.3)
EF	%	53.6 (5.6) 50.5 (2.9)	57.0 (2.2) 28.8 (2.5)	54.5 (2.8) 54.9 (2.9)	51.5 (1.8) 27.2 (2.1)
FAS-Dobu	%	58.7 (6.4) 68.4 (4.3)	69.6 (4.3) 27.7 (4.2)	71.0 (4.3) 67.7 (5.7)	68.2 (6.5) 24.0 (5.0)
LVM	mg	145.4 (14.1) 144.5 (3.6)	133.2 (8.2) 232.3 (16.2)	131.6 (8.2) 138.5 (13.2)	122.2 (6.4) 204.7 (7.2)
LVW/TL	mg/ mm	7.3 (0.8) 8.0 (0.5)	7.6 (0.5) 13.8 (0.8)	8.1 (0.6) 7.1 (0.8)	7.1 (0.3) 11.4 (0.6)
AWTh dias.	mm	0.79 (0.02) 0.90 (0.01)	0.81 (0.01) 1.18 (0.06)	0.74 (0.03) 0.75 (0.03)	0.78 (0.02) 1.12 (0.07)

Male	Unit	WT ^{Sham}	WT ^{TAC}	KO ^{Sham}	KO ^{TAC}
PWTh dias.	mm	0.78 (0.01) 0.88 (0.01)	0.79 (0.01) 1.18 (0.06)	0.74 (0.03) 0.75 (0.03)	0.78 (0.02) 1.12 (0.07)
LVEDD	mm	4.3 (0.0) 4.5 (0.1)	4.6 (0.1) 4.8 (0.1)	4.8 (0.1) 4.8 (0.1)	4.3 (0.2) 4.4 (0.2)
Heart rate	bpm	466 (23) 501 (40)	482 (20) 492 (29)	464 (17) 511 (27)	500 (24) 539 (17)
Female					
FS B-Mode	%	33.9 (2.0) 31.9 (1.3)	27.8 (2.5) 10.9 (3.9)	29.3 (1.0) 27.3 (3.0)	32.9 (3.4) 10.7 (4.8)
FAS	%	55.2 (2.5) 54.2 (0.9)	52.6 (3.4) 28.4 (4.7)	50.4 (1.7) 48.9 (4.9)	56.6 (4.7) 22.1 (5.2)
EF	%	60.5 (2.4) 59.0 (0.9)	56.0 (3.7) 34.5 (4.4)	55.4 (1.8) 54.0 (5.0)	60.4 (4.9) 27.2 (3.9)
FAS-Dobu		78.5 (3.5) 72.5 (5.6)	77.7 (3.8) 42.2 (6.0)	70.2 (11.5) 71.1 (5.6)	68.4 (7.4) 22.8 (7.4)
LVM	mg	112.3 (10.4) 119.6 (7.9)	107.8 (7.2) 192.5 (6.8)	119.6 (19.2) 116.1 (10.3)	137.3 (3.8) 236.9 (14.2)
LVW/TL-ratio	mg/ mm	7.3 (0.8) 8.0 (0.5)	6.0 (0.3) 11.4 (0.5)	8.1 (0.6) 7.1 (0.8)	7.1 (0.3) 11.5 (0.6)
AWTh dias.	mm	0.74 (0.04) 0.77 (0.04)	0.76 (0.03) 1.18 (0.06)	0.72 (0.04) 0.77 (0.07)	0.85 (0.05) 1.27 (0.05)
PWTh dias.	mm	0.74 (0.05) 0.75 (0.04)	0.76 (0.03) 1.18 (0.05)	0.73 (0.04) 0.77 (0.06)	0.86 (0.04) 1.28 (0.06)
LVEDD	mm	4.3 (0.1) 4.5 (0.1)	4.1 (0.1) 4.3 (0.0)	4.5 (0.1) 4.4 (0.0)	4.5 (0.1) 4.4 (0.1)
Heart rate	bpm	509 (17) 531 (4)	505 (21) 510 (10)	487 (5) 561 (24)	513 (27) 533 (31)